REPORT DOCUMENTATION PAGE

AFRL-SR-BL-TR-99-

0097

a sources,
ect of this
Jefferson

1. AGENCY USE ONLY *(Leave blank)*	2. REPORT DATE	3. REPORT TYPE AND DATES COVERED
	31 Aug 99	FINAL 15 Jul 96 - 14 Jul 99

4. TITLE AND SUBTITLE
DEPSCOR95 Studies of Processing Chemistry and Stability of High Temperatuare Polyimides Using TG/FTIR/MS

5. FUNDING NUMBERS

6. AUTHOR(S)
Charles W.M. Lee

7. PERFORMING ORGANIZATION NAME(S) AND ADDRESS(ES)
Western Kentucky University
1 Big Red Way
Bowling Green KY 42101

8. PERFORMING ORGANIZATION REPORT NUMBER
F49620-96-1-0338

9. SPONSORING/MONITORING AGENCY NAME(S) AND ADDRESS(ES)
AFOSR/NL
801 N Randolph St., Rm 732
Arlington VA 22203-1977

10. SPONSORING/MONITORING AGENCY REPORT NUMBER

19991220 066

11. SUPPLEMENTARY NOTES

12a. DISTRIBUTION AVAILABILITY STATEMENT
Distribution Unlimited

12b. DISTRIBUTION CODE

13. ABSTRACT *(Maximum 200 words)*

This research project addressed two fundamental aspects of carbon fiber reinforced high temperature polyimide composites, namely the curing chemistry involved for polyimide formation and then, the thermal oxidative stability of the polyimide structure so produced. The latter played a key role in controlling the composite long-term service temperature when the composite wastargeted for aircraft and aerospace applications. The TGA/FTIR and TGA/MS evolved gas analysis provided a convenient means to study these two features by monitoring the off-gas reaction producrts during cure in the former and following the off-gas degradation products in the latter. TGA served as a curing reactor in the former while FTIR and MS identified the reaction products in real time. Similarly, TGA provided the means of aging a compositein a controlled environment while FTIR and MS were used to detect the degradation products given off, also in real time. According to TGA/FTIR/MS study, the thermal curing of polyimides including AFR700B/T650-35, LARC RP-46/IM7 and VCAP-75/Glass fiber prepregs proceeded essentially by: 1. the elimination of methanol from amic-acid prepolymer formation, 2. the release of water from subsequent imidization, and 3. finally, the thermal crosslinking via a reverse Diels-Alder reaction when a NE end capping monomer was used. Thus, this polyimide curing reaction sequence confirmed the literature findings. However, the FTIR/MIS data obtained could also accommodate the alternative that the elimination of water from amide-ester formation occurred first, which was followed by the release of methanol from subsequent imidization. In the case of AFR700B/T650-35 prepreg, most off-gases were released by 430 o F (221 o C),

14. SUBJECT TERMS
Carbon Fiber
Polyimides
Prepregs

15. NUMBER OF PAGES
80

16. PRICE CODE

17. SECURITY CLASSIFICATION OF REPORT	18. SECURITY CLASSIFICATION OF THIS PAGE	19. SECURITY CLASSIFICATION OF ABSTRACT	20. LIMITATION OF ABSTRACT
UNCLASSIFIED	UNCLASSIFIED	UNCLASSIFIED	

WESTERN KENTUCKY UNIVERSITY

BOWLING GREEN, KENTUCKY 42101

August 31, 1999

Dr. Charles Y-C Lee
AFOSR
801 N. Randolph Street, Room 732
Arlington, VA 22203-1977

96-1-0388 DEPSCOR-95

Dear Charles:

Enclosed is a copy of the final technical report on "Studies of Processing Chemistry and Stabilityof High Temperature Polyimides Using TGA/FTIR/MS," a DEPSCoR research project, for your review. I hope you find it satisfactory.

To complete this report, I need a Cover and title page, Standard Form 298 for Report Documentation Page. Would you please send me one? I also need a blank form for reporting Final Invention.

I wish to thank you for the your guidance and suggestion during this work. They are very valuable. After today, I am going to take on a new and different approach to life, i.e., to learn how to be a happy retiree from Western Kentucky University.

Wish you continuing success with your Air Force research funding tasks. You have done a great job for the fundamental polymer research community.

Best regards,

Charles W. M. Lee

Charles W. M. Lee
Department of Chemistry

Tel: 502-745-3943
Fax: 502-745-5361
Email: charles.lee@wku.edu

EXECUTIVE SUMMARY

This research project addressed two fundamental aspects of carbon fiber reinforced high temperature polyimide composites, namely the curing chemistry involved for polyimide formation and then, the thermal oxidative stability of the polyimide structure so produced. The latter played a key role in controlling the composite long-term service temperature when the composite was targeted for aircraft and aerospace applications. The TGA/FTIR and TGA/MS evolved gas analysis provided a convenient means to study these two features by monitoring the off-gas reaction products during cure in the former and following the off-gas degradation products in the latter. TGA served as a curing reactor in the former while FTIR and MS identified the reaction products in real time. Similarly, TGA provided the means of aging a composite in a controlled environment while FTIR and MS were used to detect the degradation products given off, also in real time.

According to TGA/FTIR/MS study, the thermal curing of polyimides including AFR700B/T650-35, LARC RP-46/IM7, and VCAP-75/Glass fiber prepregs proceeded essentially by: 1. the elimination of methanol from amic-acid prepolymer formation, 2. the release of water from subsequent imidization, and 3. finally, the thermal crosslinking via a reverse Diels-Alder reaction when a NE end capping monomer was used. Thus, this polyimide curing reaction sequence confirmed the literature findings. However, the FTIR/MS data obtained could also accommodate the alternative that the elimination of water from amide-ester formation occurred first, which was followed by the release of methanol from subsequent imidization. In the case of AFR700B/T650-35 prepreg, most off-gases were released by 430°F (221°C), thereby marking this temperature as the time for both vacuum cut-off and application of consolidation during autoclaving to produce low void content parts. Again, this coincided with industrial autoclaving practice. Moreover, a prepreg storage lifetime study indicated that little 10°F freezer effect was noted up to 9 months.

With regard to AFR700B/T650-35 composite stability, the TGA/FTIR/MS technique successfully identified, in real time, some of the important off-gas products during aging, such as H_2O, CO, CO_2, HCF_3, HF, CH_3OH, $C_6H_5NH_2$, phenyl isocyanate, cyclopentadiene, etc. The onset temperature for the release of these degradation products from chain scissions was surprisingly small at about 190 – 220°C. Furthermore, up to this temperature the composite degradations proceeded in a similar fashion, regardless of the aging environment used. Beyond 220°C, oxidative degradations gaining in speed started to deviate from thermal degradations, resulting in a larger weight loss and hence, a less stable composite. In general, they were given off in two separate temperature ranges, suggesting the operating degradation mechanisms to be different The first peak temperature occurred between 300 – 330°C while the second peak temperature took place at about 500 – 520°C indicating the involvement of carbon fiber. Because of its ability to examine the degradation off-gases and their kinetics, the TGA/FTIR/MS technique could be employed to determine a limit temperature for accelerated aging. Based on off-gases and the trend of their release, the degradation mechanism of AFR700B/T650-35 composite appeared to be similar between 190 and 371°C, thereby marking 371°C to be

the highest accelerated aging temperature for its long-term lifetime prediction. Beyond 371°C, different degradation mechanisms would apply. This was the first time that an accelerated aging temperature limit was determined according to real-time degradation products. To expand its usefulness, an interrelationship among aging environment/temperature/time, the state of chemical degradations, and mechanical property change needs to be established.

It should be noted that with all of its capability, the above evolved gas analysis lacked the ability of examining curing reactions as well as chain scissions not involving off-gas productions. As a result, complimentary techniques such as temperature programmable FTIR, NMR including solid state NMR, etc. should be used in conjunction to fully understand these composite fundamentals.

CONTENTS

Figures

1. Introduction

In recent years, carbon fiber reinforced composites of polyimides having use temperature as high as 371°C (700°F)[1] and even up to 427°C (800°F)[2] have been developed for aircraft engine and space applications. At these high service temperatures, the thermal stability and thermal oxidative stability (TOS) of the polymer matrix are of primary concern. Any thermal decompositions or thermal oxidative degradations could, potentially, affect their high temperature applications.

For given monomer components and end groups, the stability of polyimides depends upon the processing chemistry involved.[3,4] Thus, in addition to the composition, the monomer reactivity, associated reaction mechanism and reaction kinetics also play an important role in determining the resulting cured polymer structure which, in turn, influences its stability. In the case of PMR-15, a 316°C polyimide, studies[5] have shown the effects of monomer aging during storage as well as its curing schedule. Therefore, the performance of a polymer is intimately tied to the manner by which it is formed, i.e., processing-structure-property interrelationships need to be established for the understanding and modification of material properties.

Traditionally, IR, NMR, reverse-phase liquid chromatography, and GPC have been employed[6,7] to follow the reactions PMR-15 type of polyimide and the buildup of molecular weights. Unfortunately, these techniques lack the ability of monitoring the reactions continuously. More recently, DSC, DMA, and dielectric constants have been used[5] to follow the polyimide reactions continuously. These techniques allow for the detection of the effects of these reactions in the form of heat of reaction by DSC, rheology by DMA, and ion mobility by dielectric constants. They are valuable in process control and useful for reproducibility check. But, they still lack the ability of positively identifying reaction products when they are made. Hence, a need for in-situ monitoring of monomer reactions and subsequent polymerization by direct reaction product identification exists.

Lately, Lee and Pan[8] have successfully applied on-line TGA/FTIR and TGA/MS techniques to follow the various PMR-15 reactions. The use of TGA permits one to heat the monomer mixture to reaction temperatures and to follow the evolution of condensation gaseous products by weight loss while FTIR helps one to identify, at the same time, what these small gas molecules are. When large organic species are given off, they are identified by the use of mass spectroscopy.

In this study, the same approach was applied to investigate the processing chemistry of high temperature polyimide prepregs of AFR700B[1], VCAP-75[2] and LARC™-RP46[9]. The curing time and temperature for off-gas productions were determined. The sequence of evolution of these off-gases was, then, compared to that of PMR-15 prepreg as well as literature curing chemistry for these high temperature polyimides. Processing chemistry based on this on-line off-gas monitoring was proposed. On the application side, this information would be useful to the establishment of proper processing conditions for part consolidations. For instance, the onset of

vacuum application to pull off evolved gases during cure and the subsequent application of pressure to minimize void formation in a consolidated part are two such important processing considerations for producing quality polymer composites. Furthermore, the effects of prepreg storage aging of AFR700B/T650-35 was examined to ascertain if curing occurred during freezer storage by comparing the off-gas products and the conditions for their releases.

With regard to the assessment of polymer stability, TGA is usually employed to determine the temperature of initial weight loss, which can be viewed as the onset of degradations. Moreover, it can be used to monitor continually the weight loss kinetics[10]. While the end results of thermal and/or thermal oxidative degradations in terms of weight loss are measurable by TGA, their degradation pathways are not readily assessable without the aid of an on-line evolved gas analysis. Once again, TGA/FTIR[11] and TGA/MS offer the means of identifying, in real time, small gaseous products like CO_2, H_2O, CH_4 and CO as well as large organic species.

The stability of polyimide composites has been studied extensively. Zhang et al[12] studied the thermal and oxidative stability of Cytec^R 5260/IM7, a BMI composite, by TGA/FTIR. In addition, the same BMI composite was later examined by Zhong et al[13] using TGA/MS. Mass fragments including such large organic species as phenylisocyanate, methylphenyl isocyanate, benzosuccinimide, etc. were noted. The FTIR/MS data suggested the methylene group in the backbone to be the initiation site for degradation. More recently, Alston et al[14] investigated the thermal oxidative stability of several high temperature polyimides using TGA/FTIR. The presence of degradation products such as phenyl isocyanate, p-phenylene diisocyanate, and trifluoromethane in a 3F polyimide led them to propose the degradation initiation site to be either imide or fluorinated linkages. The proposition that the degradation in a 3F or 6F polyimide started at a fluorinated linkage agreed well with the theoretical bond order calculations by Lee et al[15]. They found the C-CF_3 linkage to have the smallest bond order and thus, the largest C-C bond distance. Hence, this C-CF_3 linkage would be the initiation site of degradation.

In the present study, the stability of a post-cured AFR700B/T650-35 laminate[16] was determined using both TGA/FTIR and TGA/MS. Thermal aging of this laminate was conducted in a nitrogen environment while thermal oxidative aging was carried out in air. Both dynamic and isothermal aging were conducted for stability study. Weight loss and off-gas evolutions were measured as a function of aging time and temperature. These FTIR and MS off-gas profiles formed the basis of degradation pathway probe.

In addition to stability determination and degradation mechanism examinations, an attempt to determine the highest accelerating aging temperature for long-term durability assessment was made for this AFR700B/T650-35 composite. In general, the lifetime of a polymer composite is estimated, on the basis of its weight loss, through accelerated aging. At elevated aging temperatures, it is easy to induce degradations and thus, a large measurable weight loss. If the degradation mechanisms remain the same over a given range of aging temperatures, one can determine the weight loss kinetics and then, estimate the corresponding aging time needed to produce the same weight loss at a

lower aging temperature. If the degradation mechanisms change, this type of lifetime calculation based solely on weight loss kinetics could lead to misleading conclusions. In the absence of on-line degradation product identifications in the past, degradation mechanisms were, in general, assumed to stay the same for expediency sake. At the advent of evolved gas analysis by TGA/FTIR and/or TGA/MS, the off-gas degradation products are detectable, thereby providing the means of checking and verifying, in real time, if the degradation pathways remain the same. Moreover, one can easily determine the aging temperature beyond which degradation mechanisms have changed and thus, define the peak allowable accelerating aging temperature. To this end, the AFR700B/T650-35 composite was aged between 220 (428) and 600°C (1112°F) followed by a four hour hold at the given aging temperature. Their off-gas degradation products were analyzed for accelerated aging temperature limit determination.

2. Experimental

2.1 Material Selection

Three high temperature polyimide prepregs having T_g between 600 and 700°F were chosen for the processing chemistry study. They were AFR700B/T650-35[16], VCAP-75/Glass Fiber[17], and RP46/IM7[18], stored in a small 10°F freezer before use. Small pieces were cut for TGA/FTIR or TGA/MS measurements.

For polyimide stability study, only a post-cured AFR700B/T650-35 composite[16] was employed. This was an 8-ply 3K T650-35 fabric laminate. Its post-cure conditions as related by William McCormack of GE Aircraft Engines were as follows:

1) Heat from room temperature to 450°F in 1 hr 34 min (approximately 4°F/min)
2) Hold at 450°F for 4 hr
3) Heat from 450°F to 600°F in 1 hr 15 min (approximately 2°F/min)
4) Hold at 600°F for 16 hr
5) Heat from 600 to 650°F in 50 min (approximately 1°F/min)
6) Hold at 650°F for 4 hr
7) Heat from 650 to 675°F in 25 min (approximately 1°F/min)
8) Hold at 675°F for 4 hr
9) Heat from 675 to 700°F in 25 min (approximately 1°F/min)
10) Hold at 700°F for 4 hr
11) Heat from 700 to 725°F in 25 min (approximately 1°F/min)
12) Hold at 725°F for 4 hr
13) Heat from 725 to 750°F in 25 min (approximately 1°F/min)
14) Hold at 750°F for 10 hrs
15) Cool from 750 to 650°F in 50 min (approximately 2°F/min)
16) Cool from 650 to 150°F in 1 hr 40 min (approximately 5°F/min)

A TMA measurement of this post-cured laminate at 10°C/min gave its glass temperature at 417°C (783°F). Thus, it has reached a T_g beyond 700°F. For TGA/FTIR or TGA/MS

analysis, ground irregular shaped powders by the use of a metal file having a nominal size of 0.1-0.2 mm were employed.

2.2 Apparatus

2.2.1 Differential Scanning Calorimeter

DSC 2920, a Modulated DSC by TA Instruments, provided the thermogram of the three polyimide prepregs in nitrogen for the determination of endothermic and/or exothermic temperatures which gave an indication of the release of absorbed moisture or residual solvent and the evolution of condensation reaction products.

2.2.2 Thermomechanical Analyzer

TMA model 943 by DuPont Instruments measured the glass transition temperature of the post-cured AFR700B/T650-35 composite in air.

2.2.3 Thermogravimetric Analyzer/Fourier Transform Infrared Spectrometer

DuPont Instrument's TGA model 951 was coupled with Perkin Elmer 2000 FTIR by using an insulated teflon tube heated to a temperature of 150°C by a Powerstat Variable Autotransformer. The gas cell (25 cm x 10 cm) with KRS-5 windows used with the FTIR was heated with a Barnant Thermocouple Controller. The tubing and the gas cell were heated to prevent condensation within the tubing transfer line or the gas cell. The TGA/FTIR experimental setup is shown in Figure 1. The amount of prepreg sample used was about 1 g while the sample size for composite was approximately 0.5 g.

2.2.4 Thermogravimetric Analyzer/Mass Spectrometer

DuPont Instrument's TGA model 951 was connected to a Thermolab VG Mass Spectrometer. This VG MS has a specially designed flexible capillary tube with a fused silica liner, which was heated to 170°C to reduce memory effects. It only took 60 milliseconds in gas transit time from the TGA to the MS. Sample gases entering the ion source were ionized by collisions with electrons from a hot filament. The ions thus formed, which may undergo fragmentation, were then sorted in the quadrupole analyzer according to their mass-to-charge ratio before entering the dual detector. Two detectors will be available for use: a Faraday cup for high pressure and accurate quantitative work, and a scanning electron multiplier (SEM) for high sensitivity work. In the present work, the MS data was gathered with the SEM detector. The entire operation of the MS, including storage, analysis and presentation of data was handled by an IBM-compatible PC (386SX). Figure 2 shows the TGA/MS experimental setup. Again, the amount of prepreg sample employed was about 1 g whereas the composite sample size was close to 0.5 g.

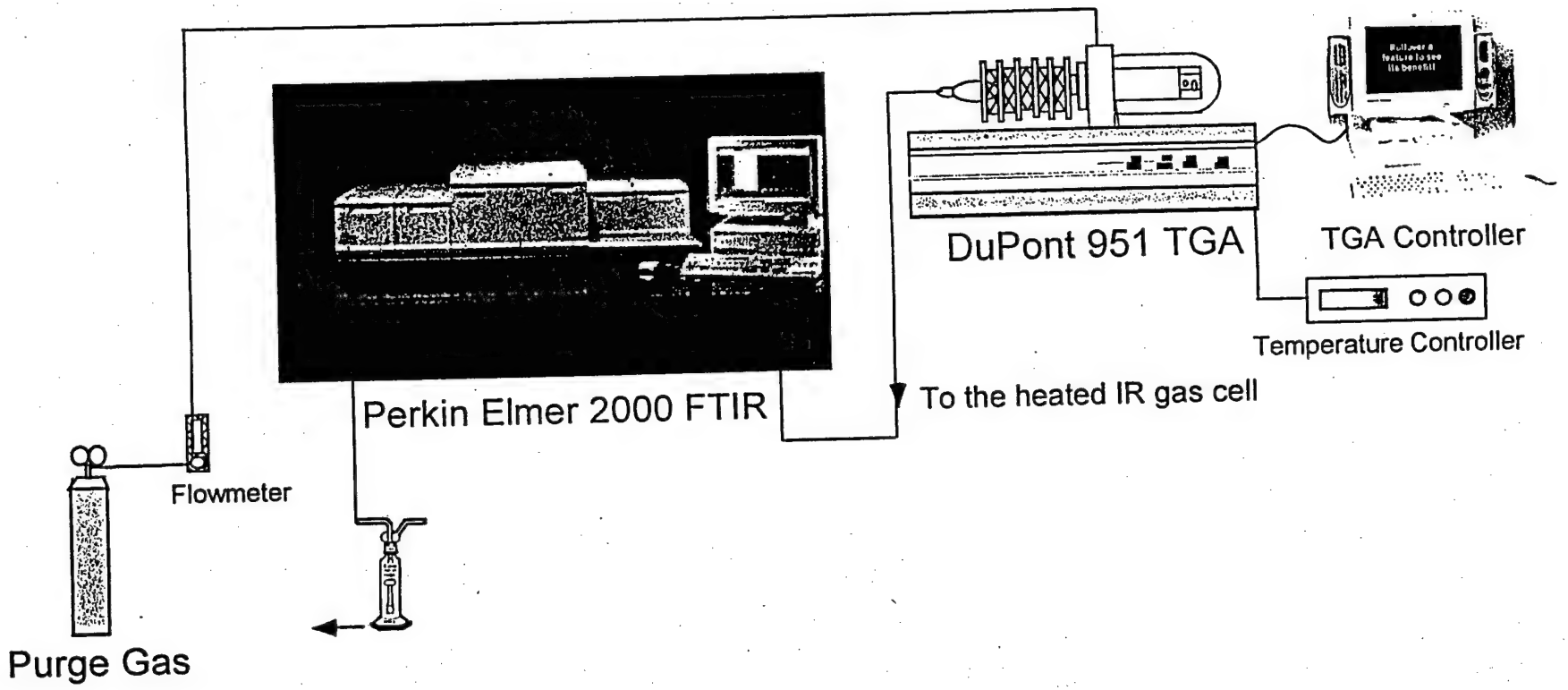

Figure 1 TGA/FTIR Experimental Setup

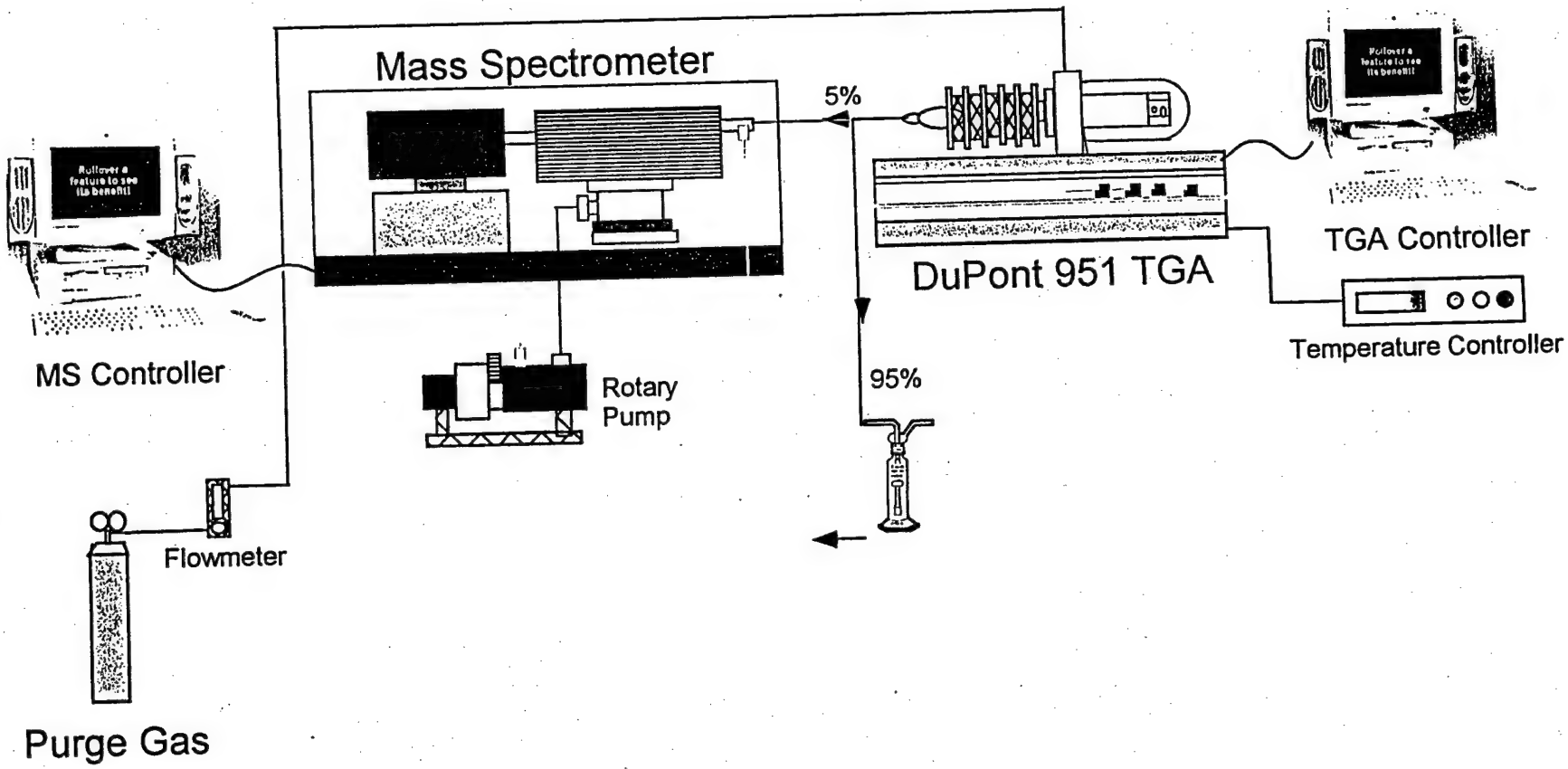

Figure 2 TGA/MS Experimental Setup

3. Results and Discussion

3.1 Curing Chemistry Study

3.1.1 Short-time Curing of AFR700B/T650-35 Prepreg

AFR700B[7], an addition polyimide, was made from monomers: NE, monomethylesteter of 5-nornbornene-2,3-dicarboxylic acid; PPDA, para-phenylenediamine; and 6FDE or HFDE, di-methylester of 4,4'hexafluoroisopropylidene bisphthalic acid using methanol as the solvent. Figure 3 displays its formulation. Reinforced with 3K intermediate modulus carbon fiber T650-35, the AFR700B/T650-35 prepreg was produced.

To explore the temperature ranges for off-gas evolution, a curing run of this AFR700B prepreg in TGA by heating to 400°C at 10°C/min in nitrogen at 50 ml/min was carried out. The TGA weight loss curves (see Figure 4) exhibited two major weight loss rate peaks at 115 and 149°C having corresponding weight losses at 1.55 and 4.28%. A shoulder appeared at about 250°C while another minor peak occurred around 340-350°C. Thus, off-gases were evolved at relatively high rates at 115, 149, 250, and 345°C.

The FTIR data was collected with Perkin Elmer 2000 FTIR from 450 – 4000 cm^{-1} at a 4 cm^{-1} resolution. At 10°C/min prepreg heating rate, each FTIR data file consisted of 9 scans, which took about 53 seconds. The average of these nine scans was stored and displayed in a file, providing the real time FTIR information in every 9°C rise. The FTIR temperature profile for the curing of AFR700B/T650-35 prepreg to 400°C at 10°C/min in N_2 is given in Figure 5. It showed peak rates of evolution of CH_3OH (1033 cm^{-1}), H_2O (3715 cm^{-1}), and cyclopentadiene (663 cm^{-1}) at 176, 180, and 360°C, respectively.

The MS data were generated by Thermolab's VG mass spectrometer at 70 eV. Figure 6 displays the corresponding MS temperature profile showing peak release rates of CH_3OH (m/e = 31 and 15), H_2O (m/e = 18), and cyclopentadiene (m/e = 66) to take place, at somewhat lower temperatures, at 150, 155, and 319°C, respectively. There was also a shoulder around 220 – 270°C for H_2O. Since the transit time for an off-gas to go from the TGA to the MS was in the order of milliseconds, MS provided a much closer on-line monitoring than FTIR. In the latter, two factors slowed down the monitoring process. The first was the residence time in the gas cell, which could amount to about 1.6 minutes for this 80 ml. gas cell at the 50 ml/min purge gas flow rate. Added to this gas cell residence time delay, another 53 sec was spent in the nine consecutive FTIR scans for data averaging and displaying. Thus, the FTIR could experience a time delay as large as 2.5 min, corresponding to a 25°C temperature lag at 10°C/min. A comparison of the MS and FTIR off-gas peak temperatures confirmed the existence of 25°C lag in the case of methanol and water. For cyclopentadiene, the peak temperature difference between MS and FTIR data was 41°C, which was greater than 25°C. Considering the fact that the FTIR peak temperature for cyclopentadiene was determined from a relatively broad peak, its determination would be less definitive, resulting in some uncertainty. It should be borne in mind that this temperature lag would vary with the heating rate, gas cell volume,

MONOMERS

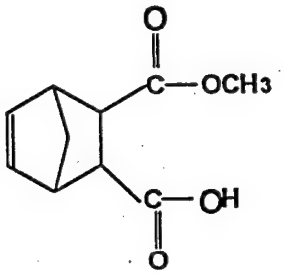

1 NE

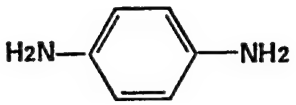

+9 PPDA

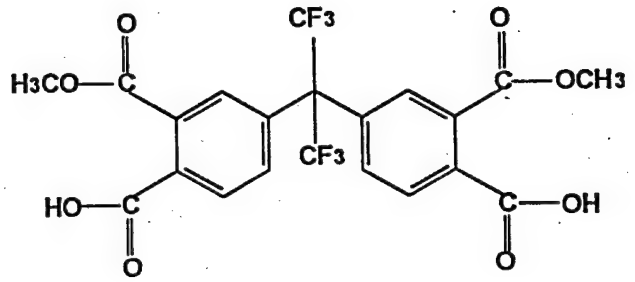

+8 6FDE

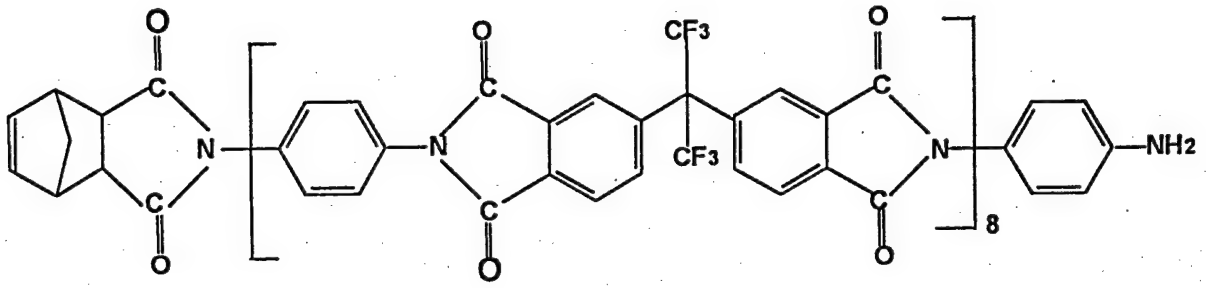

Figure 3 AFR700B Formulation

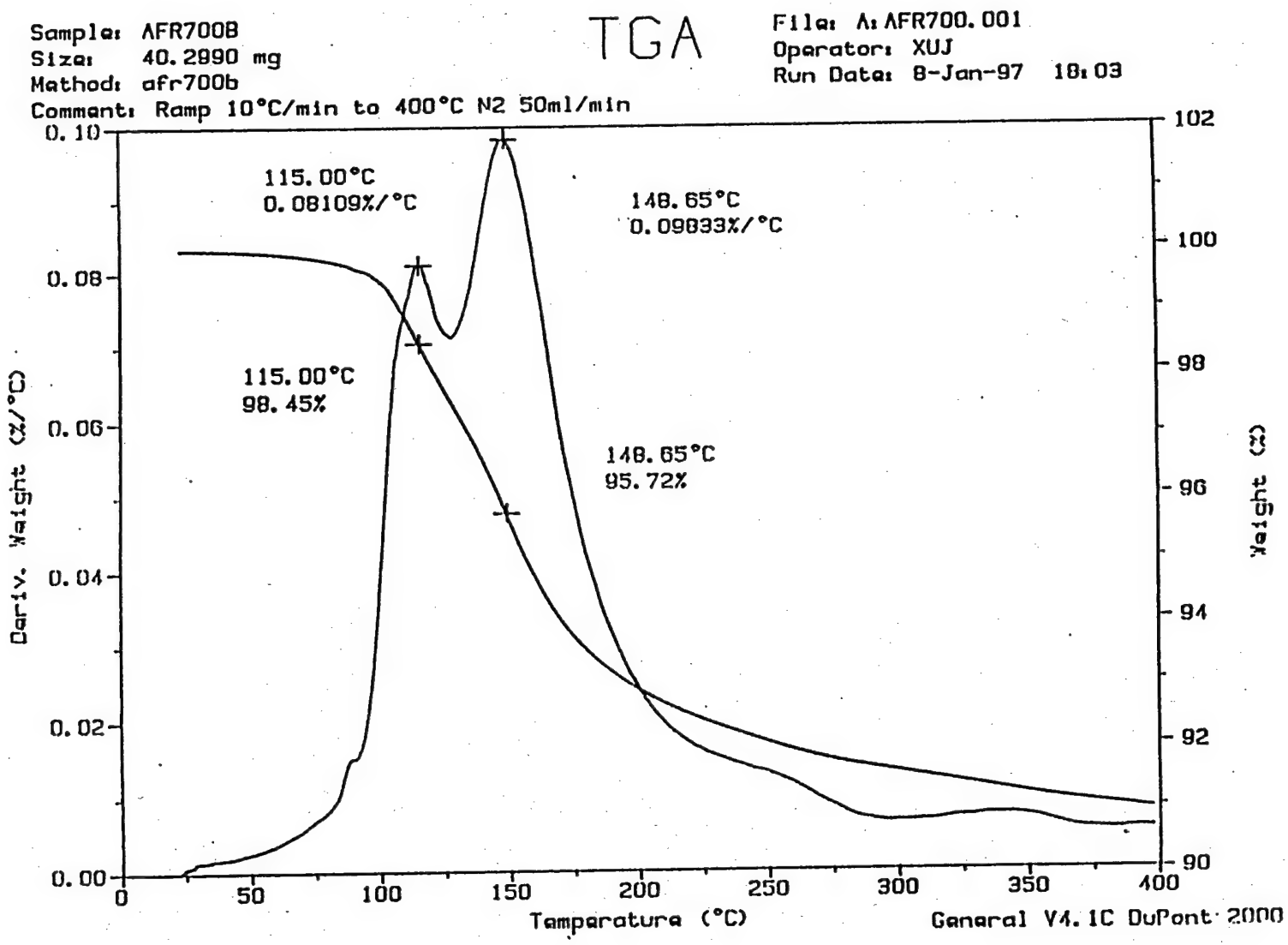

Figure 4 AFR700B/T650-35 Prepreg Weight Loss

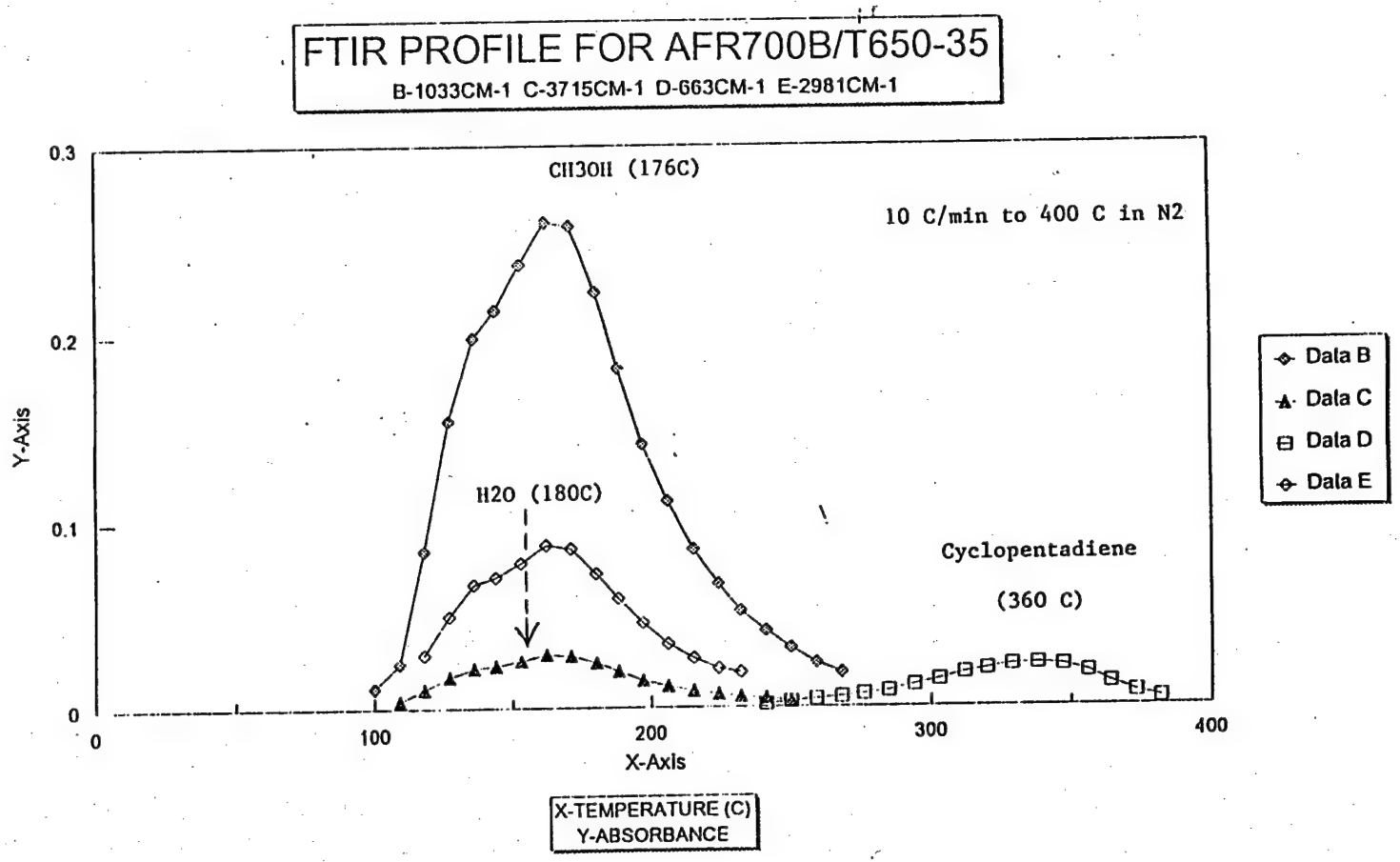

Figure 5 FTIR profile for AFR700B/T650-35 Prepreg

MS Profile for AFR700B/T650-35
at 10C/min in N2

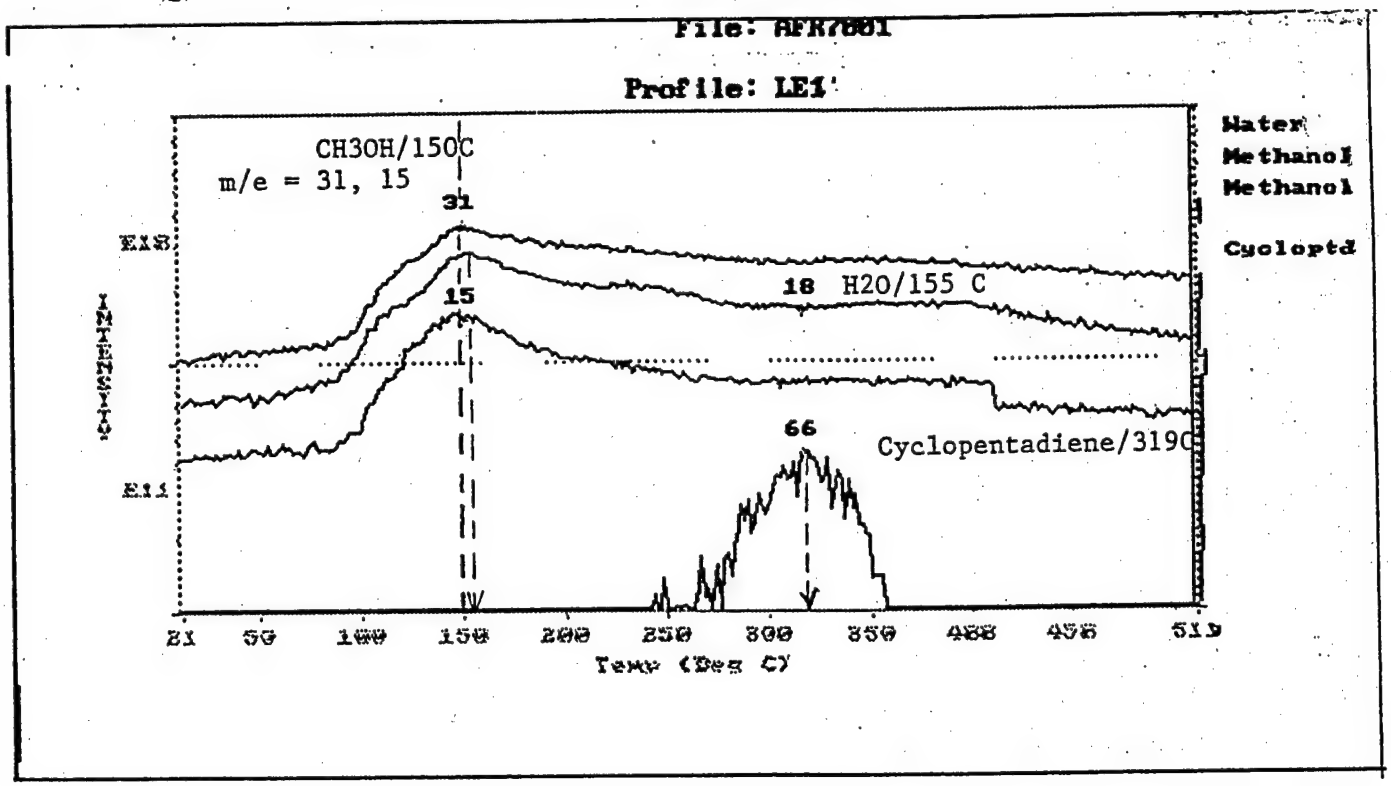

Figure 6 MS profile for AFR700B/T650-35 Prepreg

purge gas flow rate, and FTIR data acquisition rate. It is important to note that when the heating rate is small, the temperature lag is also small.

In general, one can say that the MS data furnished the closest real time cure reaction monitoring, which was also supported by the TGA weight loss rate data. The peak temperature for the AFR700B/T650-35 prepreg weight loss rate was found to be 149°C in the proximity of MS peak temperatures of 150 and 155°C, strongly suggesting the release of CH_3OH and H_2O accounted for the rapid weight loss around 149°C. Overall, these real time weight loss, FTIR, and MS data indicated that the evaporation of surface water and residual methanol solvent in the prepreg gave rise to a peak weight loss rate at 115°C. It was then followed by the evolution of methanol and water at 150°C, the continuing loss of water in 220 – 270°C, and the formation of cyclopentadiene at 320°C. It should be mentioned the detection of cyclopentadiene by TGA/FTIR/MS was possible because no applied pressure was used, in contrast to autoclave prepreg consolidation. When cyclopentadiene was formed via reverse Diels – Alder reaction[19], it was given off and detected. As a result, it would be difficult to verify the existence of reverse Diels – Alder reaction during prepreg autoclaving even if these TGA/FTIR and/or TGA/MS techniques are accessible.

The FTIR and MS data obtained can also be used to determine the onset temperature for the release of vapors and gases from a TGA curing run. These onset temperatures, of course, depended upon the detection threshold of the characteristic absorption bands. By and large, both methanol and water were given off at about 75 – 80°C, while the formation of cyclopentadiene started at about 245°C and ended at 355°C according to the MS data. FTIR indicated the ending of methanol evolution at approximately 270°C. For reasons unknown, it was difficult to ascertain the termination of water release from both FTIR and MS data.

A curing run of the AFR700B/T650-35 prepreg was also made in a DSC from ambient temperature to 400°C at 10°C/min in nitrogen at 50 ml/min to see if additional information could be obtained. The thermogram in Figure 7 exhibited a minor endotherm at 100°C, a major higher temperature endotherm at 142°C, and a broad exotherm from 165 to 325°C. The first endotherm appeared to be related to the evaporation of surface water. The second large endotherm might have come from the combined effect of methanol evaporation (endothermic) and amic-acid reaction (exothermic). The net result was endothermic due to the presence of a large amount of methanol solvent present in the prepreg. For this reason, the heat of formation for the amic-acid reaction could not be determined. Moreover, these DSC peak temperatures were fairly close to the TGA weight loss rate peak temperatures at 115 and 148°C lending partial support to the origin of these weight losses. Ensuing to the second large endotherm a broad exotherm starting at 165°C and extending to 325°C was noted. The heat given off by imidization and subsequent crosslinking might well be responsible for this broad exotherm. Its temperature range was certainly broad enough to cover those for both imidization and crosslinking.

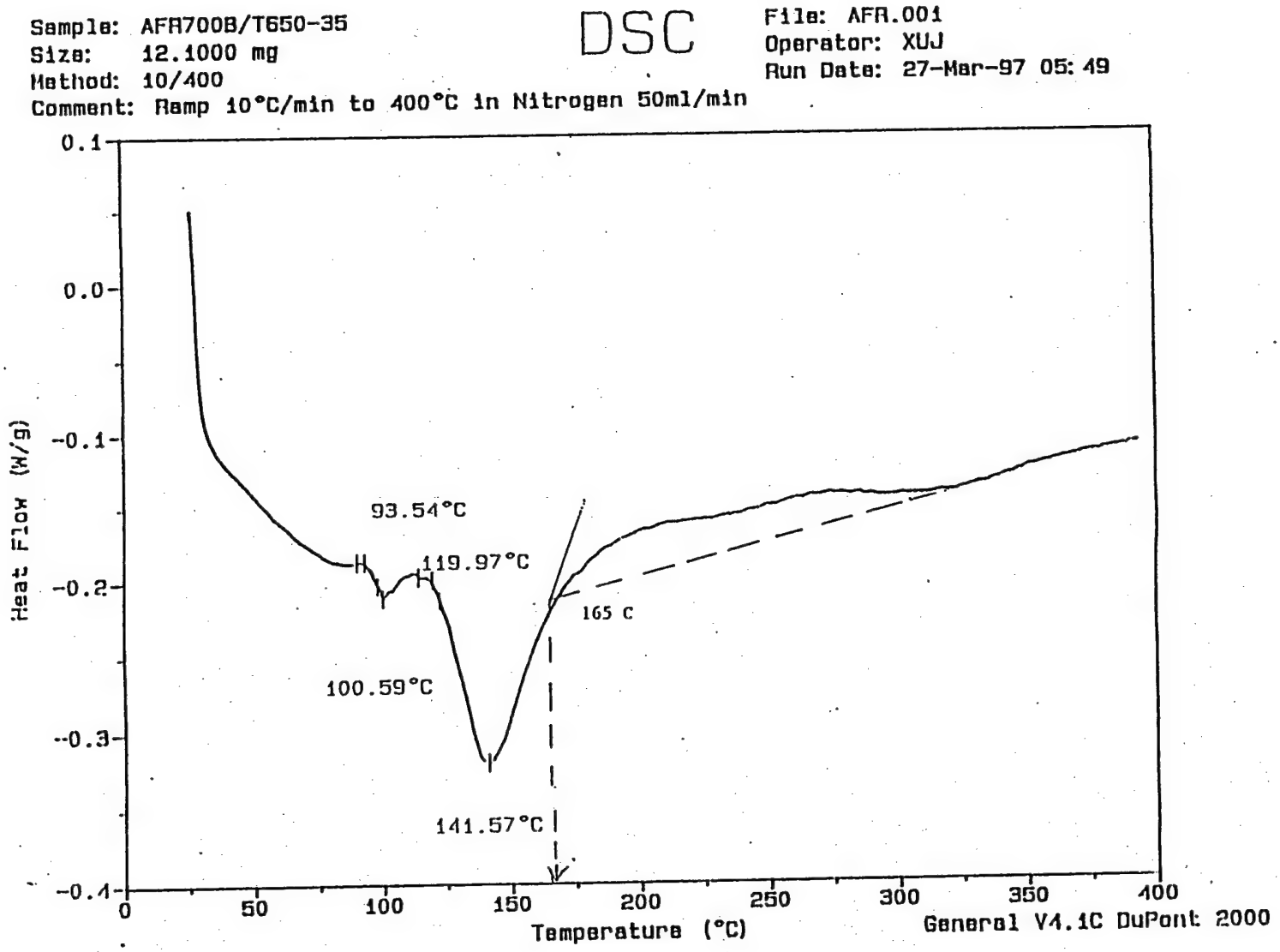

Figure 7 DSC for AFR700B/T650-35 Prepreg

The curing rate affected the peak release temperatures of methanol and water mainly due to thermal lag. As a result, at 3°C/min the water and methanol peak release temperatures moved toward lower temperatures. FTIR profile showed their occurrence at 128 and 130°C, respectively. Similarly, the MS profile gave rise to a methanol evolution peak temperature of 125°C and a peak temperature for cyclopentadiene formation at 314°C. Therefore, the prepreg heating rate exerted a dominating effect of the rate of gas evolution, which needed to be recognized. Although a single TGA 10°C/min ramp rate was, in general, used for expediency and curing temperature range finding, a slow heating rate comparable to commercial practice or better yet, a real cure schedule may be required to examine the actual curing chemistry involved.

Up to this point, the overall TGA/FTIR and TGA/MS results indicated that at 3°C/min the following curing chemistry paths for the AFR700/T650-35 prepreg:

1. the elimination of methanol through an amic-acid prepolymer formation at about 125°C;

2. the release of water from imidization at approximately 220°C;

3. the thermal crosslinking of polyimide at 314°C via a reverse Diels-Alder[19] reaction where cyclopentadiene was formed resulting in its detection in the absence of applied pressure in a TGA.

3.1.2 Curing of AFR700B/T650-35 Prepreg Using an Autoclave Schedule

The AFR700B/T650-35 prepreg was cured in TGA using General Electric Aircraft Engines autoclave cure schedule. It should be pointed out that due to equipment limitations, no application of vacuum and consolidation pressure was made. Thus, only the prepreg curing heat history was simulated. Furthermore, the slow cooling cycle during autoclave curing and its subsequent post-curing were eliminated in the interest of saving instrumentation use time. The absence of off-gas products during the cooling cycle and post-cure period was assumed. Hence, the use of TGA/FTIR and/or TGA/MS would not yield additional information anyway. The actual cure schedule[16] used for this processing chemistry study was as follows:

1. 1.1°C/min (2°F/min) to 221°C (430°F) from room temperature
2. 3 hour hold at 221°C (430°F)
3. 5.9°C/min (11°F/min) to 372°C (702°F)
4. 4 hour hold at 372°C (702°F)
5. cure in nitrogen at 50 ml/min.

Figures 8, 9, and 10 show the corresponding TGA weight loss, FTIR profile, and MS profile for this 10 hours plus curing run.

TGA weight loss data indicated a total weight loss of 9.66% at the end of the cure schedule. However, most of this weight loss took place in the first heating step from

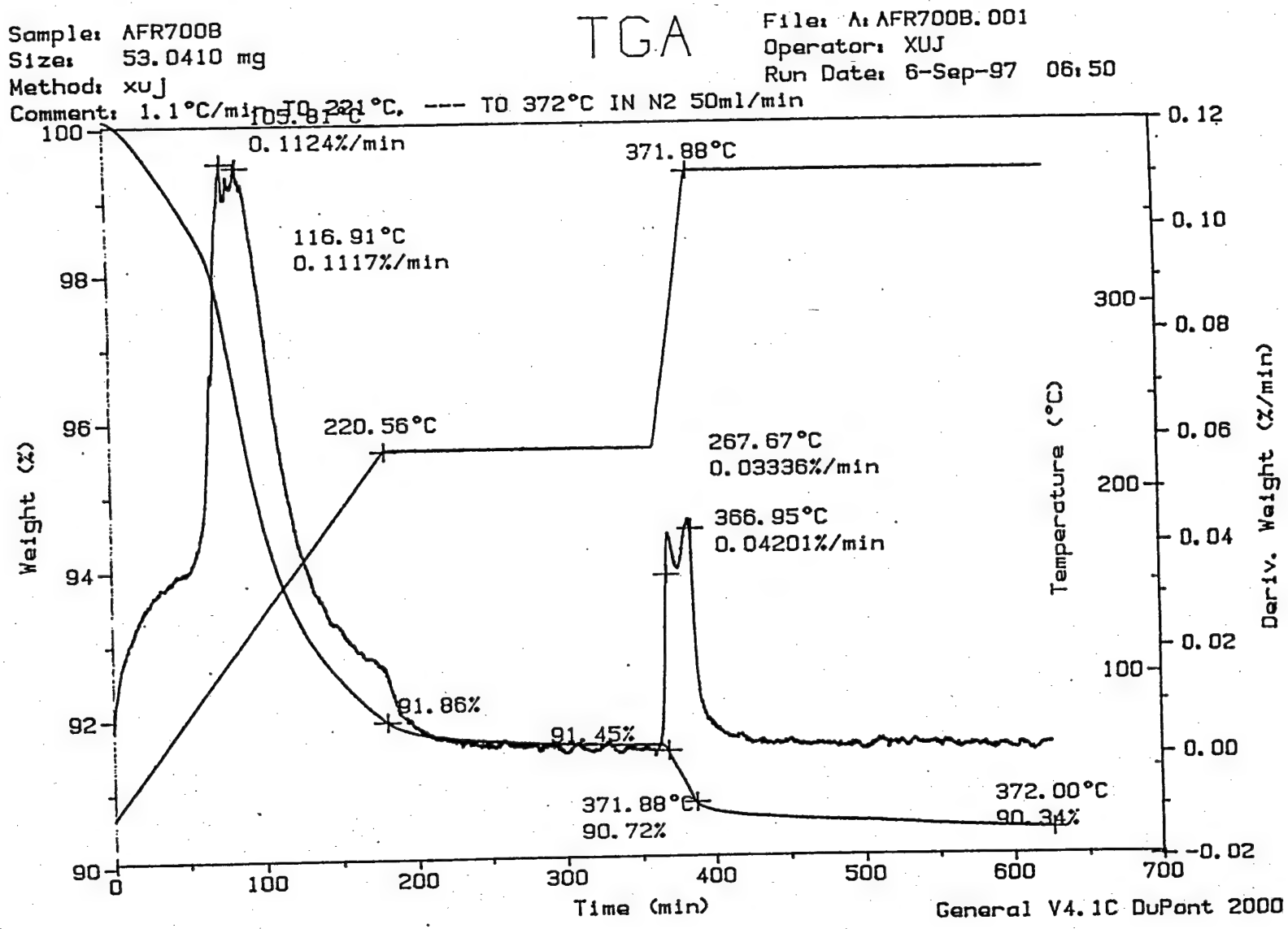

Figure 8 TGA Weight Loss of AFR700B/T650-35 Prepreg based on a Cure Schedule

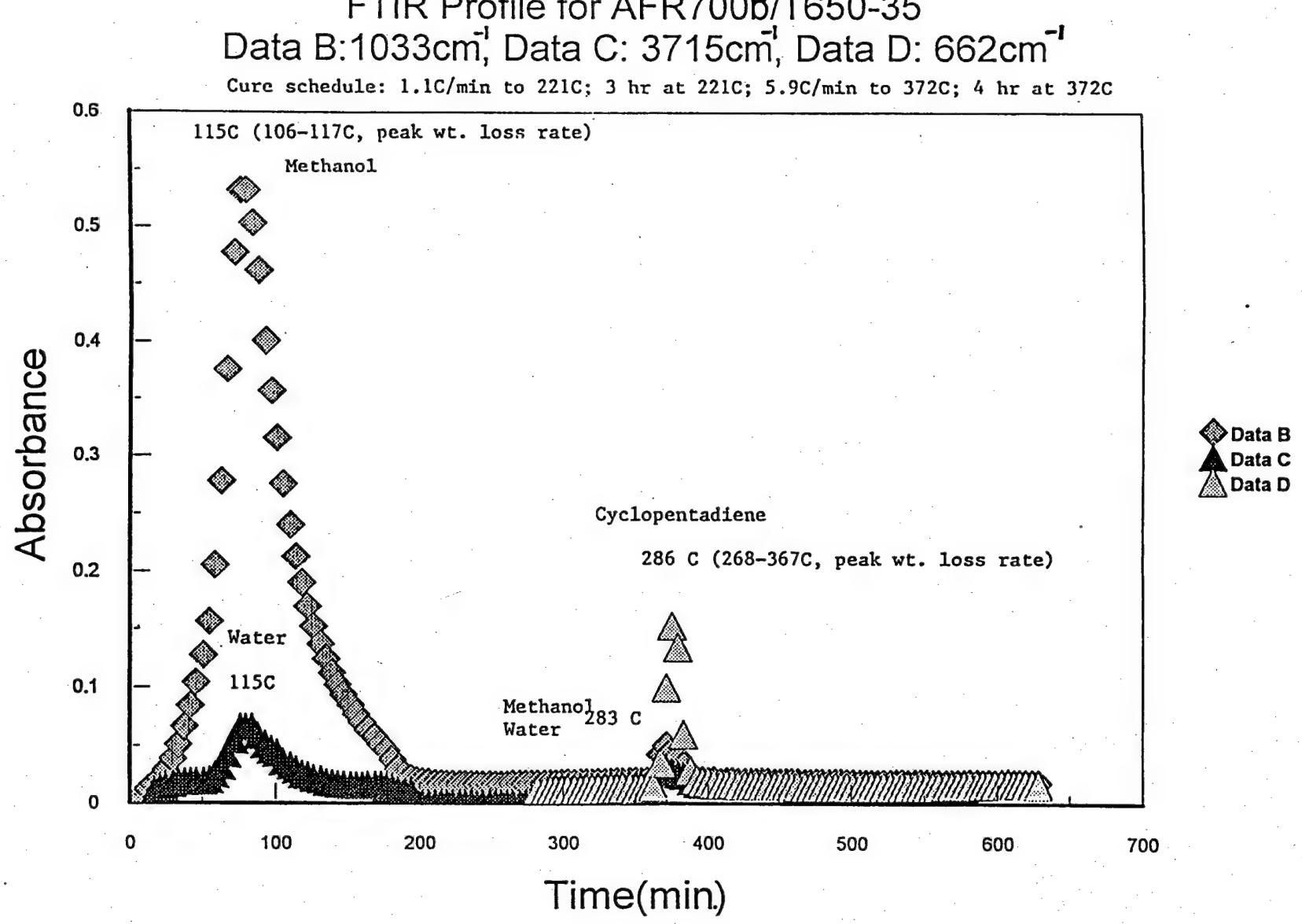

Figure 9 FTIR Profile of AFR700B/T650-35 Prepreg heated according to a Cure Schedule.

TGA/MS Profile for AFR700B Prepreg Cure Schedule

m/e = 18; Water

m/e = 15, 31; Methanol

m/e = 66; Cyclopentadiene

Cure Schedule: 1. 21-221C at 1.1C/min

2. 3 hr hold at 221C

3. 221-372C at 5.9C/min

4. 4 hr hold at 372C

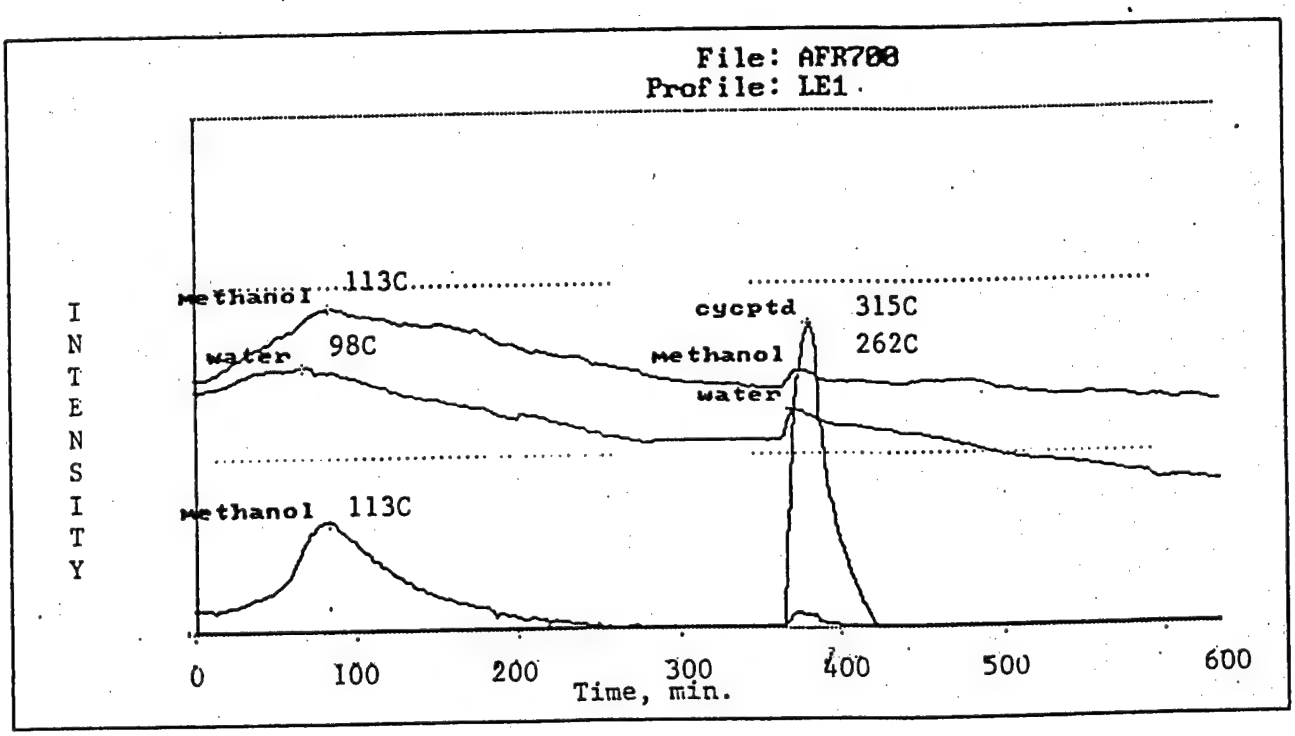

Figure 10 MS Profile of AFR700B/T650-35 Prepreg heated according to a Cure Schedule

room temperature to 430°F at 8.14%. Little weight change occurred during the 3 hours hold at 430°F. Then, the second heating stage from 430 to 702°F brought about another 0.73% weight loss. Thus, most off-gases should appear between room temperature and 430°F (221°C) with a small amount released between 221 and 372°C. It was also interesting to note that regardless of the TGA heating rate, the total prepreg weight loss was about the same. At 10°C/min to 400°C, the total weight loss was about 9.0% while heating at 3°C/min produced a total weight loss of 11.0% upon reaching 400°C. Since these total weight loss values were fairly close to the 9.7% weight loss from the long-time cure, it might be surmised that most of the off-gases had been released. This small difference in total weight loss might have come from the initial absorbed moisture and residual solvent present in the various prepreg samples used.

FTIR data showed the release of water and methanol peaked at 115°C shortly after curing started. This 115°C peak temperature lied within the 105 – 117°C peak temperature range for the TGA weight loss rate, thereby suggesting water and methanol to be the major off-gases from prepreg curing. Their releases tapered off when the prepreg reached 221°C (430°F). Therefore, for prepreg autoclaving the application of vacuum should be extended to 221°C to minimize bubble or void formation. A much smaller FTIR peak occurred for both water and methanol at 283°C (541°F). In addition, the loss of cyclopentadiene produced a FTIR peak at 286°C (547°F). All these events took place in the second heating stage from 221 to 372°C at 5.9°C/min. Two observations can be made:

1. the releases of methanol and water was not complete even after the 3 hours of hold at 221°C;

2. the presence of cyclopentadiene confirmed the crosslinking of AFR700B via a reverse Diels-Alder reaction[19].

Very little additional weight loss occurred after the second heating step, thereby suggesting that curing reactions and crosslinking were almost complete. In order to retain the cyclopentadiene formed in the prepreg for crosslinking, the application of pressure for part consolidation should be made after 221°C (430°F). The use of 430°F as the time for both vacuum cut-off and application of consolidation pressure, was, in fact, practiced by the industry for AFR700B prepreg autoclaving.

The MS profile showed similar results as the FTIR profile. The MS peak intensity temperatures differed slightly from the FTIR peak temperatures. If the formation[19] of amic-acid prepolymer (resulting in the release of methanol) followed by imidization (producing water) was complete by 221°C, the presence of second set of methanol and water peaks in FTIR and MS at higher temperatures was surprising. If these reactions were not complete, higher reaction temperatures (260 – 290°C) might be required to increase the polyimide mobility to advance the reactions further. If so, one would wish to know whether additional reactions could be advanced at even higher temperatures close to the top post-cure temperature of 750°F (399°C). To test this hypothesis, a longer and higher temperature cure of the AFR700B/T650-35 prepreg was

made in TGA/FTIR/MS by adding onto the above GE cure schedule a third heating step, also at 5.9°C/min, to 427°C (800°F). No additional methanol or water was detected suggesting that either the amic-acid prepolymer formation and imidization reaction had been completed below 427°C or additional reaction sequence not involving off-gas productions could still be taking place.

The close proximity of the FTIR and MS peak temperatures for methanol and water (Figures 9 and 10) has rendered the determination of this AFR700B prepreg curing reaction sequence somewhat difficult. There were seen in the 98 – 115°C range below 221°C and also, between 262 and 283°C above 221°C. Thus, it became less certain, at least based on the evolved gas study, if amic-acid prepolymer reaction with the elimination of methanol followed by imidization with the loss of water (Figure 11) and crosslinking by reverse Diels–Alder reaction or Michael addition reaction (Figure 12) was the preferred curing mechanism. It appeared that amide-ester formation with the loss of water followed by imidization with the loss of methanol (Figure 13) could fit the FTIR/MS as well. It should be pointed out that the latter would produce a prepolymer having a larger molecular weight (MW = 776 for amide-ester prepolymer vs. MW = 748 for amic-acid prepolymer) and thus, a higher viscosity for the subsequent imidization reaction to overcome. To resolve this curing reaction sequence uncertainty, independent investigative methods such as NMR[7] (hopefully in real time), isothermal GC/MS, etc. might be required.

The TGA/FTIR/MS data from the long-time cure schedule were compared to those made at 3°C/min and 10°C/min. Even though the various curing reaction steps, i.e., amic-acid prepolymer formation (or amide-ester formation) followed by imidization and crosslinking, were identified, their peak temperatures were different depending upon the heating rate and hence, the rate of cure. The larger the heating rates, the greater the peak reaction temperatures were. For instance, FTIR showed the initial release of methanol and water to be at 115°C for the long-time cure, 128 – 130°C for the 3°C/min heating rate and 176 – 180°C for the 10°C/min heating rate. Therefore, the use of test results obtained at large curing rates to draw conclusions should be made with caution.

In general, the prepreg for a polymer composite is stored in a freezer at sub-ambient temperature to minimize the advancement of curing reactions. In this study, the AFR700B/T650-35 prepreg was kept in a freezer at –12°C (10°F). To determine its storage lifetime, TGA/FTIR/MS measurements were made at different time intervals. In three cure-schedule runs, the effects of freezer storage for 3 and 9 months were checked. The evolved gas analysis indicated that a smaller amount of off-gases was detected at 221°C (430°F) with increasing prepreg freezer storage time. But, the other features relating to the release of methanol, water, and cyclopentadiene remained essentially the same. Thus, little 10°F freezer storage effect was noted up to 9 months.

3.1.3 Short-time Curing of Larc RP46/IM7 Prepreg

The curing of RP46/IM7 prepreg in nitrogen was examined by TGA/FTIR and

AFR700B Monomers

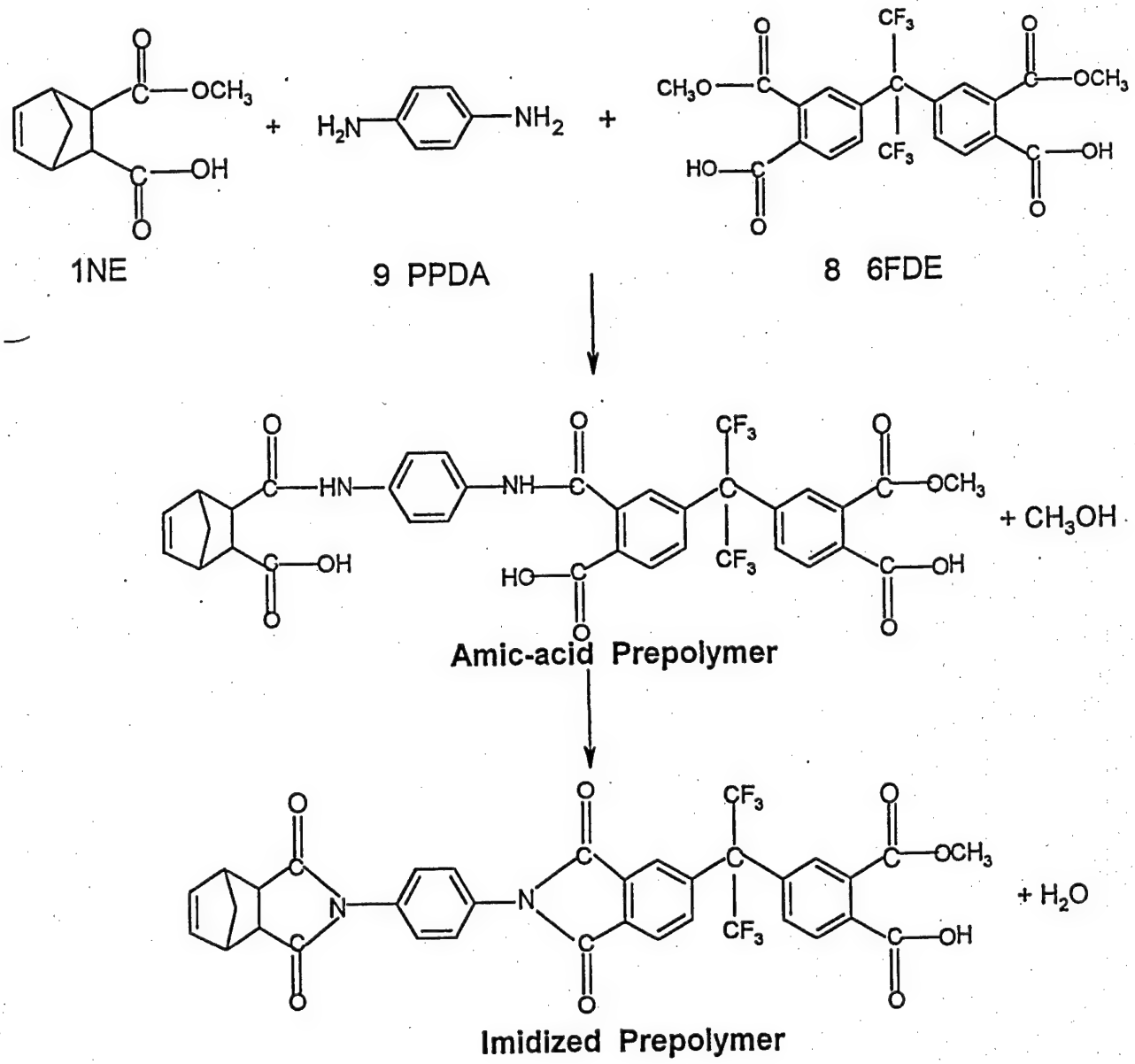

Figure 11 Literature[19] AFR700B Cure Reaction Sequence

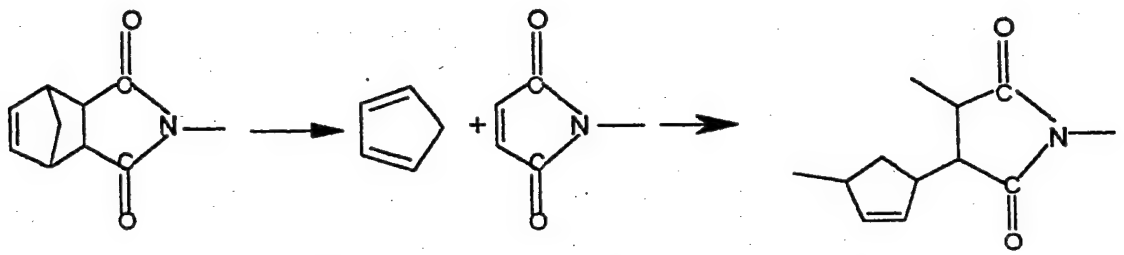

Crosslinking via the reverse Diels-Alder reaction

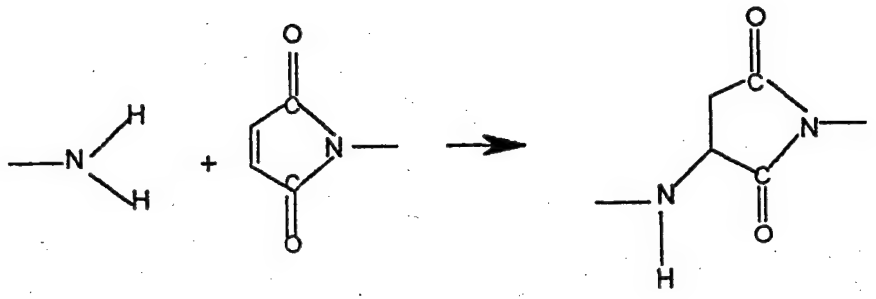

Michael addition reaction

Figure 12 Literature[19] AFR700B Crosslinking during Cure

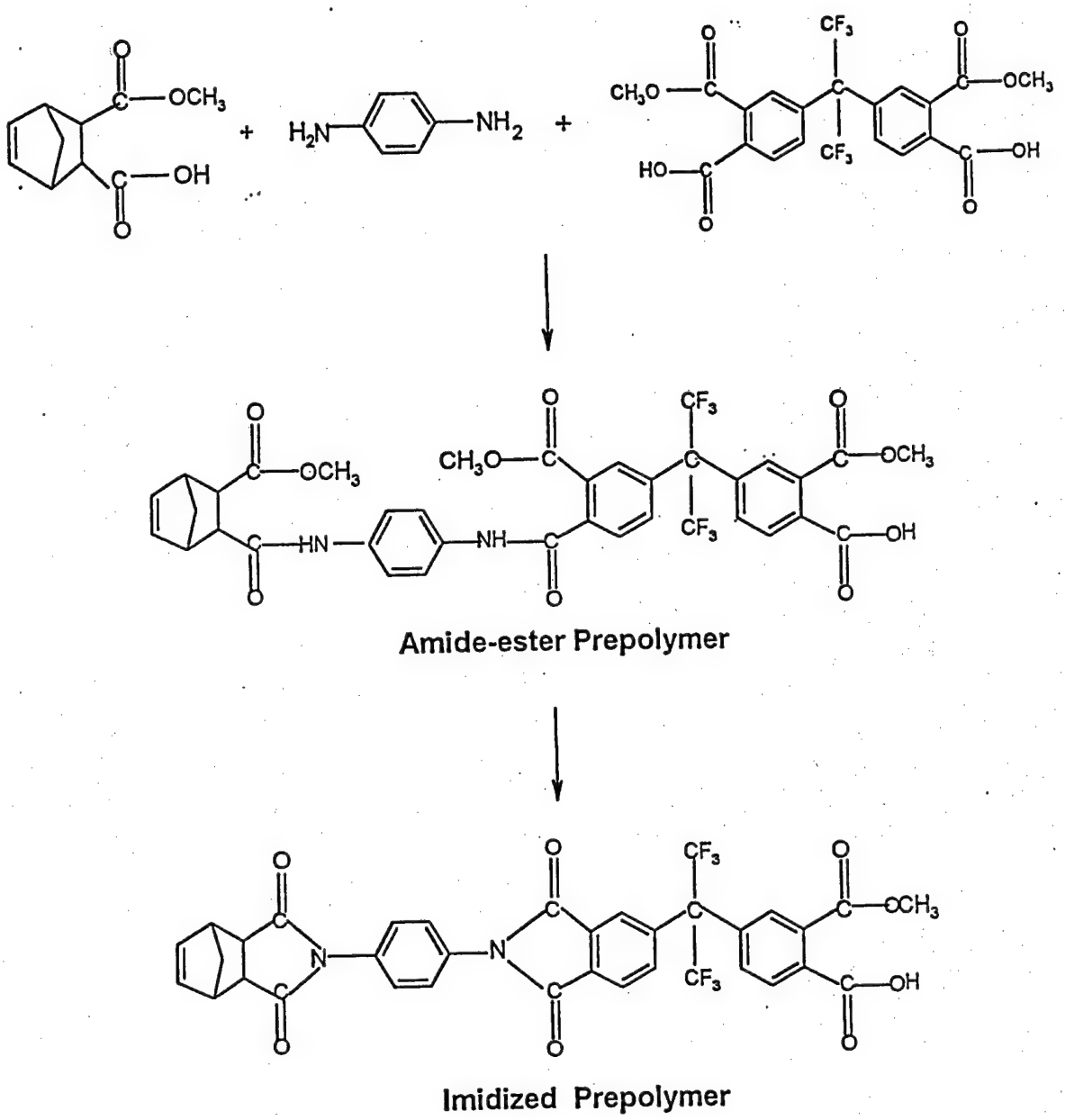

Figure 13 Alternative[19] AFR700B Cure Reaction Sequence

TGA/MS from room temperature to 400°C at 10°/min. The monomer reactants for RP46 were NE, the monomethyl ester of 5-norbornene-2,3-dicarboxylic acid; 3,4'-ODA, 3,4'-oxydianiline; and BTDE, dimethyl ester of 3,3,4,4'-benzophenonetetracarboxylic acid. Figure 14 displayed its formulation. The prepreg was produced with the reinforcement of IM7, an intermediate modulus carbon fiber. The research group[20] at NASA Langley Research Center proposed the following reaction steps:

1. the formation of pre-imidized prepolymer by the elimination of methanol and water at 150 - 200°C;

2. an endo-exo isomerization of the imide prepolymer at 200 – 250°C;

3. subsequently, thermal crosslinking around 316 – 325°C.

The TGA weight loss data in Figure 15 exhibited a major weight loss rate peak at 138°C, a weak shoulder at 230°C, and a minor peak at 338°C. Again, the total weight loss at 400°C was about 9.5%, similar to that seen in the AFR700B/T650-35 prepreg. It seemed to indicate that as long as the monomer functional groups remained the same, they would undergo similar reaction sequences, thereby giving off the same off-gas products. A DSC run was made under identical experimental conditions as the TGA run. Figure 16 showed its thermogram. Its main features displayed an endothermic peak at 138°C, a broad exotherm between 165 and 325°C, and an exotherm at 342°C. The endothermic peak temperature was, in fact, identical to the first weight loss rate peak temperature of 138°C, strongly suggesting the release of water and methanol vapors. The exotherm at 342°C corresponded to the TGA peak temperature at 338°C.

The FTIR profiles for the RP46/IM7 prepreg was depicted in Figure 17 showing a peak temperature of 162°C for both methanol and water release. The peak temperature for cyclopentadiene formation occurred at 356°C. Applying the 25°C thermal lag due to the FTIR gas cell residence time and signal averaging, these two peak temperatures became 137°C (= 162 – 25) and 331°C (= 354 – 25), very close to the TGA weight loss rate peaks at 138 and 338°C, respectively. Thus, the evolution of methanol and water was responsible for the first TGA weight loss rate peak and the DSC endotherm while cyclopentadiene formation was accountable to the last TGA weight loss rate peak and DSC exotherm. The corresponding MS profiles (Figure 18) exhibited a peak at 140°C for methanol based on the m/e = 15 intensity data. The intensity for water at m/e = 18 was very broad and thus, difficult to determine its peak temperature. The peak temperature for cyclopentadiene at m/e = 66 was found to be 342°C, not too far from the thermal lag corrected FTIR peak temperature of 331°C.

When the TGA weight loss data, the DSC thermogram, the FTIR profile, and the MS profile were taken into account in total, they supported one another and were useful to impart important curing chemistry. In the case of RP46/IM7 prepreg curing, the overall analysis seemed to suggest:

1. the release of methanol and water between 100 and 280°C with a peak at 138 -

MONOMERS

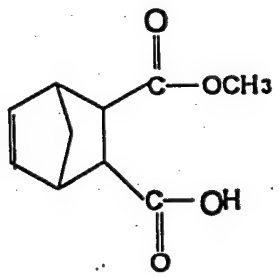

2 NE

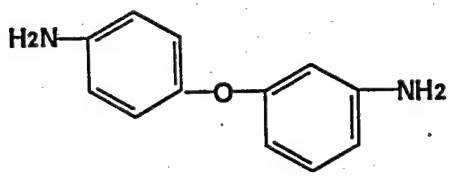

3.087 3,4'-ODA

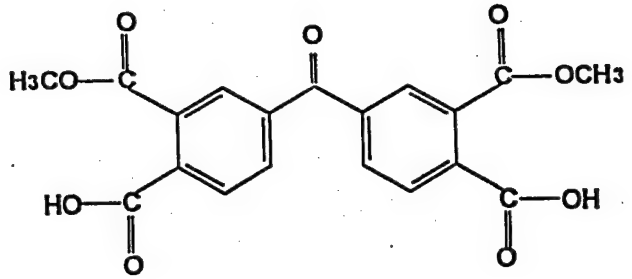

2.087 BTDE

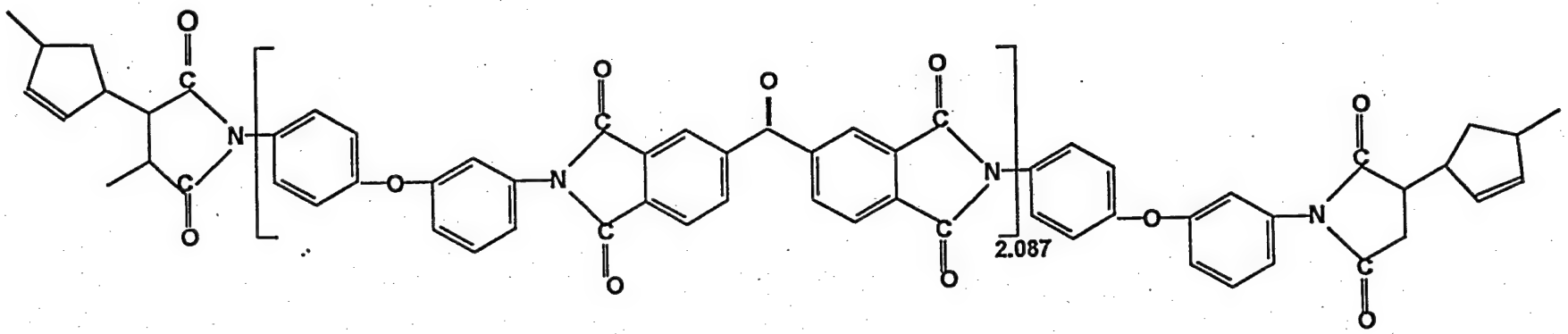

Figure 14 LARC® RP46 Formulation

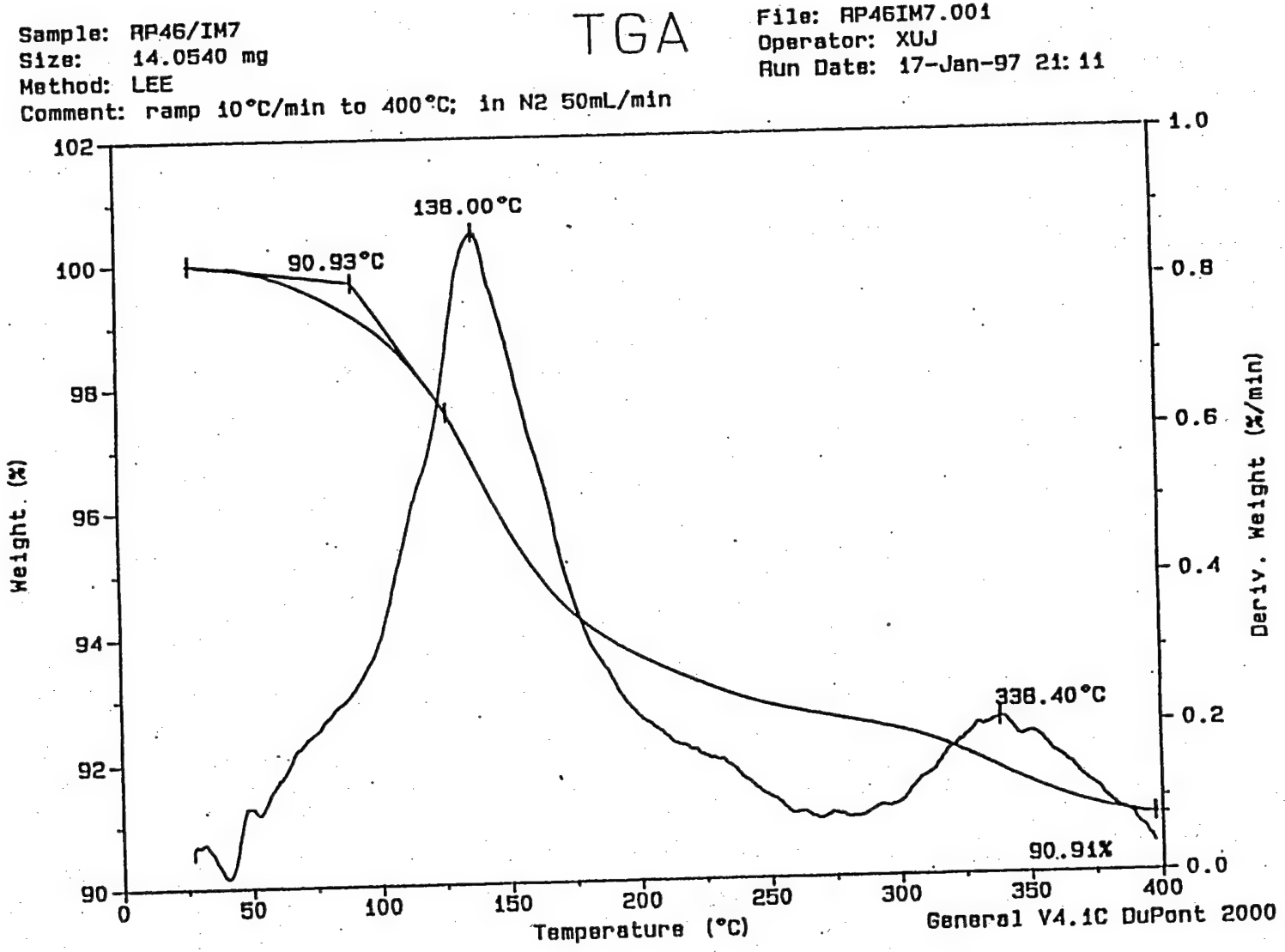

Figure 15 TGA Weight Loss of RP46/IM7 Prepreg

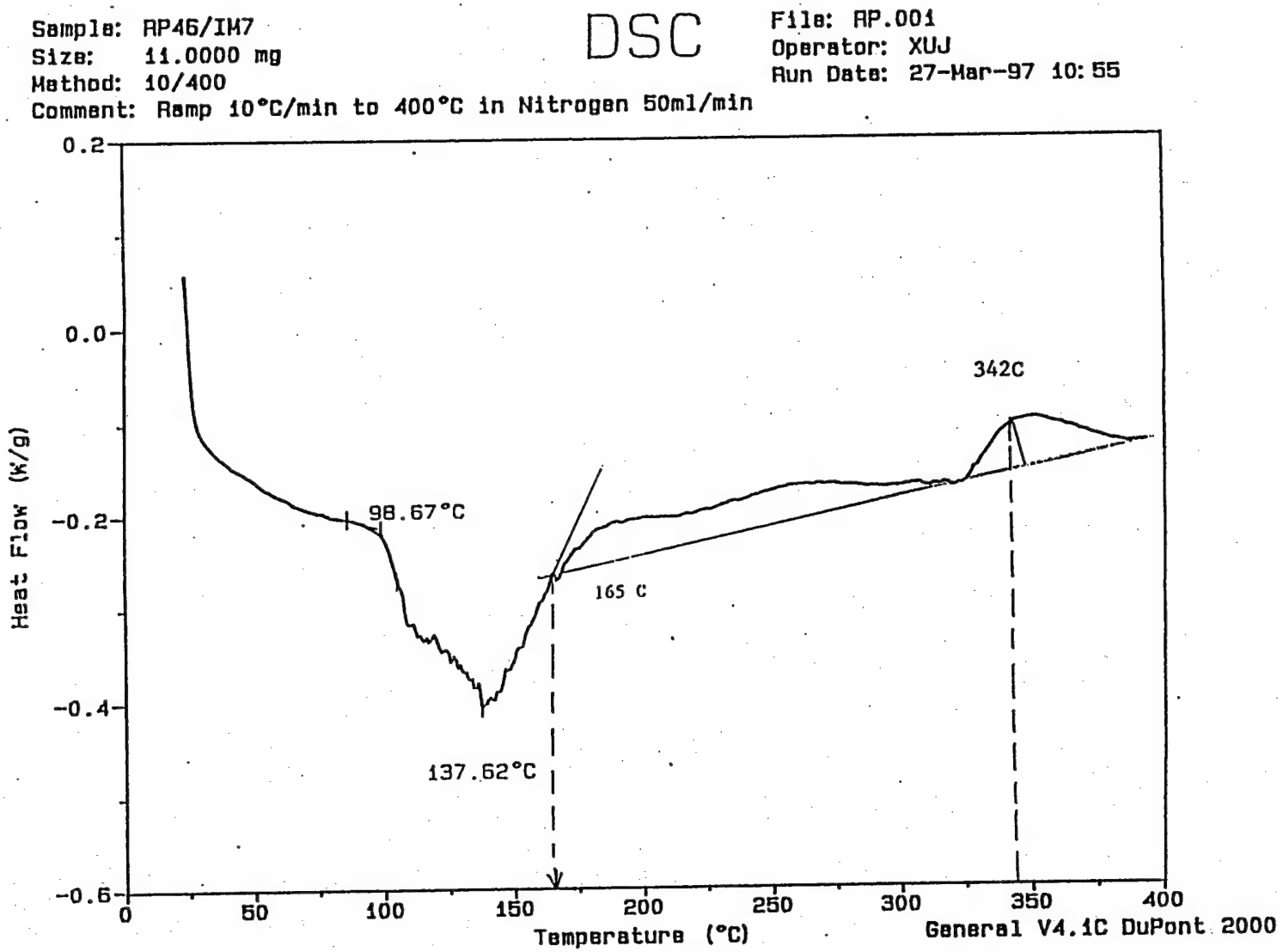

Figure 16 DSC Thermogram of RP46/IM7 Prepreg

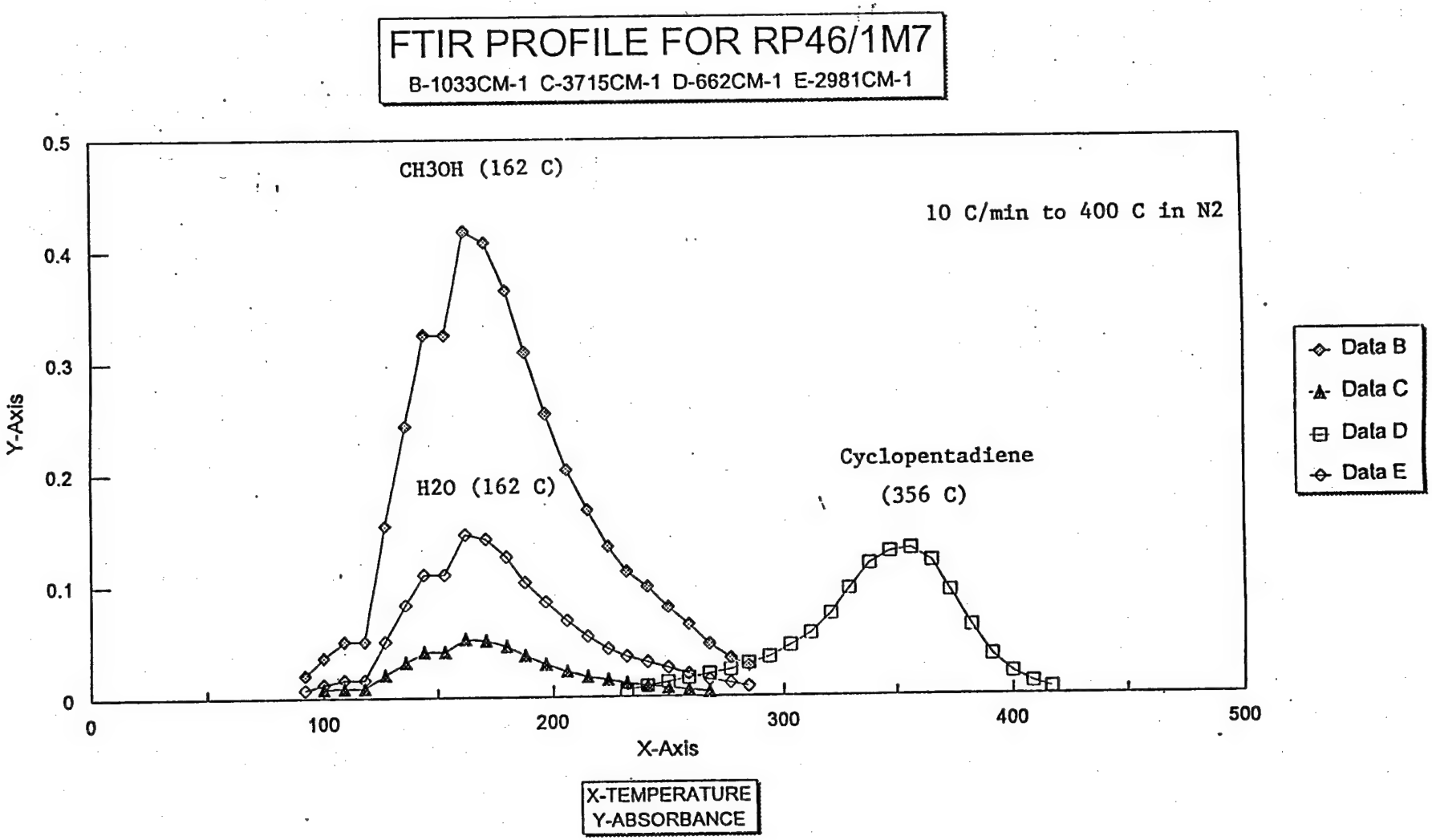

Figure 17 FTIR Profile of RP46/IM7 Prepreg

Mass Profile for RP/IM7 at 10C/min in N2

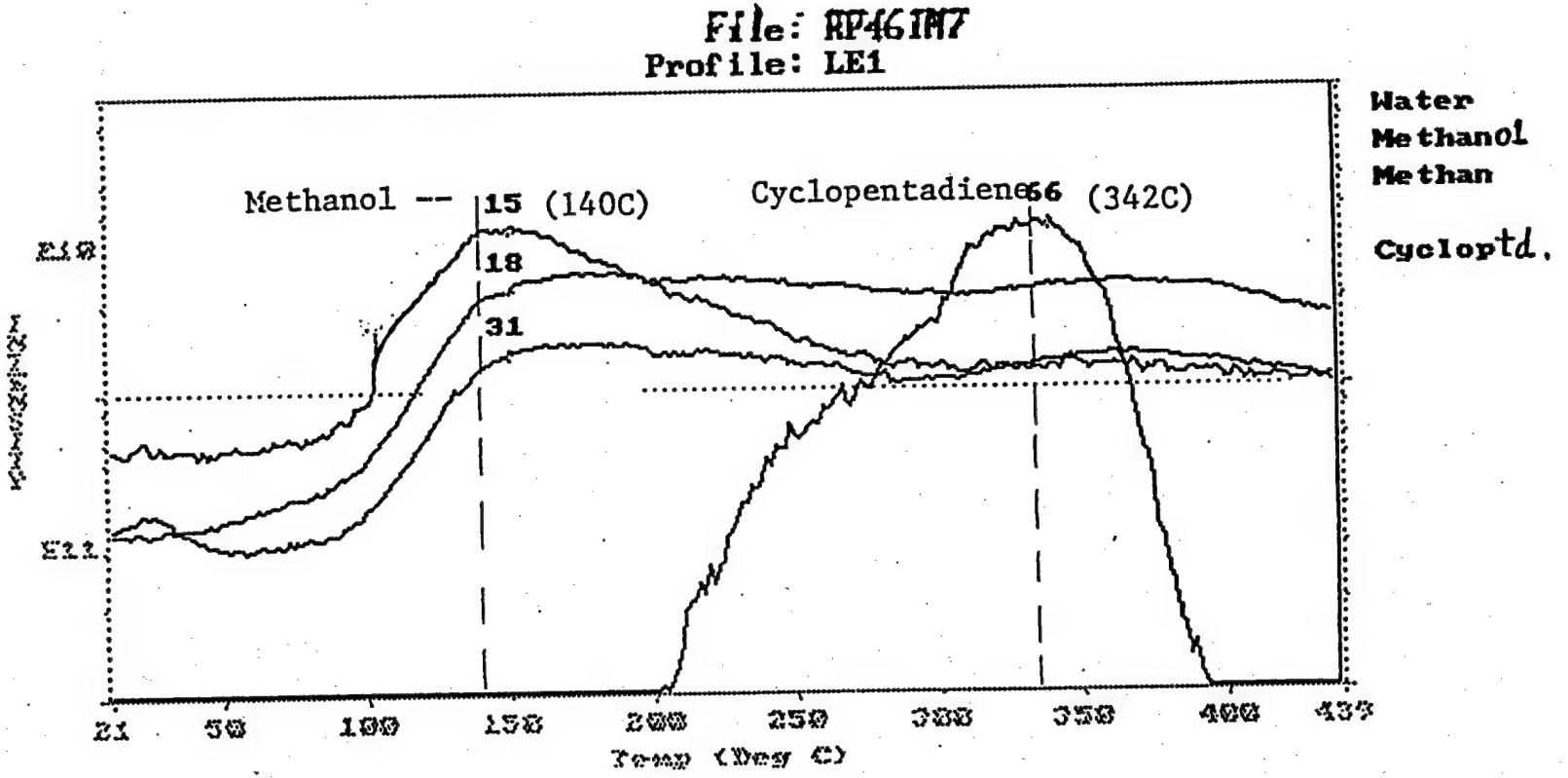

Figure 18 MS Profile of RP46/IM7 Prepreg

140°C for both indicating the loss of absorbed moisture and residual methanol as well as that from the formation of imidized prepolymer;

2. the formation of cyclopentadiene between 200 and 400°C having a peak in 310 - 350°C range.

Thus, the prepolymerization and thermal crosslinking reaction sequence proposed by the NASA Larc group was confirmed by this real time evolved gas analysis. They essentially followed the curing reaction paths for the AFR700B/T650-35 prepreg. It should, however, be pointed out that this evolved gas analysis was not capable of probing the endo-exo isomerism reaction because no off-gases were generated and given off.

3.1.4 Short-time Curing of VCAP-75/Glass Fiber Prepreg

Even though a 6F polyimide as AFR700B, VCAP-75 (Figure 19) has a different set of end groups. It was formulated in methanol with (n + 1) moles of HFDE, di-methylester of 4,4'hexafluoroisopropylidene bisphthalic acid; n moles of PPDA, para-phenylenediamine; and 2 moles of PAS, para-aminostyrene; where n = 14. VCAP-75 was capped with a vinyl group at both ends. Due to this end capping, its crosslinking did not involve the reverse Dield-Alder reaction. Hence, no cyclopentadiene would be detected.

A short time curing run of VCAP-75/Glass Fiber prepreg was made in TGA at 10°C/min from room temperature to 400°C in nitrogen at 50 ml/min. Its TGA weight loss rate (Figure 20) exhibited a peak at 149°C, almost identical to that for AFR700B/T650-35. There was a distinct shoulder between 180 and 225°C. At about 300°C, there was another minor shoulder. The first peak at 149°C was probably related to the evolution of methanol and water. The large shoulder was believed to be due to the release of water. At the end of curing run, this prepreg lost a total of 10.3% of its weight, fairly close to that from AFR700B/T650-35 at 9.0% and RP46/IM7 at 9.0%.

Figure 21 depicted the thermogram of VCAP-75/Glass Fiber, also obtained at 10°C/min in nitrogen. Its major features were a large endotherm having a peak temperature of 142°C with a tailing shoulder extending to about 240°C. This thermogram resembled the weight loss rate curve well. Furthermore, their first peak temperatures (142 vs. 149°C) were fairly close to each other. The tailing shoulders also extended out to similar ending temperatures (240 vs. 225°C). The evaporation of methanol and water was mainly the source of its large endotherm. Due to the large amount of water produced (n = 14 for the repeating backbone structure) from condensation reaction, the large heat of evaporation would overtake its heat of reaction, thereby resulting as a tailing shoulder of the endotherm. As a result, no exotherm was observed in the DSC thermogram.

The FTIR profile of VCAP-75/Glass Fiber prepreg shown in Figure 22 displayed a 171°C peak temperature for methanol as well as water. Taking into account the 25°C thermal lag inherent in the collection of FTIR data at 10°C/min, the "real" peak

MONOMERS

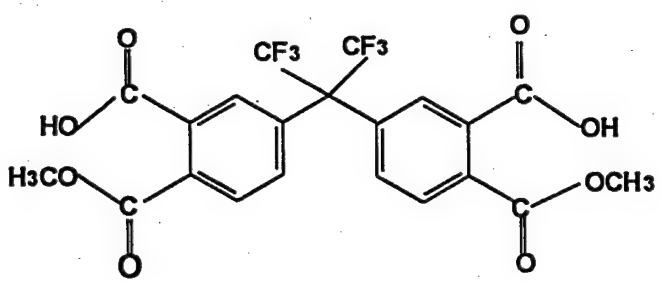

(n+1) HFDE

n PPDA

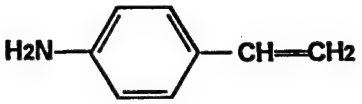

2 PAS

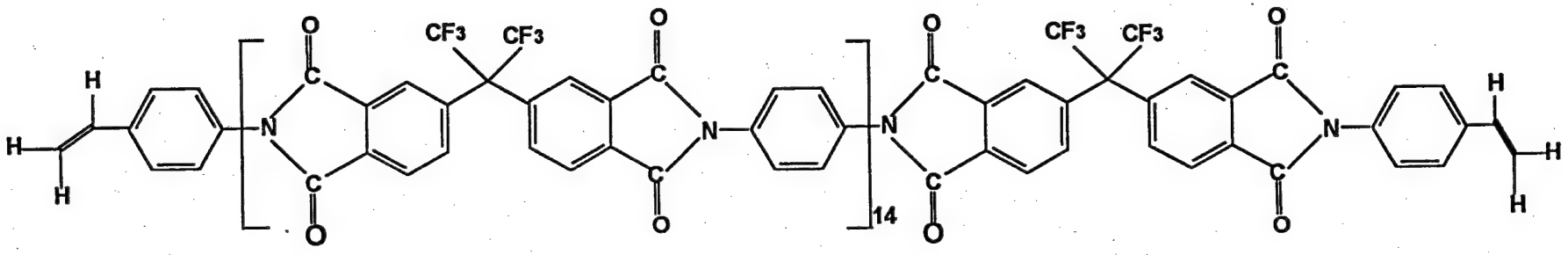

Figure 19 VCAP-75 Formulation

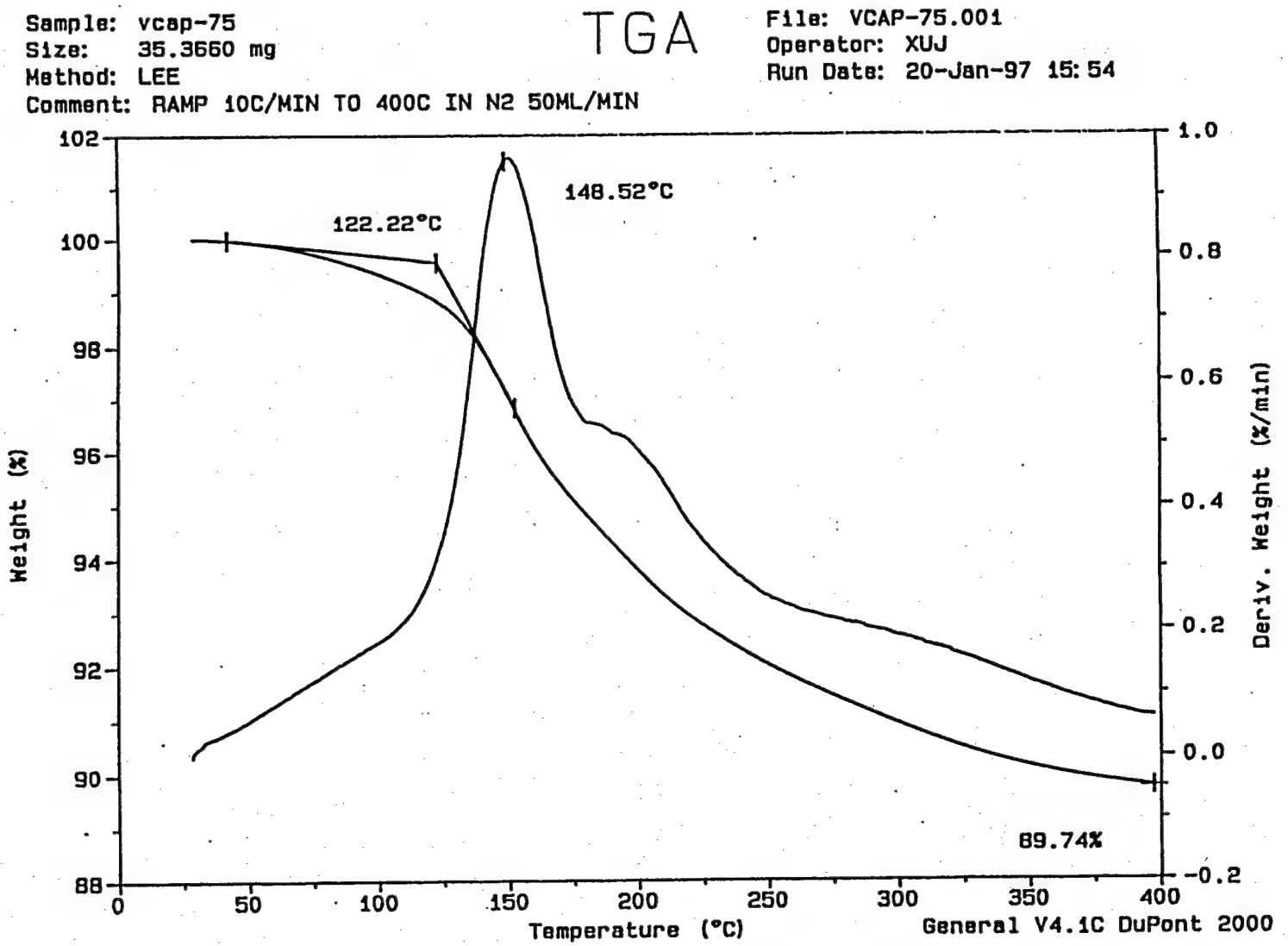

Figure 20 TGA Weight Loss of VCAP-75/Glass Fiber Prepreg

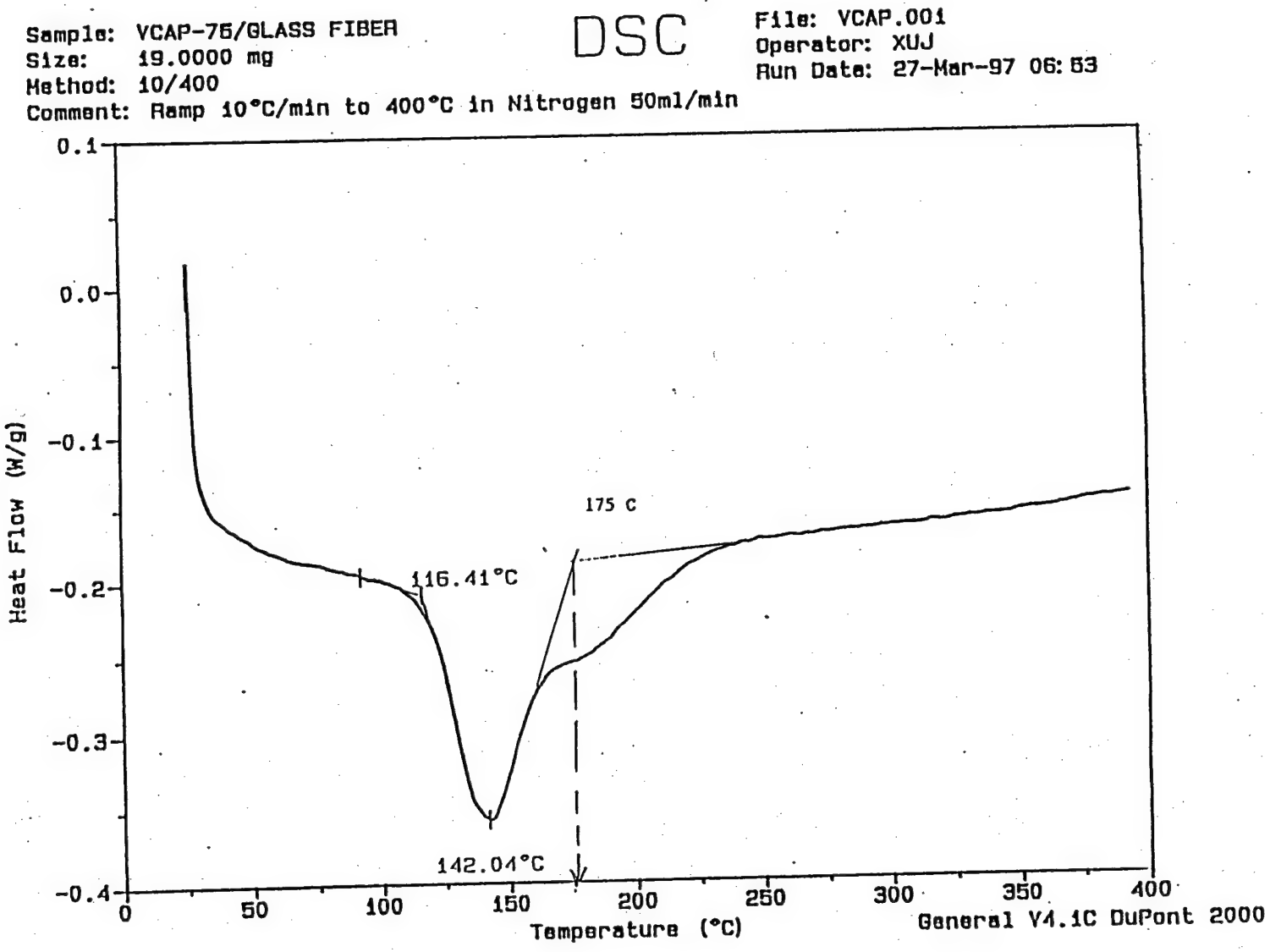

Figure 21 DSC for VCAP-75/Glass Fiber Prepreg

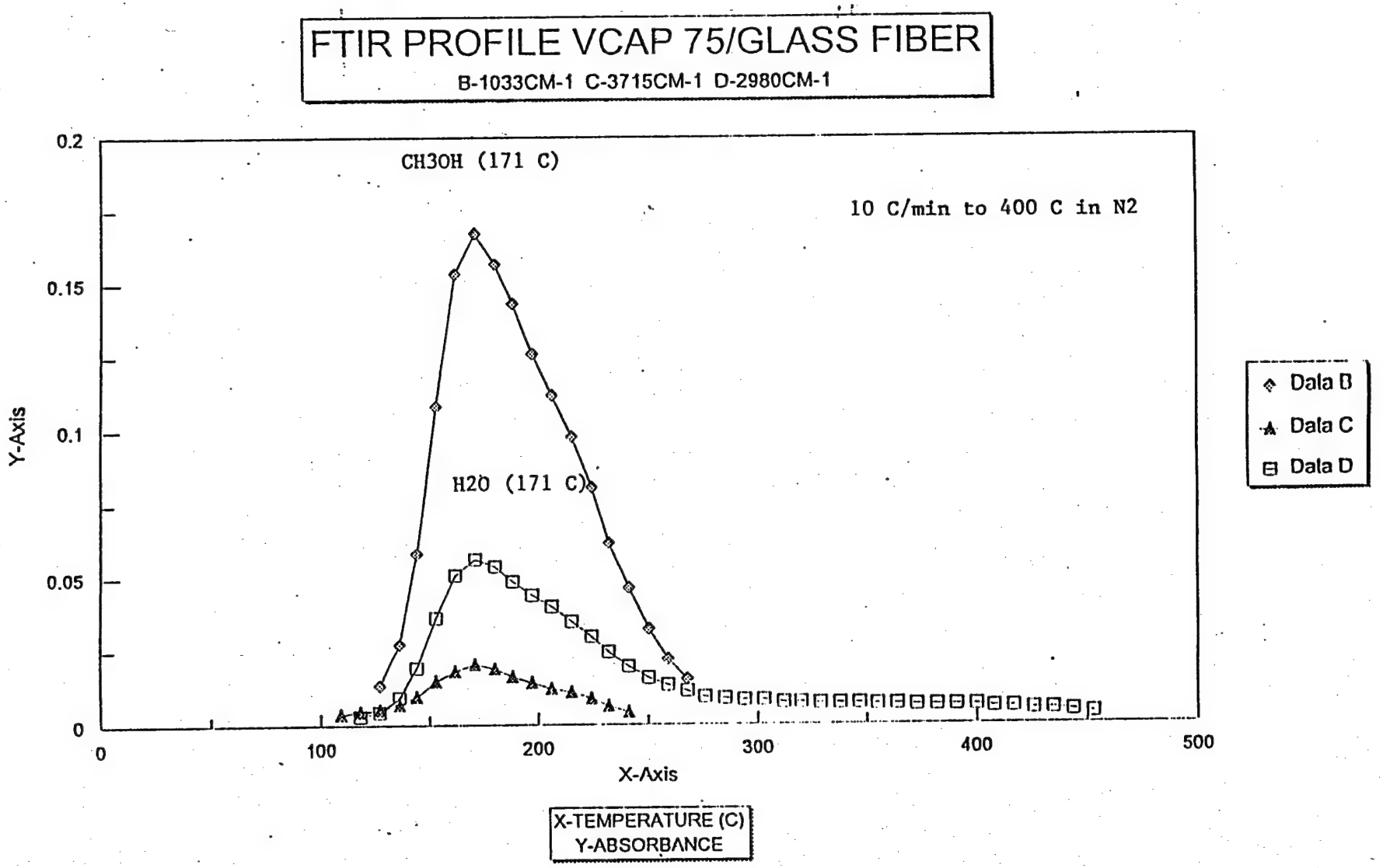

Figure 22 FTIR Profile for VCAP-75/Glass Fiber Prepreg

temperature for these two off-gases was 146°C (171 – 25 = 146) which was not too different from the 149°C peak temperature for its weight loss rate. Hence, the evolution of both methanol and water definitely made up the major portion of this weight loss rate peak. Again, the identical peak temperature of 146°C for both methanol and water made the assignment of imidization prepolymer reaction sequence difficult. They could fit either an amic acid formation/imidization reaction path or an amide-ester formation/imidization curing sequence. The FTIR profile for water covered a temperature range of 110 and 240°C having a nominal peak temperature at 171°C. Between 200 and 240°C, its water absorption intensity appeared to have leveled out slightly resulting in a minor shoulder. This shoulder might have derived from the imidization reaction releasing condensation water in the process. No cyclopentadiene as m/e = 66, 65, etc. was detected by MS, which was consistent with its end capping chemistry.

3.1.5 Summary on Curing Chemistry Study

Overall, the in-situ monitoring of the major curing reactions involved in a high temperature polyimide by using TGA/FTIR and TGA/MS has been successfully demonstrated. It should be noted that both techniques might involve some thermal lag depending upon the TGA heating rate. Moreover, the TGA/FTIR technique could result in some thermal lag due to the way FTIR data were collected in the gas cell and displayed. Therefore, whenever applicable, TGA/MS would be the preferred technique for real time monitoring.

In essence, the thermal curing of polyimides studied proceeded in the following fashion:

1. the elimination of methanol from amic-acid prepolymer formation
2. the release of water from subsequent imidization
3. finally, thermal crosslinking.

These polyimide curing reaction steps are in agreement with the literature. However, the FTIR/MS data obtained could also accommodate the alternative that the elimination of water from amide-ester formation was followed by the release of methanol from subsequent imidization. When a NE end capping monomer was used, cyclopentadiene was detected, thereby confirming the contention that final crosslinking proceeded through a reverse Diels-Alder reaction.

It should be pointed out that the TGA/FTIR and TGA/MS techniques had their limitations. They could be used only to monitor reactions, which gave off vapors and gases. Consequently, they would not be able to probe into reaction sequence, which no off-gas was produced. Thus, in the case of polyimide cure, ring opening reaction, endo-exo isomerization, and those thermal crooslinking reactions not involving cyclopentadiene formation would evade detection. A possible in-situ monitoring of those reactions could be the use of a temperature programmable conventional FTIR or a FTIR microscope. Even so, one should exercise cautions to vent the off-gas products. If these

off-gas products are detected, their gas phase FTIR may interfere with the FTIR signals of the reacting mass left behind. For instance, water vapor in its gas form possesses mainly two groups of IR bands[21], one in 3500 – 3900 cm^{-1}, and another in 1300 – 1900 cm^{-1} (see Figures 23 – a, b, c, d). The latter IR broad band covers the many carbonyl IR bands important to the conversion of acid or ester type of carbonyl functional group into an imide carbonyl. The reason that water vapor has so many characteristic IR bands is, of course, due to its many rotational freedoms as a gas. By the token, methanol as a vapor also has many IR bands (Figure 24 – a, b) derived from its rotational characteristics.

In the present study, the cure chemistry of three high temperature polyimides was examined in a prepreg form using TGA/FTIR and TGA/MS evolved gas analysis techniques. Therefore, the effects of the reinforcing fiber, if any, had been included. This approach was taken to simulate autoclave curing as close as possible. Because of it, the determination of the temperature and time for off-gas productions can be translated into autoclaving process control, i.e., vacuum application should be continued until the off-gases were gone and then, followed with consolidation pressure application. But, at the same time the cure of the reactive monomers in the absence of reinforcement can not be separated out completely. Since the resulting polyimide cure reaction mechanism did match the literature cure chemistry on neat resins, their essential features would have been determined. Most importantly, they had been established in "real time."

3.2 AFR700B/T650-35 Composite Stability Study

3.2.1 TGA Weight Loss

GE Aircraft Engines provided the post-cured AFR700B/T650-35 composite. Its glass transition temperature measured by TMA in air at 10°C/min was 417°C (783°F), as shown in Figure 25. Its thermal stability was determined in nitrogen from room temperature to 600°C at 10°C/min while its oxidative stability was studied in air at both 5 and 10°C/min. Evolved gas analysis was carried out with TGA/FTIR as well as TGA/MS. The purge gas flow rate used was 50 ml/min. It should be noted that for this stability study, powdered samples obtained by filing of the AFR700B/T650-35 laminate were employed.

Regardless of the purge gas type, less than 3% weight loss in the composite occurred below 500°C (932°F) at 10°C/min. In general, the largest weight loss rate took place at about 550 - 570°C (1022 - 1058°F) in both nitrogen and air. Most of the off-gas products came about between 550 and 600°C (1112°F). At 10°C/min, this composite lost 17% of its weight at 600°C in nitrogen whereas the weight loss reached 35% in air. Thus, this composite lost more of its weight in air. Consequently, the composite is much more stable in nitrogen than in air. In other words, its thermal stability is greater than its oxidative stability. The composite lost 34% of its weight in air at 5°C/min. Compared to its 35% weight loss at 10°C/min, the heating rate did not appear to affect the composite weight loss kinetics at all.

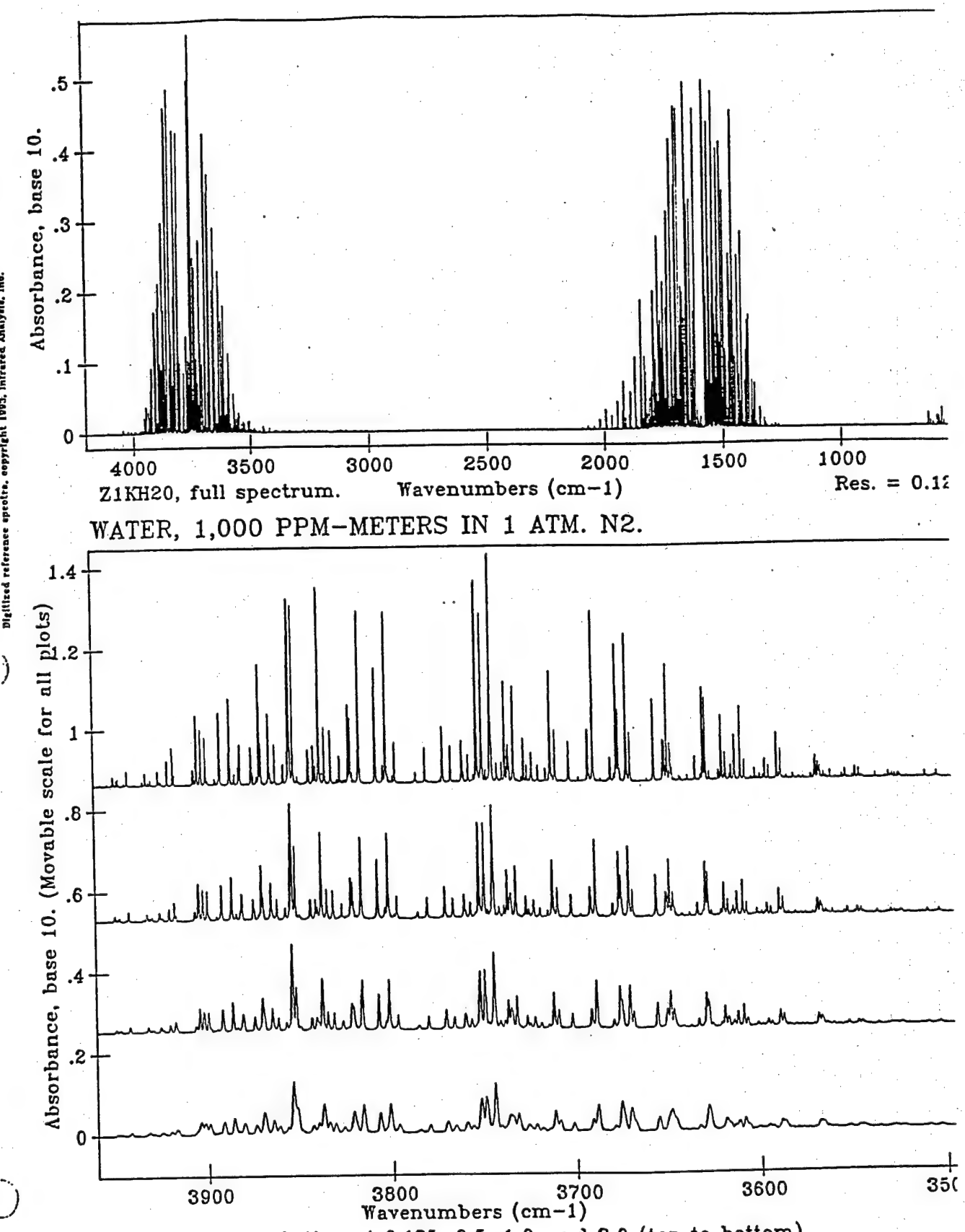

Figure 23-a FTIR of Water Vapor, 3500-3900 cm^{-1}

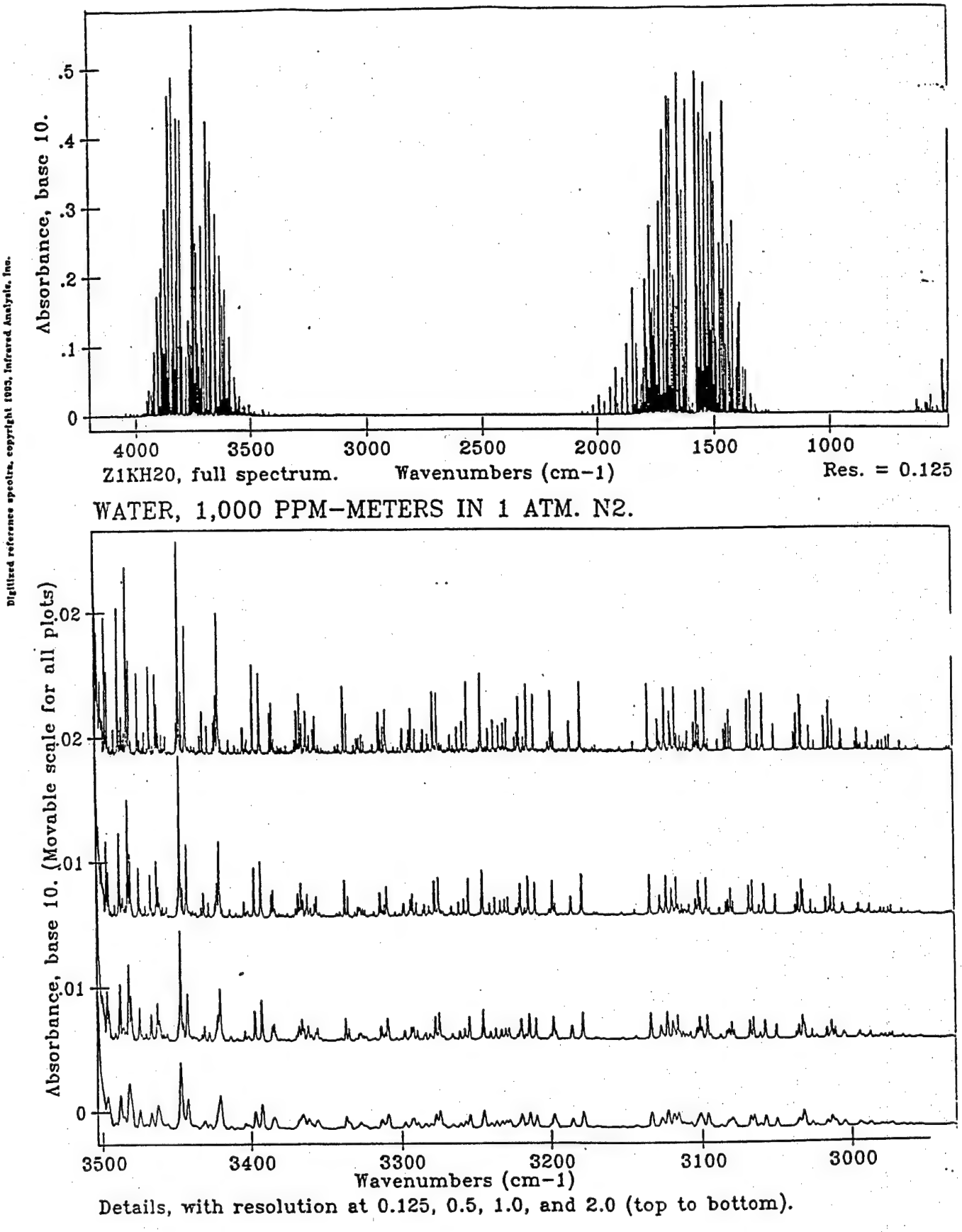

Figure 23-b FTIR of Water Vapor, 3000-3500 cm^{-1}

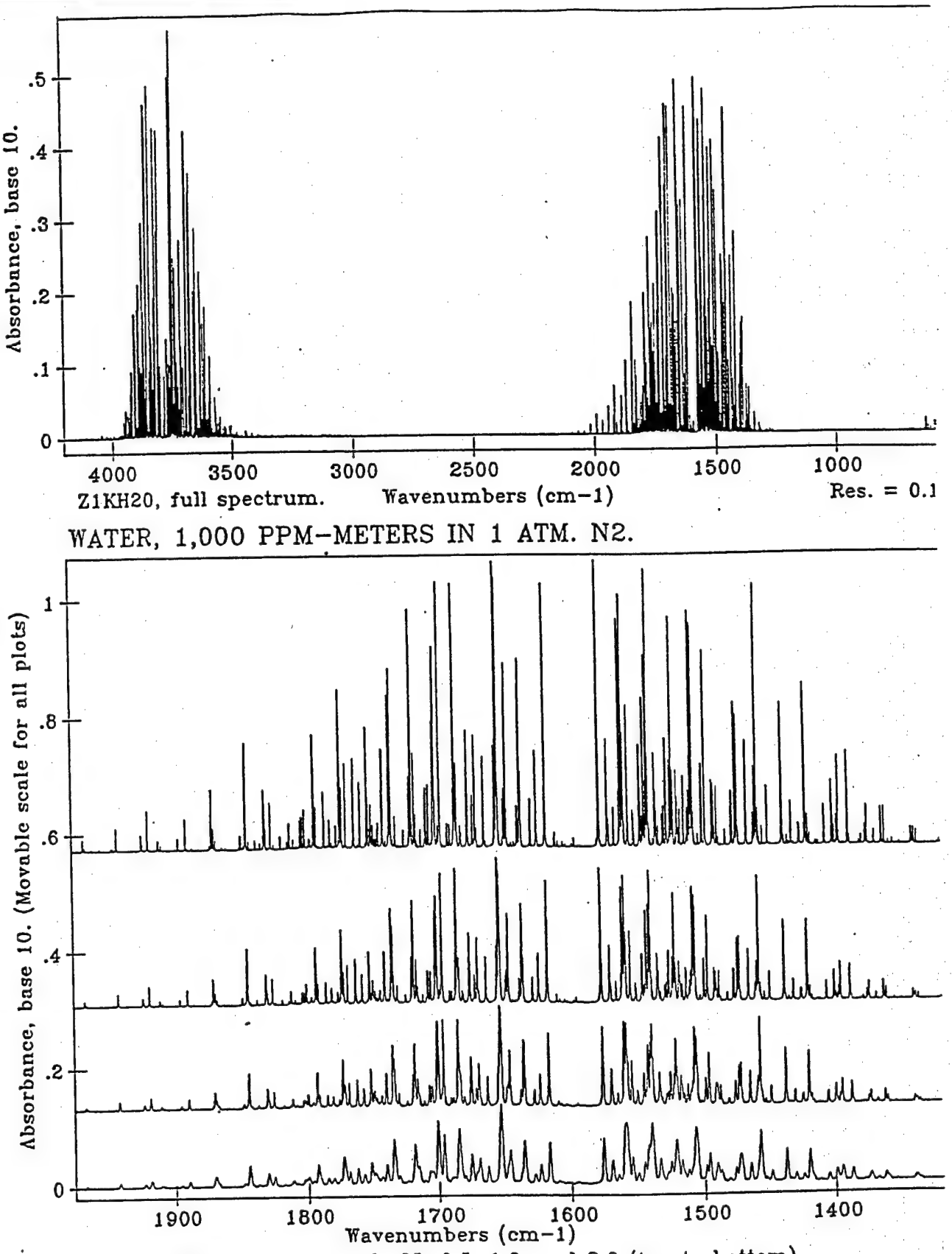

Figure 23-c FTIR of Water Vapor, 1400-1900 cm^{-1}

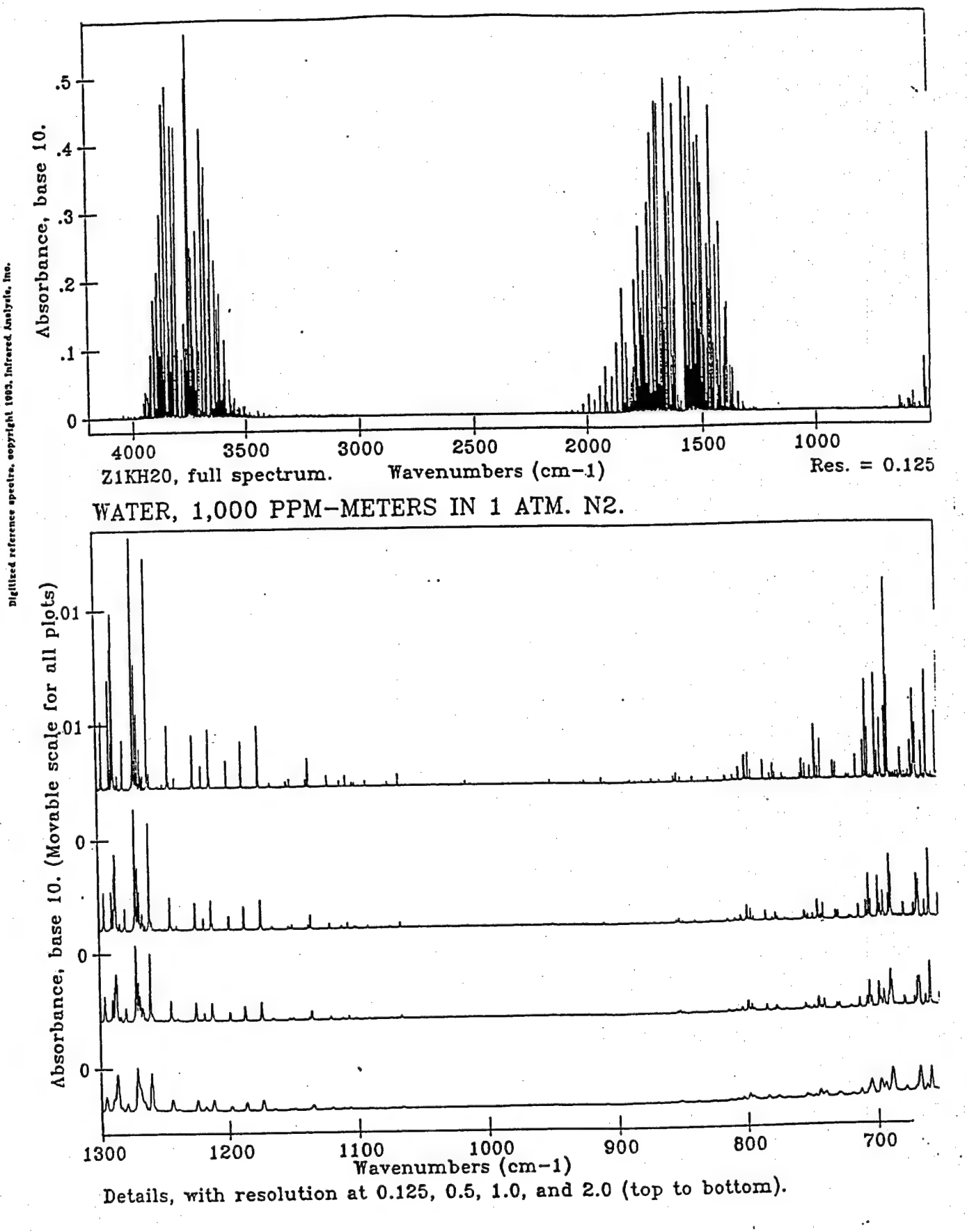

Figure 23-d FTIR of Water Vapor, 700-1300 cm^{-1}

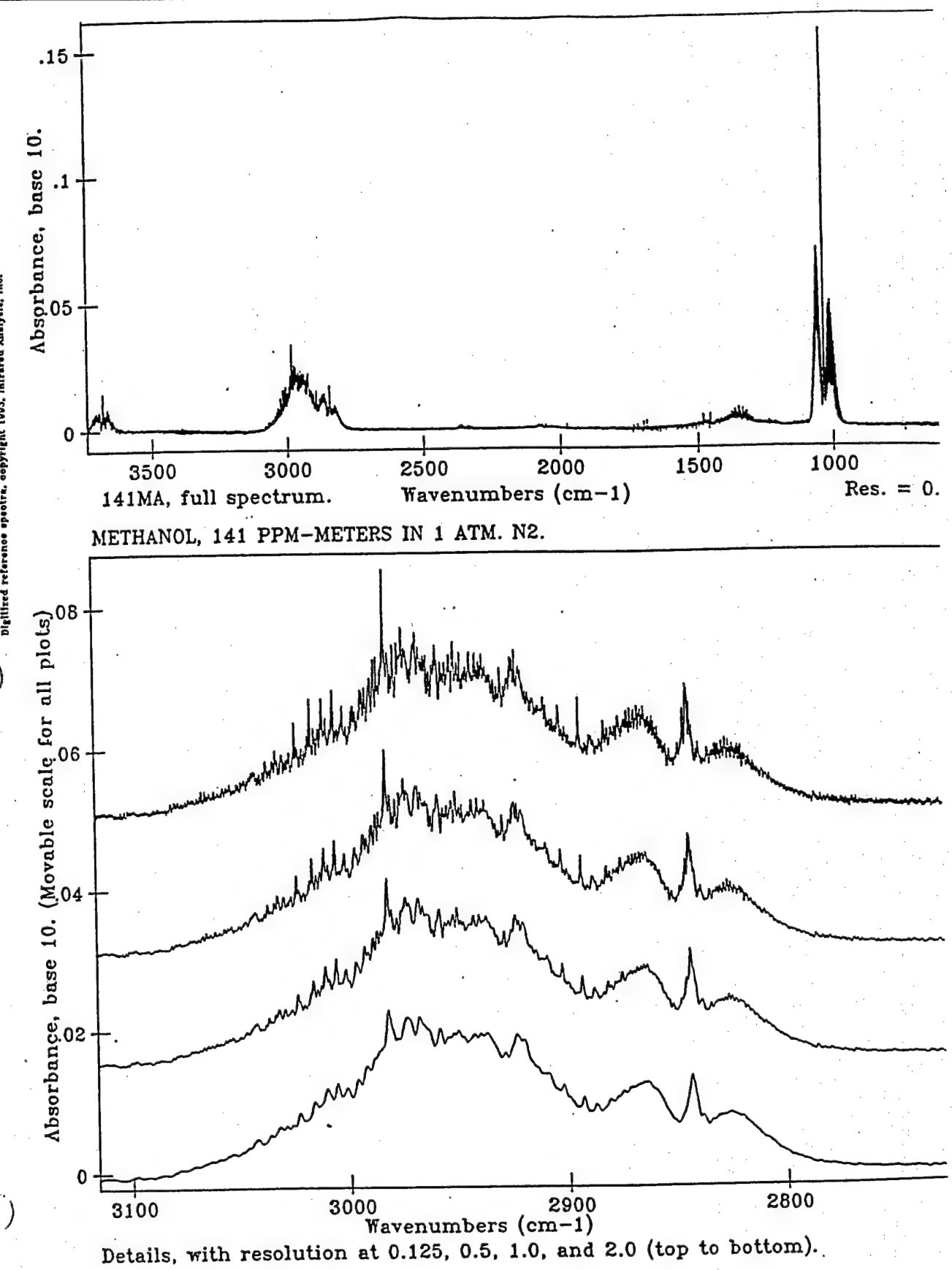

Figure 24-a FTIR of Methanol Vapor, 2800-3100 cm^{-1}

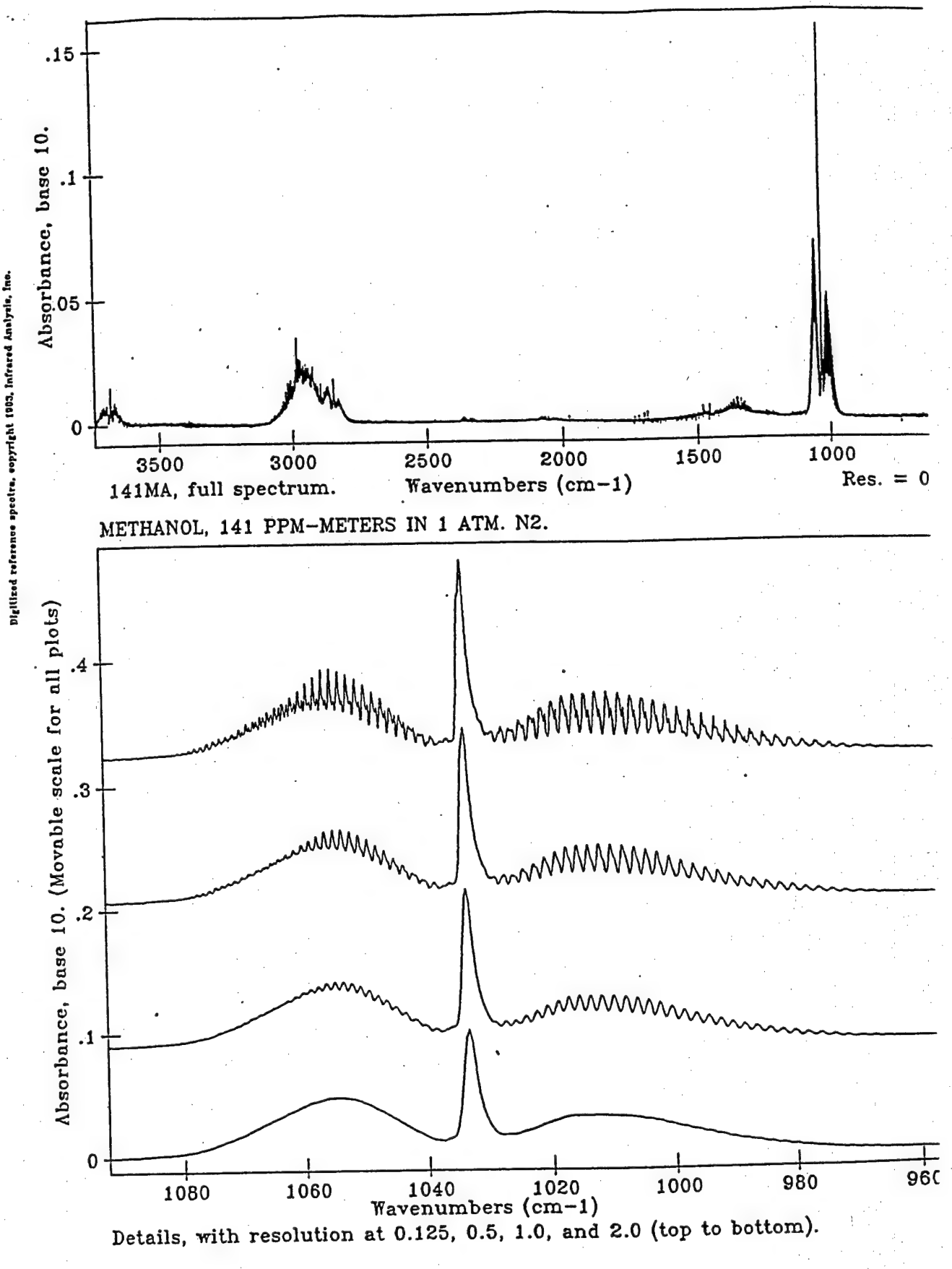

Figure 24-b FTIR of Methanol Vapor, 980-1080 cm^{-1}

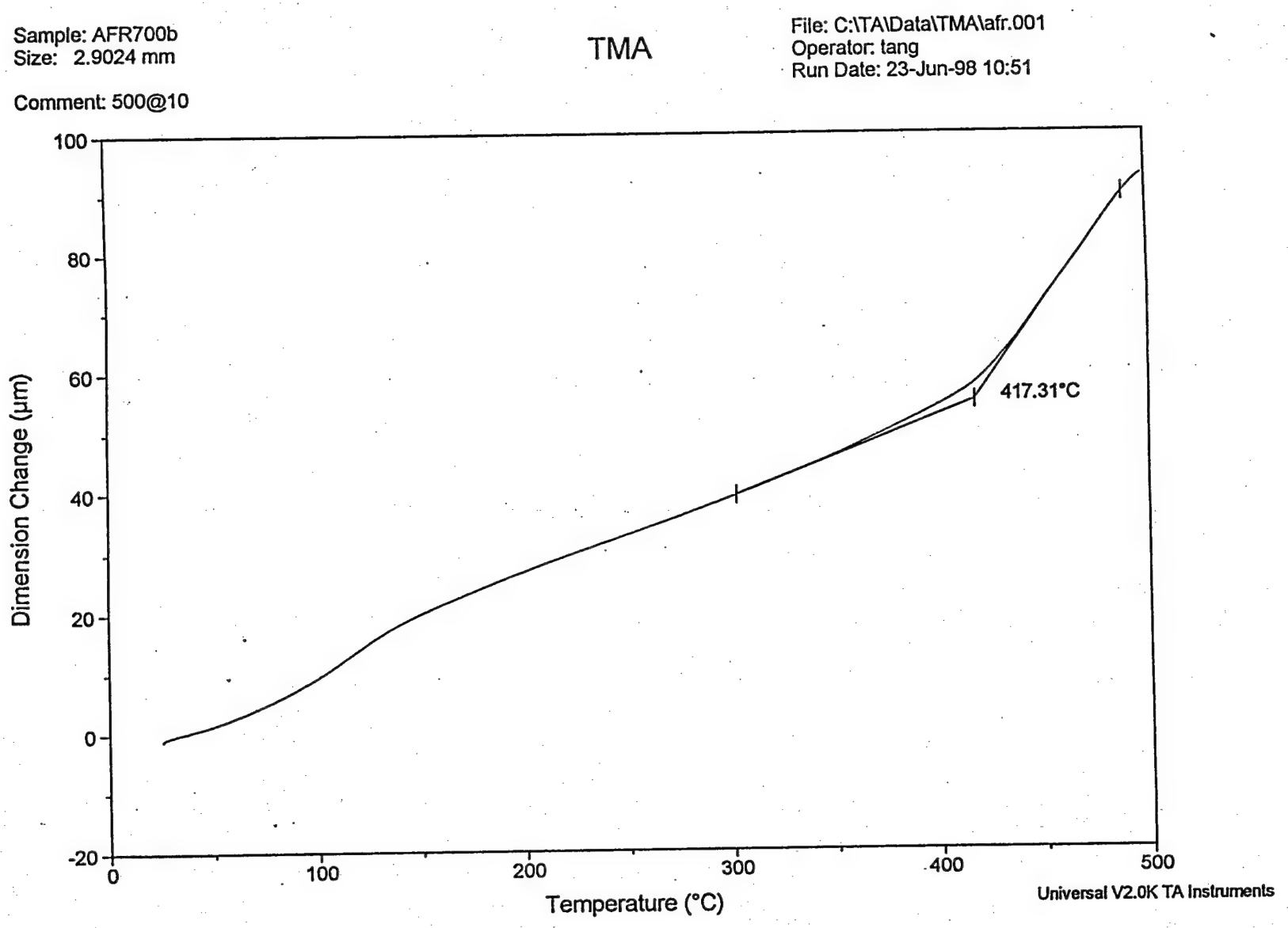

Figure 25 Glass Transition Temperature Measurement of AFR700B/T650-35 Composite by TMA.

3.2.2 Off-gas Products Identification by TGA/FTIR and TGA/MS

Figure 26 showed a three dimensional FTIR spectra of the AFR700B/T650-35 composite when heated to 600°C in air at 10°C/min. The release of H_2O, CO_2, CO, CH_3OH, $-CF_3$, and –N=C-O was evident. The mass spectra of this composite were generated at 5°C/min in air. Figures 27 – a, b, c exhibited its mass spectra at 24, 324, and 600°C, respectively. The m/e intensity covered a range of 10^{-13} to 10^{-7}. One can see that even at 24°C, a large number of mass fragments were present. Some mass fragments were present at fairly low intensities initially. Their intensity increased with increasing temperature, indicative of the evolution of off–gas products from thermal oxidative degradations. Much more large mass species were detected at 600°C. Figure 28 displayed the mass profile for a few mass fragments with increasing temperature. It is interesting to note that water (m/e = 18) had three peaks at 78, 311, and 500°C, respectively. Moreover, its first peak at 78°C appeared to be the major species given off below 100°C. The second water peak covered a broad temperature range between 230 and 455°C. The third one began at 455°C (851°F) and extended to 600°C. These three water peak temperatures might vary depending upon the heating rate used. Their presence, however, revealed the existence of three separate release mechanisms. The evolution of absorbed water or surface moisture was responsible for the first peak. The second peak might be due to oxidative degradations of the neat resin while the third one might also involve carbon fibers[10]. There was indication that residual methanol (m/e = 31) was given off shortly after heating started.

The second mass fragment detected was HCF_3 (m/e = 70) beginning at 220°C (428°F). it reached a peak at 302°C (577°F). This finding was in agreement with the theoretical bond order calculation of Lee[15] predicting –C-CF_3- to be the weakest bond in a 6F polyimide. HCF_3 also displayed a second peak at 498°C (928°F). Shortly after the release of HCF_3, HF (m/e = 20) was given off. Similar to the former, HF possessed two peaks as well at approximately the same peak temperatures. Close to the initial presence of HCF_3 and HF, the second CH_3OH peak started to come off and continued to develop into a larger third peak with peak temperatures in proximity to those of H_2O, HF, and HCF_3. Next, -C_6H_3-NH_2 or –C_6H_4-NH- (m/e = 91) began to come off at about 250°C (482°F) indicating that the AFR700B end group, -C_6H_4-NH_2, may be vulnerable to oxidative degradation. It reached a peak at 300°C (572°F). Its release was complete at 366°C (691°F). At 275°C (527°F), the evolution of –C_6H_3-CO- (m/e = 103) commenced. It possessed two peaks, one at 330°C, and the other at 500°C. Its first mass peak ended at 455°C. A single mass peak for cyclopentadiene (m/e = 66) at 500°C was seen. Its release started at about 450°C and continued on to 600°C suggesting the vulnerability of the AFR700B NE end group to oxidative degradation. Carbon dioxide, CO_2, at m/e = 44 began to show up at 250°C and its evolution increased throughout the entire TGA/MS run. Its rate of release accelerated greatly at 450°C (842°F) hinting strongly the onset of carbon fiber oxidation. A comparison with the TGA/MS evolve gas analysis of AFR700B neat resin may provide an insight to the onset point of carbon fiber involvement.

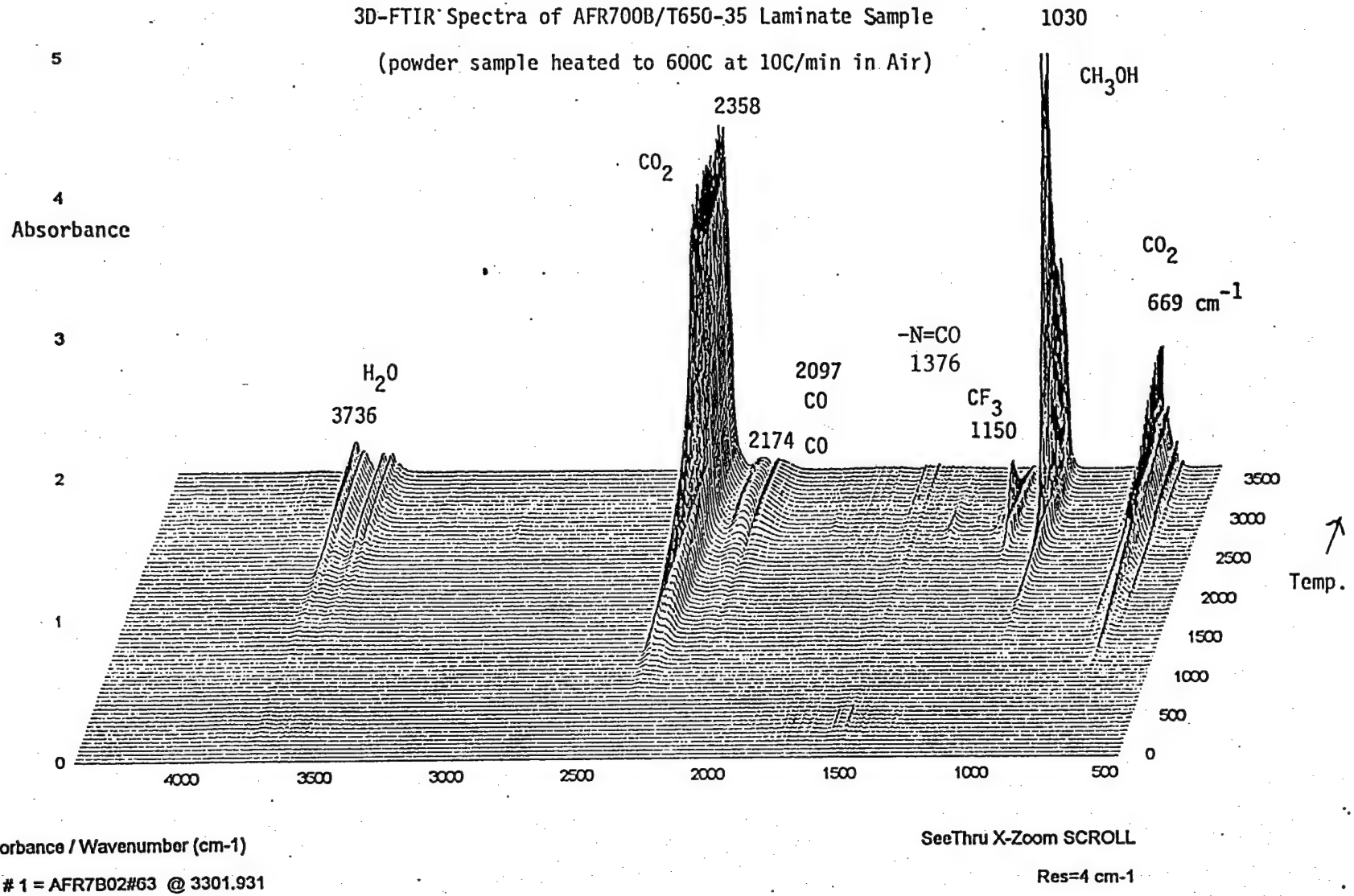

Figure 26 3D-FTIR of AFR700B/T650-35 Composite, Heated to 600°C in Air at 10°C /min

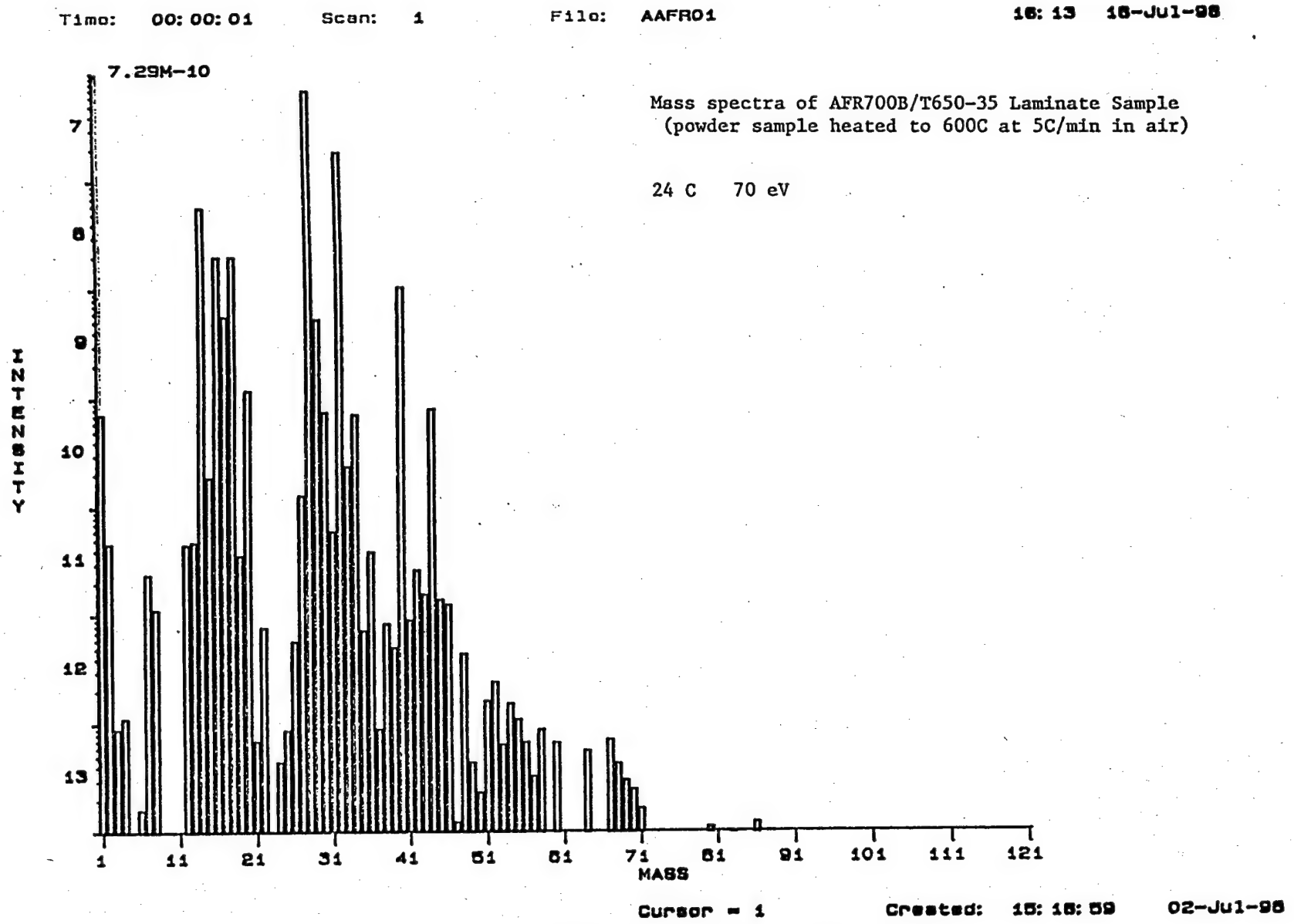

Figure 27-a Mass Spectra of AFR700B/T650-35 Composite at 24°C

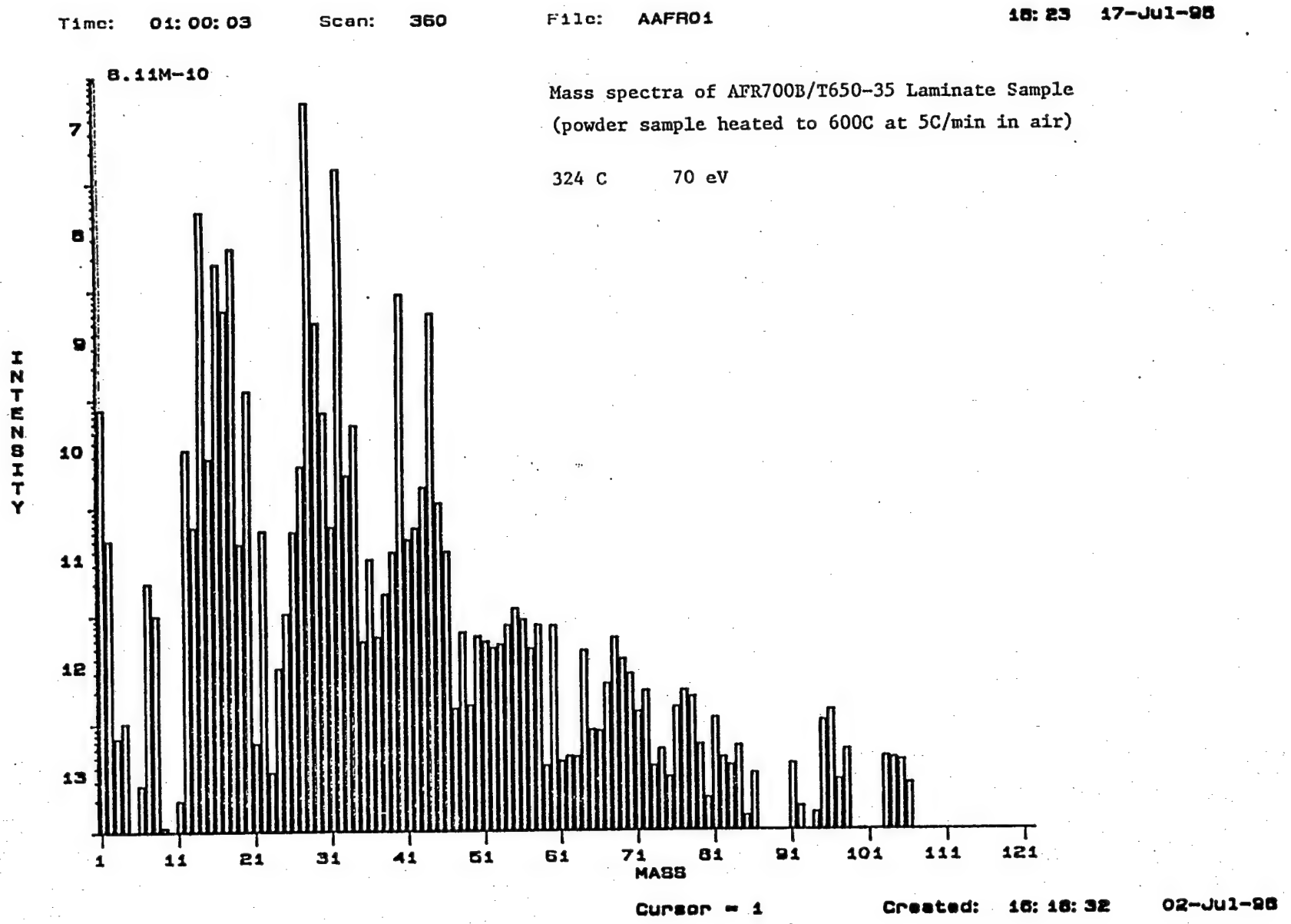

Figure 27-b Mass Spectra of AFR700B/T650-35 Composite at 324°C

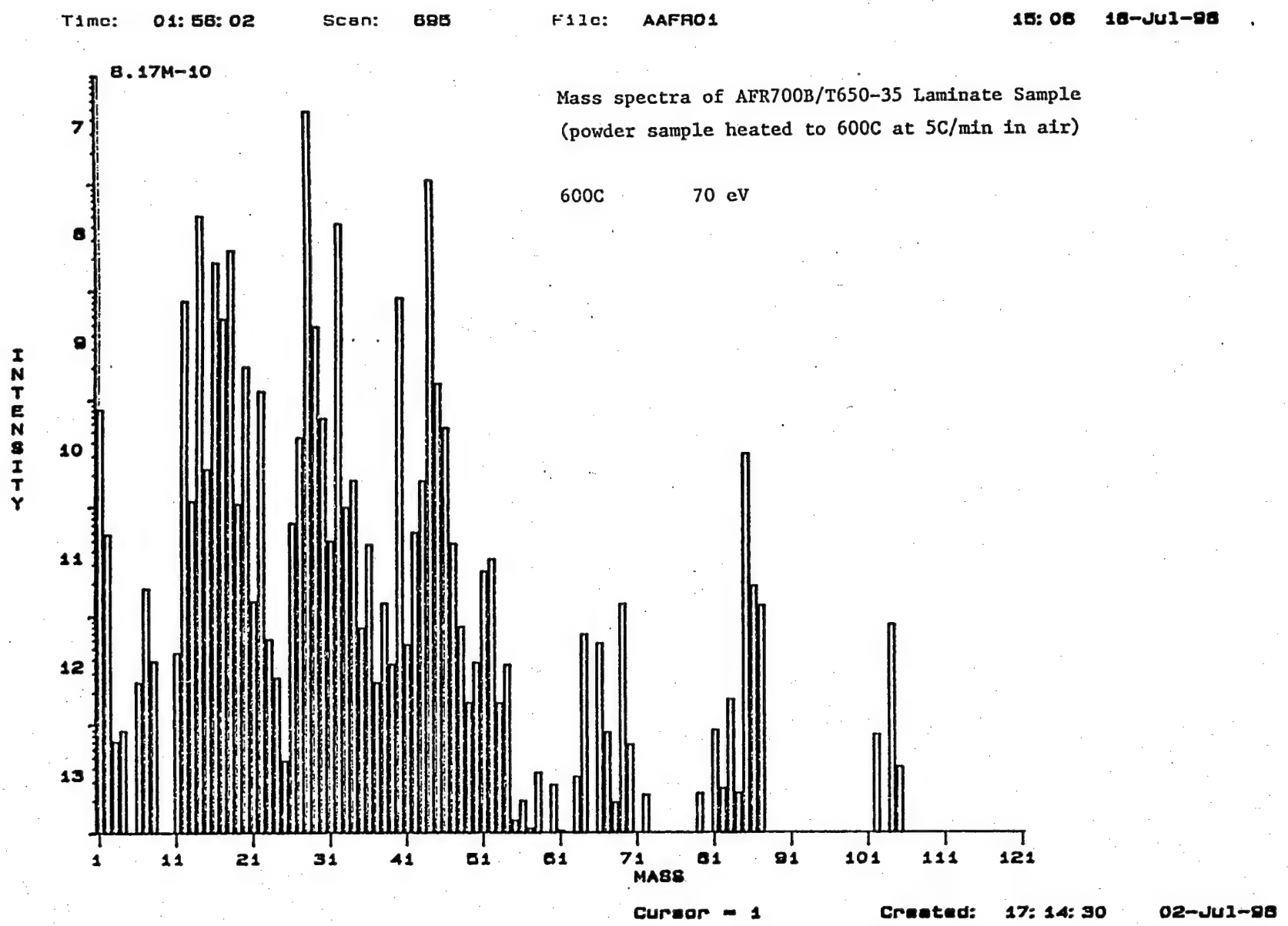

Figure 27-c Mass Spectra of AFR700B/T650-35 Composite at 600°C

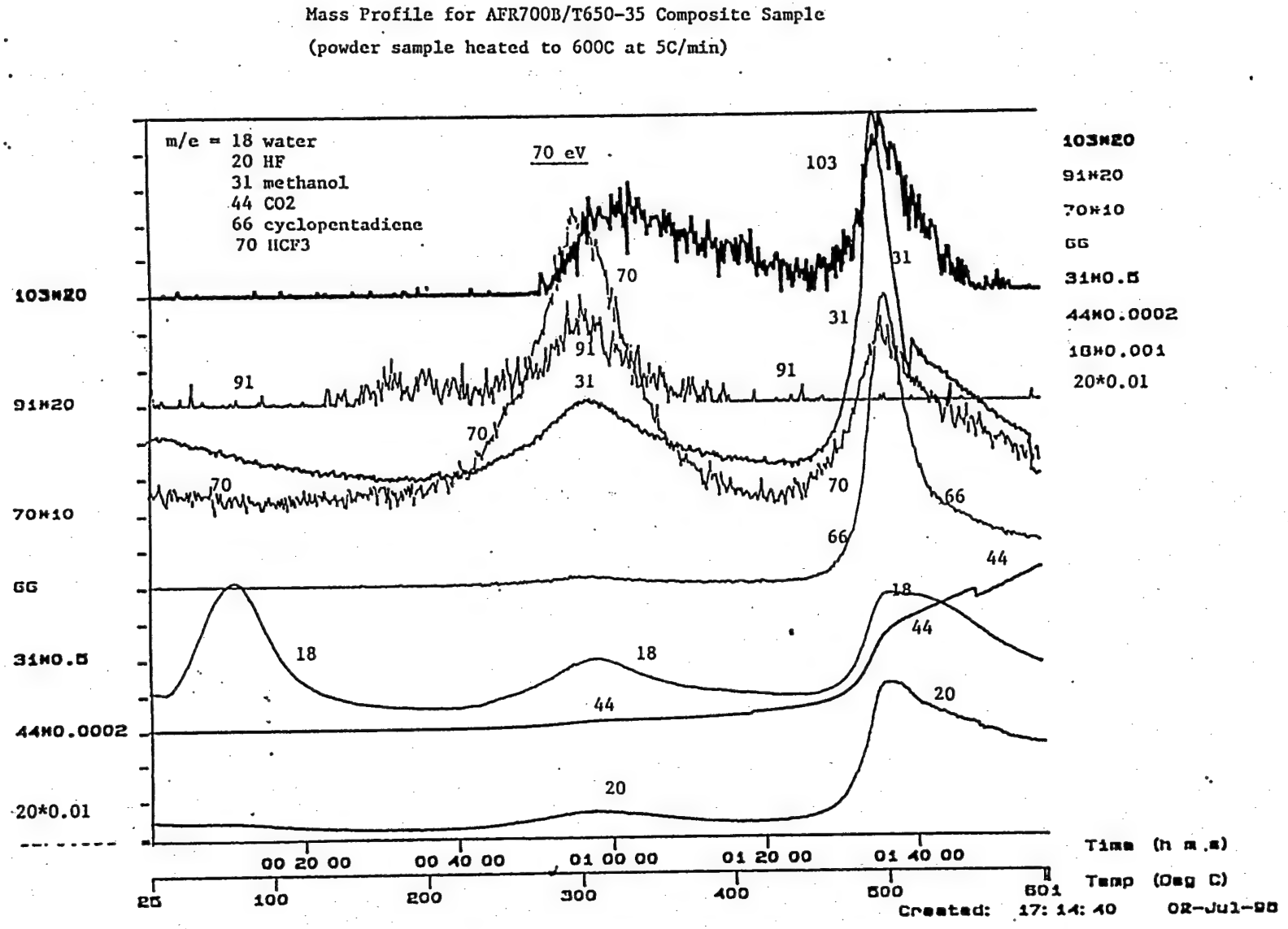

Figure 28 MS Profile for AFR700B/T650-35 Composite, Heated to 600°C in Air at 5°C/min

Several observations can be made from the above TGA/FTIR/MS evolve gas analysis. A number of off-gases were detected having peak rates of release close to 300-330°C (572-626°F). The presence of CH_3OH, H_2O, HCF_3, HF, $-C_6H_4-NH_2$, and $-C_6H_3-CO-$ would suggest that extensive oxidative degradations had already taken place. The weight loss of AFR700B/T650-35 composite between 100 and 300°C was just 0.9% (2.2 – 1.3 = 0.9), which translated to a 3% neat resin weight loss at a 70/30 carbon fiber/resin weight content in the composite. After the initial loss of absorbed moisture, the polyimide resin would have undergone substantial degradations to produce a 3% weight loss. Thus, it is fair to say that at 300°C, oxidation has started and progressed to backbone chain scissions. It is also important to note that most off-gas products were given off in two stages. The second stage commenced at 450°C. Their evolutions picked up in speed and resulted in a second peak close to 500°C. Even though detailed degradation mechanisms for the second peak are not yet known, it is doubtful they were the same as the first peak. Moreover, their kinetics may be different. To complicate the situation further, new off-gases were seen (Figure 27-c) in the elevated temperature region. Therefore, the use of elevated temperatures above 500°C for accelerated aging would have serious limitations. It appeared that for durability assessment, long-term isothermal aging should be made at lower temperatures, which need to be determined experimentally.

Figure 29 displayed another MS profile for this AFR700B/T650-35 composite, when heated to 600°C in air at 5°C/min. Instead of the linear scale used in Figure 28, a logarithmic intensity scale was employed. It can be seen that the essential feathers remained the same. In addition, a few related m/e peaks were plotted in these two figures separately. For instance, HCF_3 (m/e = 70) was shown in Figure 28 while $-CF_3$ (m/e = 69) was given in Figure 29. Since they represented related mass fragments, their shapes and peak temperatures stayed the same. Similarly, the mass profile for m/e = 103 (Figure 28) resembled that for m/e = 104 (Figure 29). Thus, some mass fragments might be present in more than one m/e values.

Figure 30 showed the corresponding mass profiles for the AFR700B/T650-35 composite, when heated to 600°C in nitrogen at 5°C/min. A comparison of Figures 29 and 30 would shed some insight into the difference between aging in air/oxidative degradation and aging in nitrogen/thermal degradation. First of all, the same mass fragments, i.e., at m/e = 18, 20, 31, 40, 44, 45, 55, 66, 69, 85, and 104 were present in both aging environments. It implied that the major degradation pathways involved might be similar. For m/e between 18 and 45, little difference in the mass profile shape existed although the mass intensity differed. The overall mass intensity in air was greater than that in nitrogen. Starting with m/e = 55 and up, the mass profile shape also began to differ. For instance, for m/e = 55 the mass profile in air displayed a peak at about 300°C whereas the mass intensity in nitrogen continued to rise to 485°C and then, leveled off toward 600°C. For m/e = 66, 69, 85, and 104, their mass intensity exhibited two peaks in air. The first peaks were smaller having a peak temperature close to 308°C while the larger second peaks occurred at 500°C. The first peaks ended between 350 and 400°C. On the other hand, when the same composite was aged in nitrogen only a shoulder appeared around 308°C, which developed into a single peak at about 520°C. Moreover,

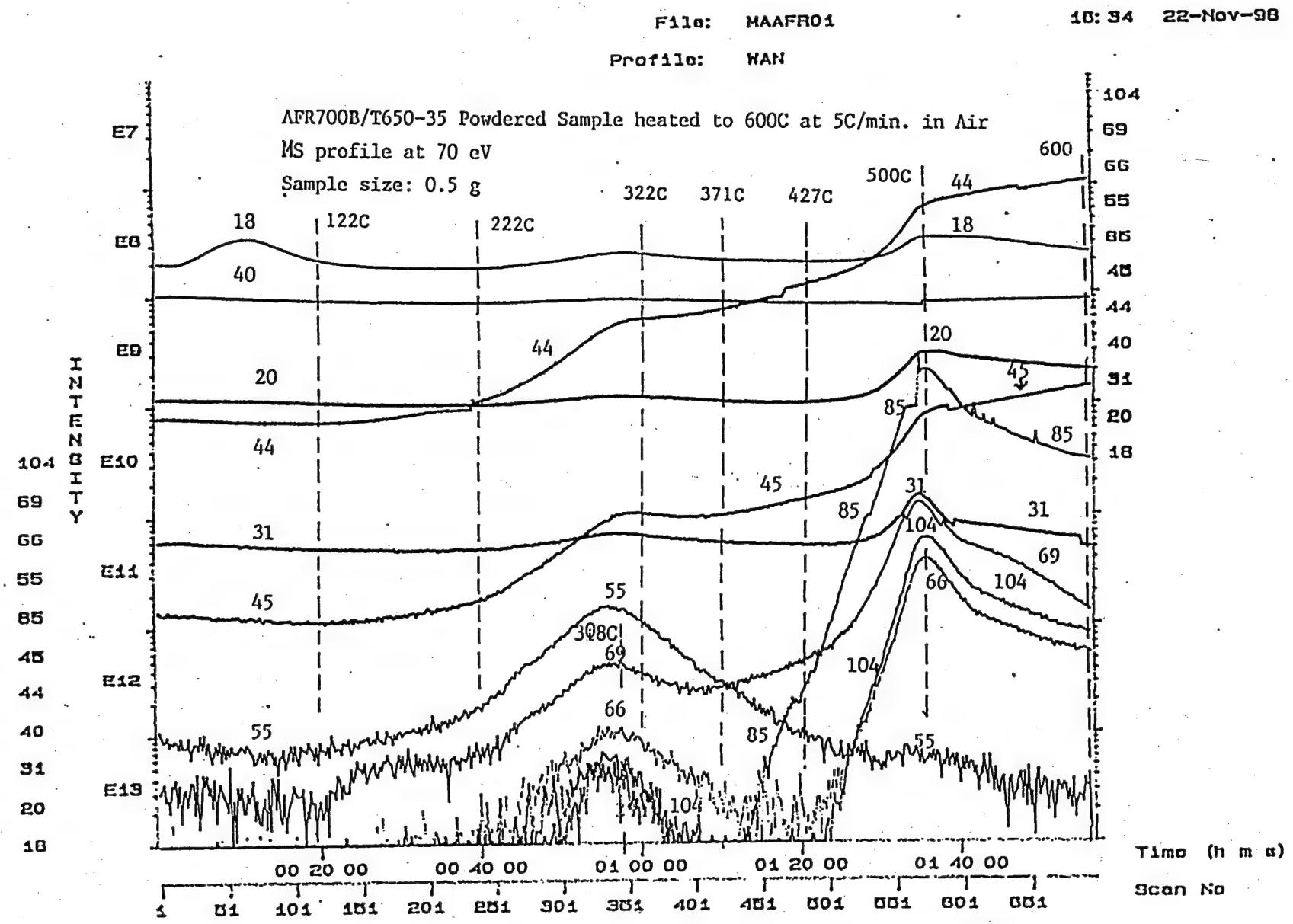

Figure 29 MS Profile at 70eV for AFR700B/T650-35 Composite, Heated to 600°C in Air at 5°C/min

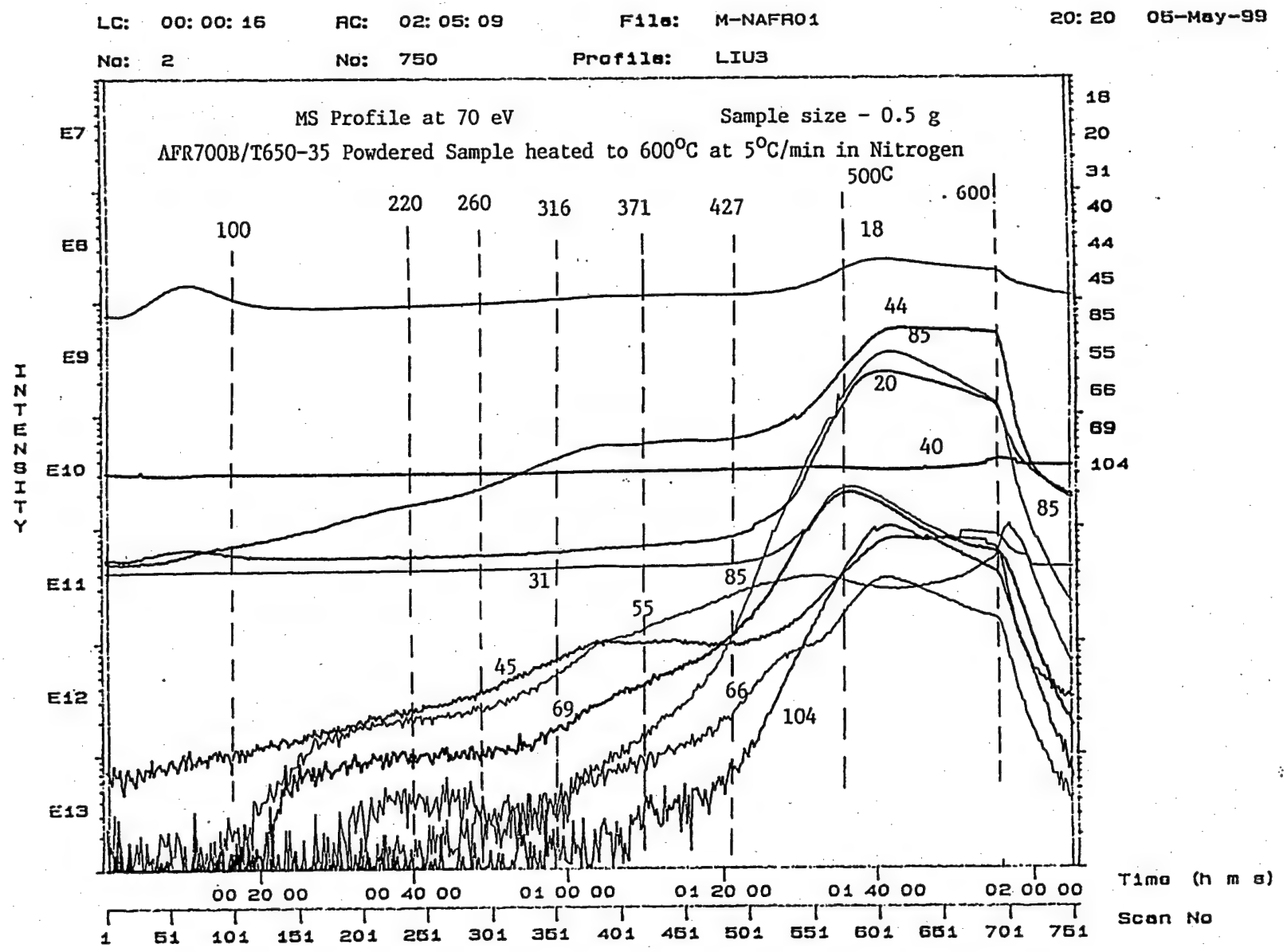

Figure 30 MS Profile at 70eV for AFR700B/T650-35 Composite, Heated to 600°C in Nitrogen at 5°C/min

for m/e = 69 ($-CF_3$) it was surprising to see that its release began as early as 120°C in both air aging and nitrogen aging regardless of the aging environment used. For m/e = 66, 85, and 104, their evolution took place at about the same temperature range (220 – 260°C) in air as well as in nitrogen. However, their release in air diminished to nil at the end of the first peak and restarted to grow into a larger second peak. It would be difficult to ascertain the details of their degradation pathways on the basis of this MS data alone. Nevertheless, one could surmise that the composite degradation mechanisms started to change between 220 and 260°C depending upon the aging environment used. Of course, one should bear in mind that this temperature range would vary with the heating rate during aging due to thermal lag. A smaller heating rate, which is closer to an isothermal aging, would decrease the temperature range for the onset of this degradation mechanism change.

3.2.3 Degradation Pathway Study

The off-gas products identified with the aid of FTIR and MS were employed to probe the degradation pathways of AFR700B/T650-35 composite. Many gas products were detected during aging. Some of these off-gas products may be the intermediate mass fragments produced by electron collisions in the mass spectrometer. For this degradation pathway study, only those ions and mass fragments related to and derivable from the AFR700B polymer structure (Figures 3 and 31) were taken into consideration. They included H_2O, CO, CO_2, $-CF_3$, HF, CH_3OH, $-C_6H_3-NH_2$, $-C_6H_3-CO-$, -N-C=O (phenyl isocyanate), and cyclopentadiene. Therefore, the emphasis was placed on the initial breakdown of the polymer backbone, instead of following the actual oxidation and subsequent reaction sequence leading to the various degradation products. Thus, this degradation mechanism study addressed mainly the onset of polyimide chain breakdown while leaving out the degradation pathway details[22]. The motivation behind this approach was that once polymer chain breakdown commenced, those neat resin dominated composite properties would have deteriorated rapidly.

Once absorbed or trapped moisture and residual volatile were driven off by heating, thermal and/or oxidative aging of the AFR700B/T650 composite started. Figure 31 showed the potential chain breakdown sites:

(1) the intermediate and complete oxidation of $-C_xH_y-$ or $R-C=O-R'$ producing H_2O and CO_2;

(2) the loss of HCF_3 or $-CF_3$ from the $-C-CF_3$ bond of $CF3-C-CF_3$ commencing at 220°C, which was the weakest bond (also a side chain) in AFR700B, to be followed by the break-off of – F from $-CF_3$ to form a HF molecule;

(3) the split off of imide carbonyl, $-C=O-$, by breaking the $-N-C$ single bond of $-N-C=O-$ and the $-C-C-$ single bond of the adjacent $-C-C_6H_3-$ group;

(4) the break-off of a –CH - attached imide carbonyl group from the nornbornene

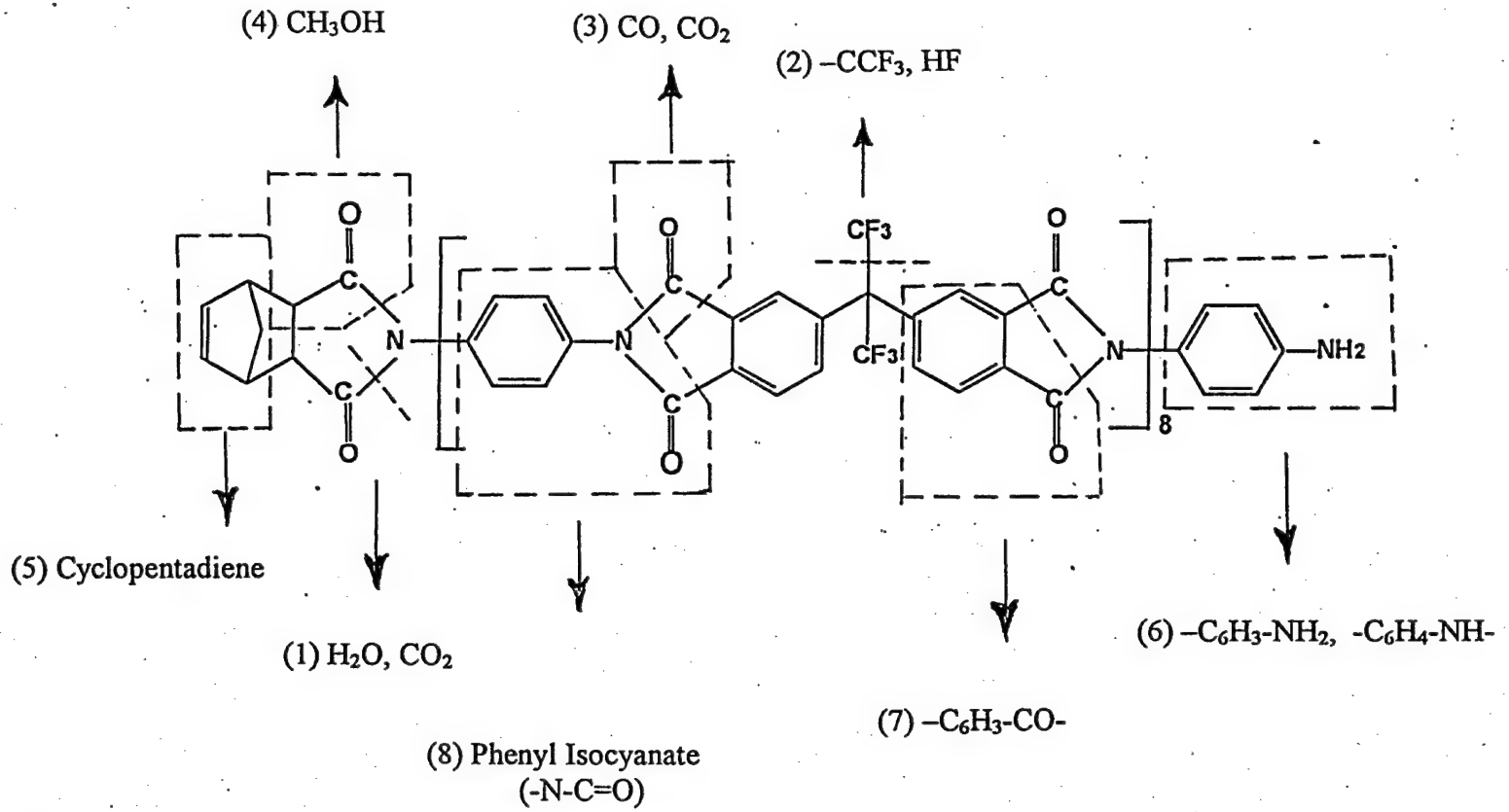

Figure 31 Proposed Degradation Pathways for AFR700B in Air, Based on Evolved Gas Analysis

ring to form CH_3OH;

(5) the loss of cyclopentadiene from the end nornbornene group;

(6) the split off of the end aniline group, - $C_6H_3 - NH_2$;

(7) the break-off of $- C_6H_3 - C = O$ from the phenyl imide ring;

(8) the release of phenyl isocyanate, $C_6H_5 - N - C = O$, from the phenyl imide group.

The release of these degradation products began at slightly different temperatures according to their relative stability. Some off-gases occurred at about the same temperatures suggesting the possibility that they were concurrent and competitive degradation processes. Nevertheless, it was quite interesting to note that these off-gas products were in general agreement with the degradation events reported by Alston et al[14] for 3F and 6F polyimides.

3.2.4 Accelerated Aging Temperature Determination

Accelerated aging was usually the methodology adopted for assessing long-term durability of a composite. For a first-order approximation, expediency, and simplicity, weight loss, instead of composite property measurements was used. The underlying principle involved was the hidden assumption that once a significant weight loss took place, polymer chain breakage followed resulting in property deterioration. Furthermore, the use of high accelerated aging temperatures to reduce the aging time needed and then, extrapolated to the lower service temperature required that the degradation mechanisms remained the same throughout the entire temperature range. Without the knowledge of degradation products occurring in real time and thus, the corresponding degradation mechanism, the weight loss kinetics was used, in the past, for service lifetime prediction. As a result, lifetime prediction was, in general, not accurate. With the aid of this TGA/FTIR/MS evolved gas analysis, the degradation products could be determined in real time. Consequently, one could use the off-gas products as a guide for assessing if similar degradation mechanism occurred. Simply stated, if the same set of degradation products was detected and also, given off at similar kinetics within a prescribed temperature range, the high-end temperature would, then, be the highest accelerated temperature allowable. The accelerated aging temperature for AFR700B/T650-35 composite was determined in 220 – 600°C by the following scheme.

The weight loss in AFR700B/T650-35 composite was shown in Figures 32, 33, 34, and 35 for its aging under varying heating conditions and aging environments. The composite was heated at 5°C/min to 600°C in air (Fig. 32) as well as in nitrogen (Fig. 33). It was also heated at 10°C/min to 600°C in both air (Fig. 34) and nitrogen (Fig. 35).

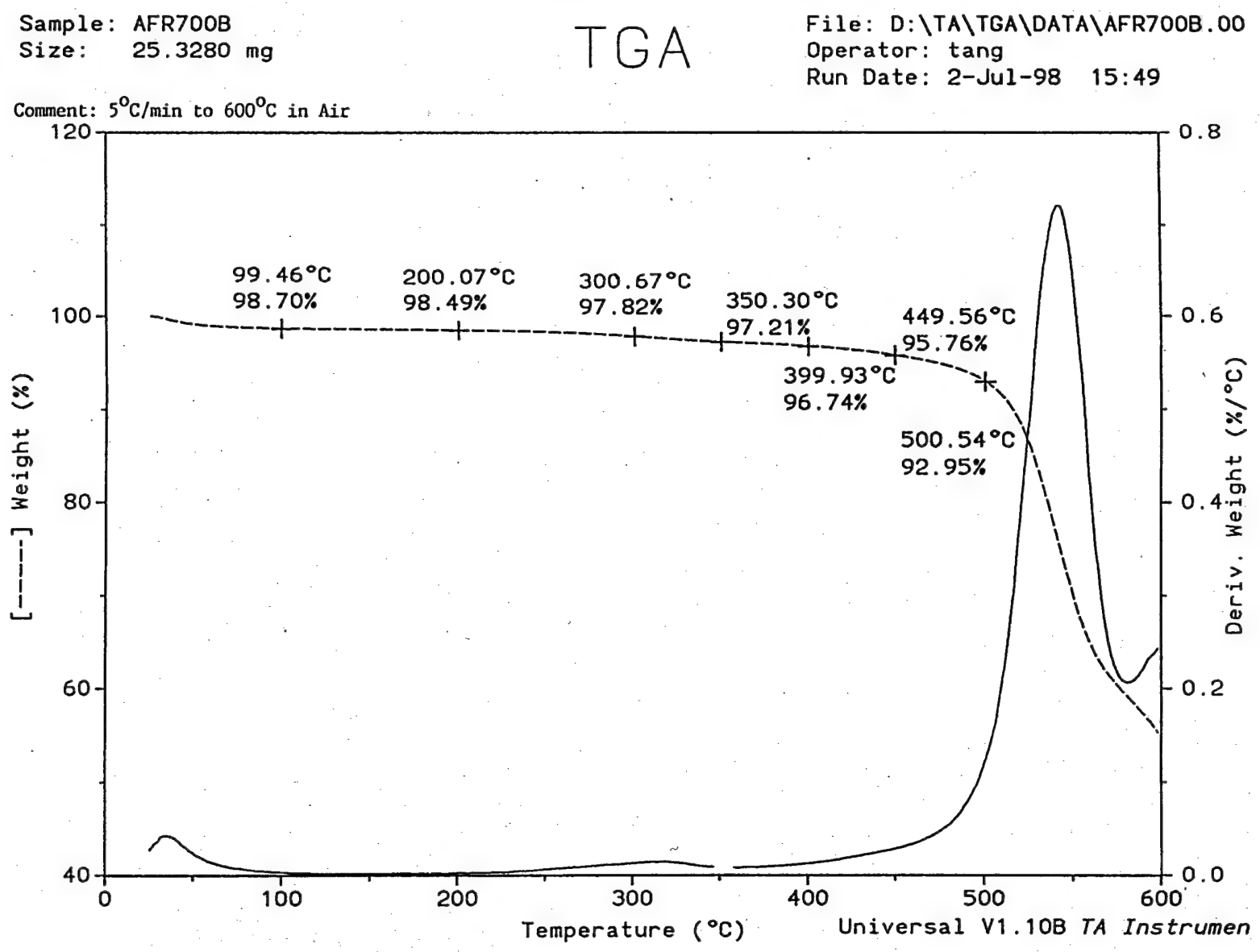

Figure 32 TGA Weight Loss of AFR700B/T650-35 Composite, Heated to 600°C in Air at 5°C/min

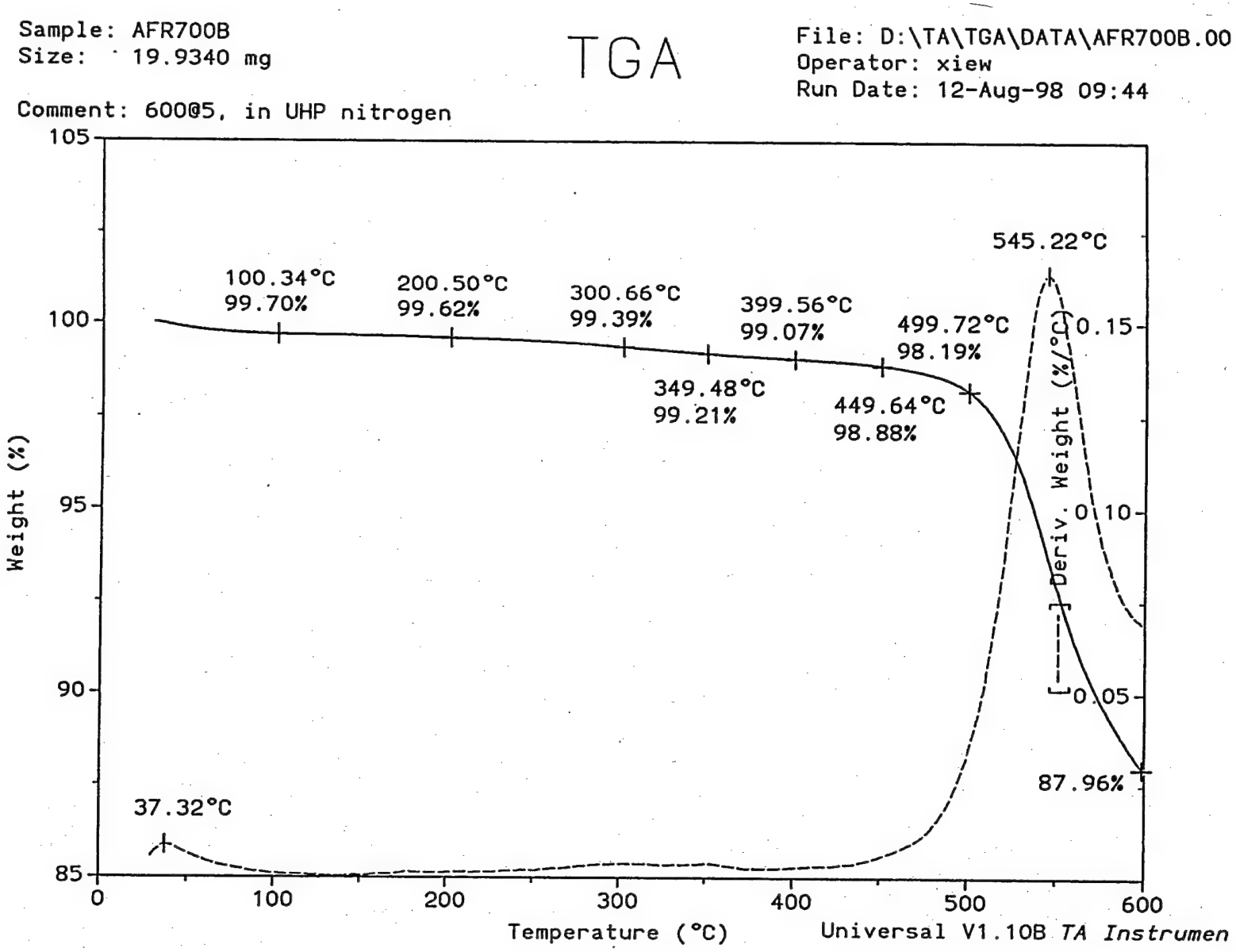

Figure 33 TGA Weight Loss of AFR700B/T650-35 Composite, Heated to 600°C in N_2 at 5°C/min

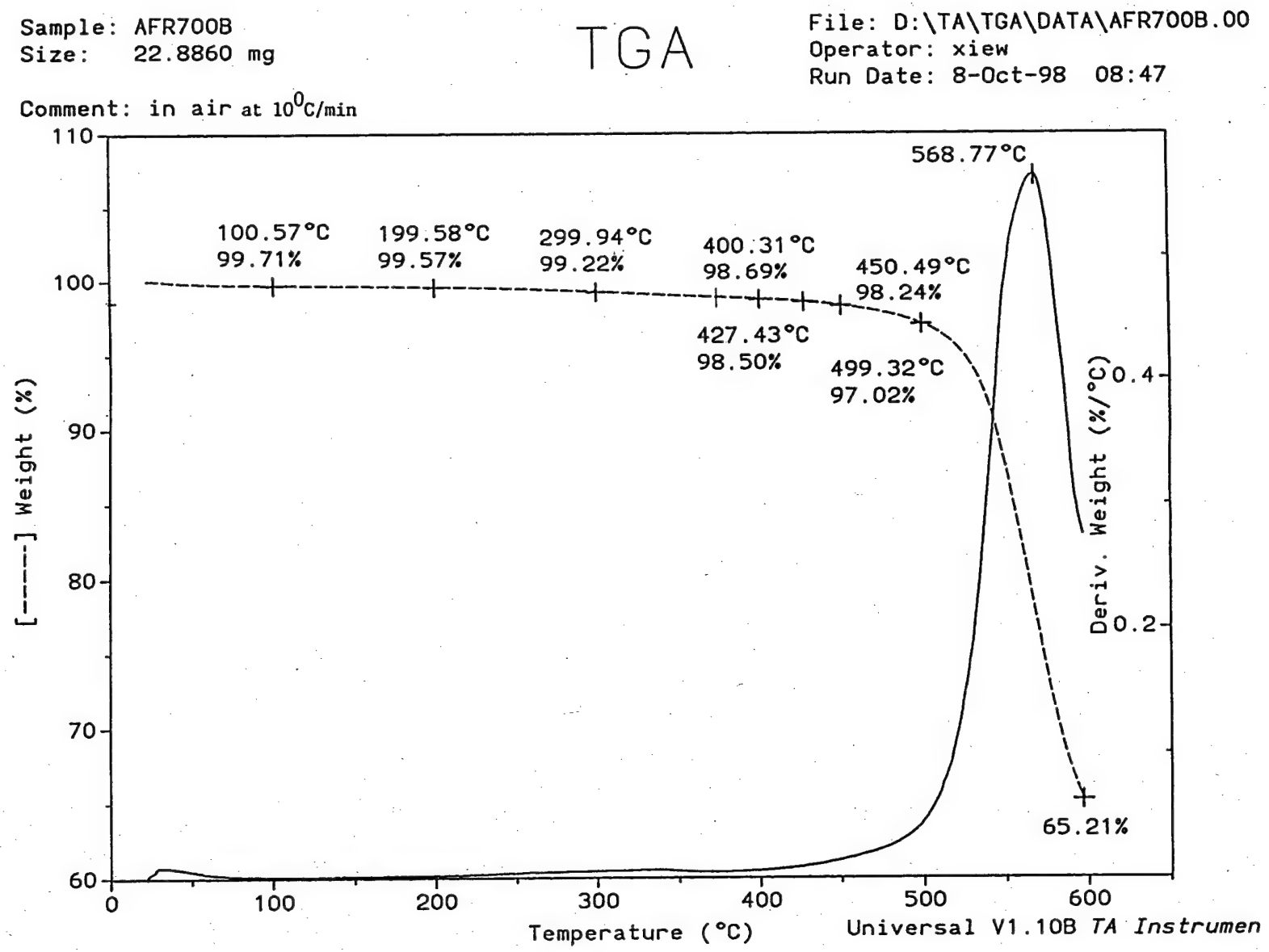

Figure 34 TGA Weight Loss of AFR700B/T650-35 Composite, Heated to 600°C in Air at 10°C/min

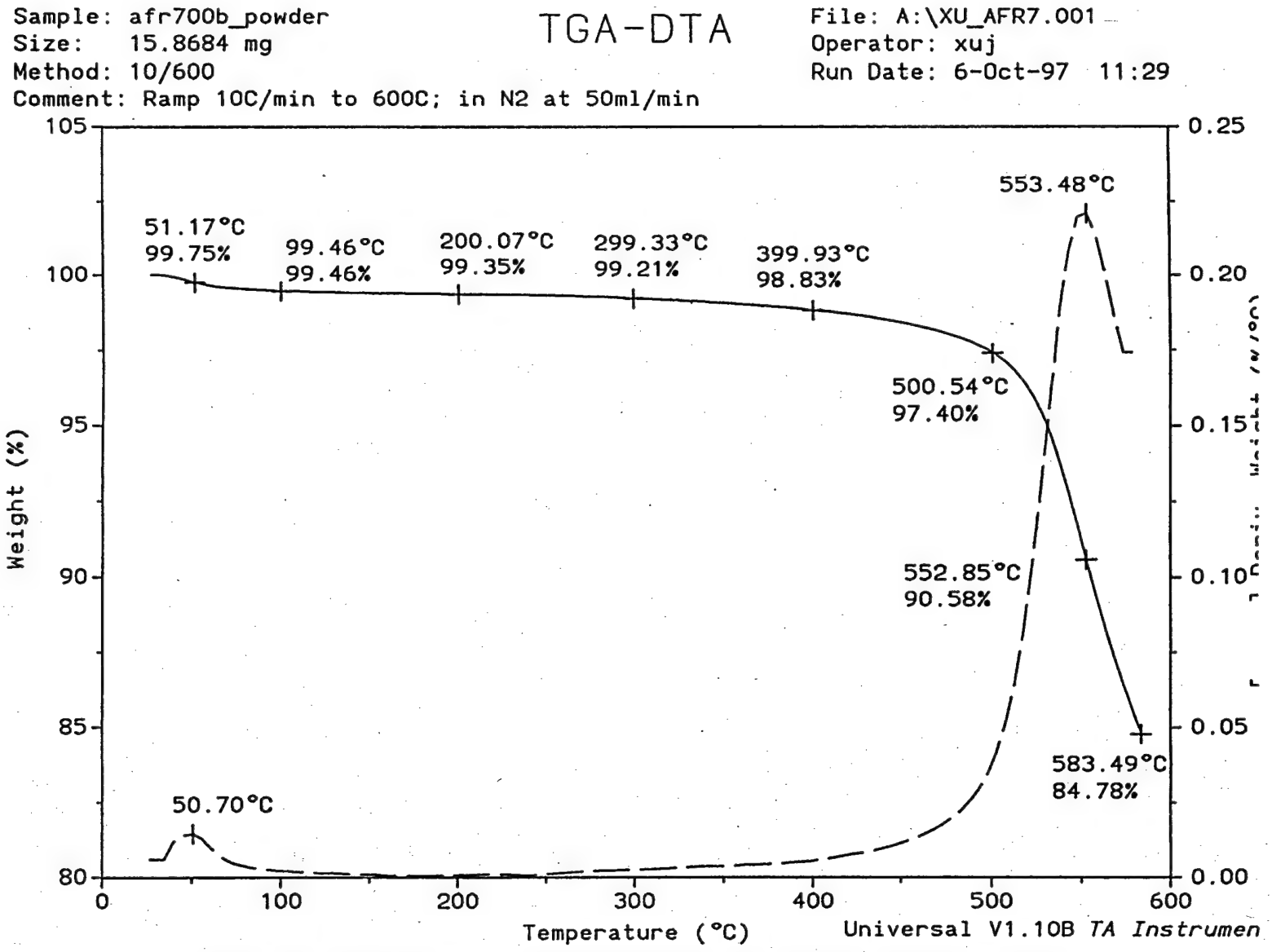

Figure 35 TGA Weight Loss of AFR700B/T650-35 Composite, Heated to 600°C in N_2 at 10°C/min

The weight losses at 100, 200, 300, 400, 500, and 600°C are tabulated below:

		weight loss, %					
		100	200	300	400	500	600°C
5°C/min	air	1.30	1.51	2.18	3.26	7.05	44.0
	nitrogen	0.30	0.38	0.61	0.93	1.81	12.0
10°C/min	air	0.29	0.43	0.78	1.31	2.98	34.8
	nitrogen	0.54	0.65	0.79	1.17	2.60	16.5

The greater stability in an inert aging environment such as nitrogen was evident. The heating rate also affected the weight loss rate. The larger the heating rate, the less the residence time at a given temperature, and the smaller the weight loss became.

Considering the case of aging in air at 10°C/min, the composite lost 1.31% of its weight upon reaching 400°C. Between 400 and 500°C, an additional 1.67% weight was lost. But, most of the weight loss occurred between 500 and 600°C amounting to 31.8%. Assuming a 70/30 carbon fiber/neat resin weight composition, the necessity of carbon fiber participation in oxidative degradations should be obvious. An examination of the corresponding MS profile for m/e = 18, 20, 31, 40, 44, 45, 55, 66, 69, 85, and 104 (see Figure 36) revealed a declining intensity for most of the above mass fragments, except for CO_2 at m/e = 44. This also tended to support the contention that oxidation of carbon fiber was involved. If the AFR700B/T650-35 composite was heated to 600°C and then, allowed to cool down in ambient condition for about 20 minutes, one could see in Figure 37 that all the above mass fragments including CO_2 decreased in intensity. When AFR700B/T650-35 composite was aged to 600°C at 10°/min in nitrogen, a similar trend in its MS profile to that obtained in aging in air was noted in Figure 38. Another nitrogen aging of AFR700B/T650-35 composite was carried out to 600°C at 10°C/min and held at 600°C for 4 hrs. Its MS profile in Figure 39 showed little effect from the additional four hour 600°C hold. All the mass fragments continued to decline in intensity. Thus, both the weight loss and the MS profile seemed to indicate that 600°C was too high a temperature for accelerated aging.

When a composite was heated to an aging temperature at a relatively large heating rate as 10°C/min, not necessarily all the degradation products that could be given off were released due to its short residence time. If they could be given off at a lower aging temperature with the aid of a holding period at the lower aging temperature, an equivalent heating history or aging temperature with regard to degradation events could then be established. An attempt to determine the equivalent aging temperature was made by heating AFR700B/T650-35 composite according to the heat history listed below:

1. heated in air to 600°C at 10°C/min
2. heated in air to 500°C at 10°C/min and held for 1 hr at 500°C
3. heated in air to 427°C at 10°C/min and held for 4 hrs at 427°C

4. heated in air to 371°C at 10°C/min and held for 4 hrs at 371°C
5. heated in air to 316°C at 10°C/min and held for 4 hrs at 316°C
6. heated in air to 260°C at 10°C/min and held for 4 hrs at 260°C
7. heated in air to 220°C at 10°C/min and held for 4 hrs at 220°C.

As the aging temperature was decreased from 600 to 220°C, its holding time should be lengthened exponentially. It was, however, held at a four hours interval for saving FTIR/MS instrument time. This four hours hold time also kept the holding time a constant in aging temperature reduction experiments.

The MS profiles for m/e = 18 (H_2O), 44 (CO_2), and 69 ($-CF_3$) were plotted for accelerated aging temperature determination in Figures 40 – 46 according to decreasing aging temperature. Thus, the evolution of H_2O, CO_2, and $-CF_3$ for the 600°C aging was displayed in Figure 40 while Figure 46 showed that for the 220°C aging temperature followed by a 4 hr. hold at 220°C. A comparison of Figures 40 and 41 (500°C aging) indicated that the release of H_2O, CO_2, and $-CF_3$ followed very similar trend. Water possessed three peaks. Carbon dioxide gave rise to a plateau first, which was followed by a peak at elevated temperature. The mass species, $-CF_3$, had two peaks with the second peak at a greater intensity than the first. Their evolution was almost identical, except for the slightly continuing upward turn of CO_2 between 500 and 600°C in the 600°C aging. On the other hand, CO_2 intensity leveled off shortly after reaching 500°C for the 500°C aging. With regard to $-CF_3$, the former reached a second peak at 520°C whereas the latter also attained to a second peak shortly after reaching 500°C, the target aging temperature. Since this 500°C aging temperature was so close to the peak temperature in the former at 520°C, the release of $-CF_3$ would have almost attained its peak. Hence, it was reasonable to expect that given additional aging time at 500°C, a peak in $-CF_3$ intensity would be and was, in fact, observed. Due to the close resemblance of the release of these off-gases, one can surmise that the 600°C aging in air could be substituted with a 500°C aging and one hour hold at 500°C.

If the aging temperature was further lowered to 427°C but augmented with a 4 hour hold at 427°C (Figure 42), the release of H_2O, CO_2, and $-CF_3$ still retained similar characteristics as those seen for the 600°C aging and the 500°C aging with one hour hold at 500°C. The major effect of this lowered aging temperature was to decrease the intensity of the third water peak, the carbon dioxide peak and the second $-CF_3$ peak. The lack of adequate thermal energy at 427°C to sustain certain degradation processes became evident. Consequently, their peak intensity was greatly reduced. If this aging temperature lowering trend continued, it could reach a point that no peaks would appear. The aging of AFR700B/T650-35 composite at 371°C (700°F) in air with a 4 hour hold confirmed such a trend. Figure 43 clearly indicated that 371°C was too low a temperature to initiate those degradation reactions involved in giving rise to the next peak for water, carbon dioxide, and $-CF_3$.

By the same reasoning, the preceding peak intensity of H_2O, CO_2, and $-CF_3$ could be reduced by continued decreasing aging temperature. This trend was, indeed, noted in Figures 44, 45, and 46 for aging at 316, 260, and 220°C, respectively. In aging at 220°C,

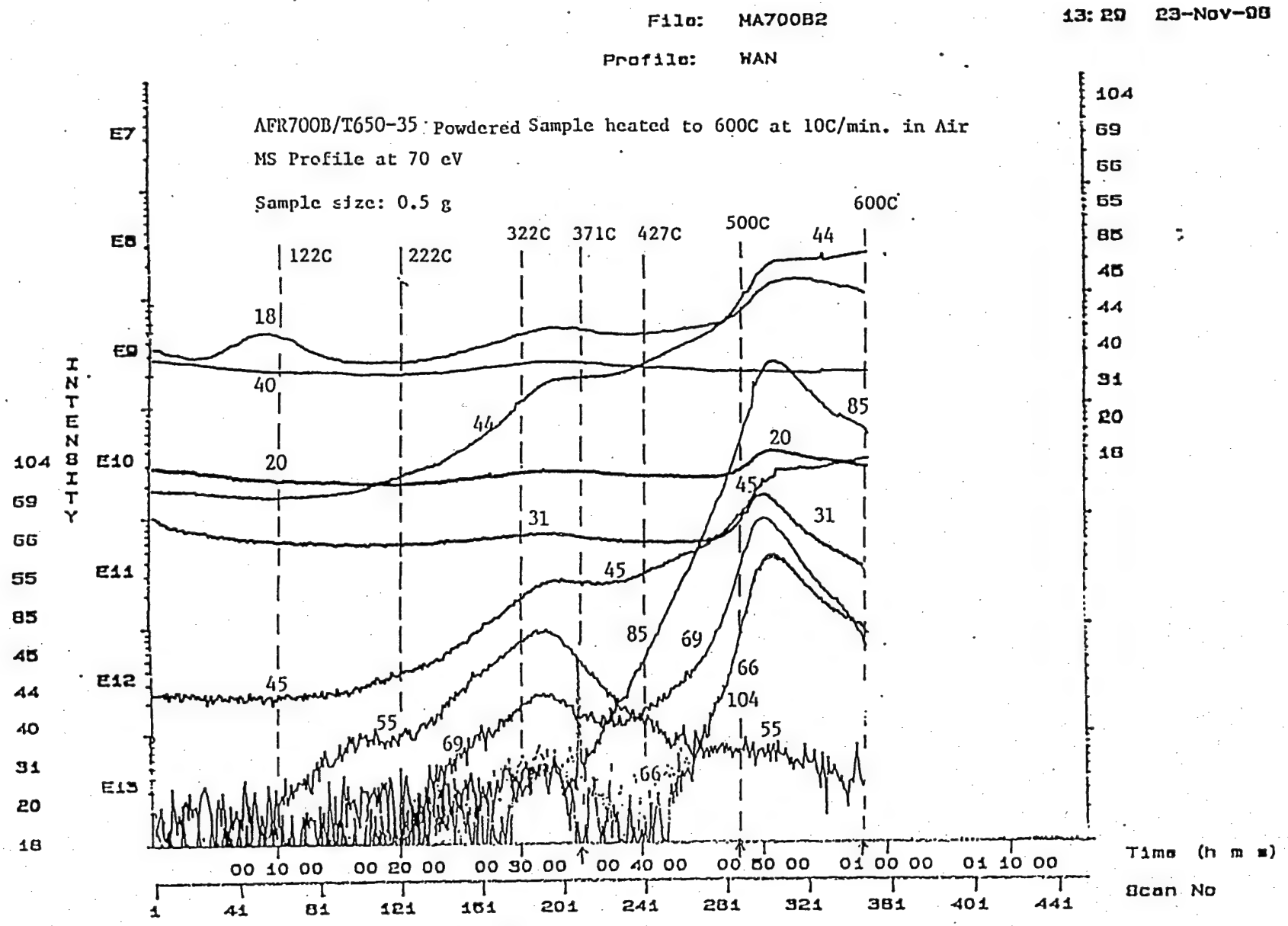

Figure 36 MS Profile for AFR700B/T650-35 Composite, Heated to 600°C in Air at 10°C/min

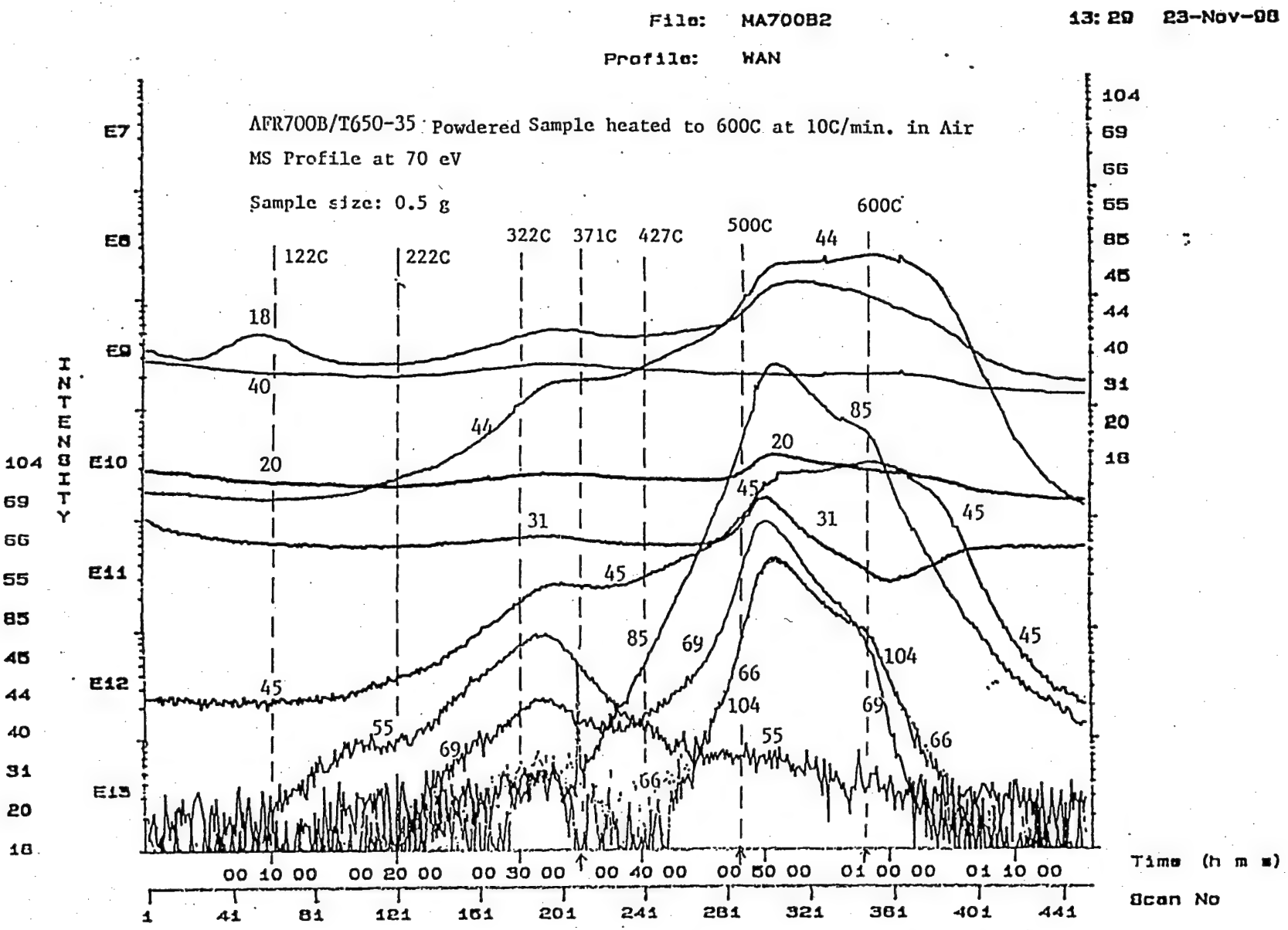

Figure 37 MS Profile for AFR700B/T650-35 Composite, Heated to 600°C in Air at 10°C/min and then cooled down for about 20 min

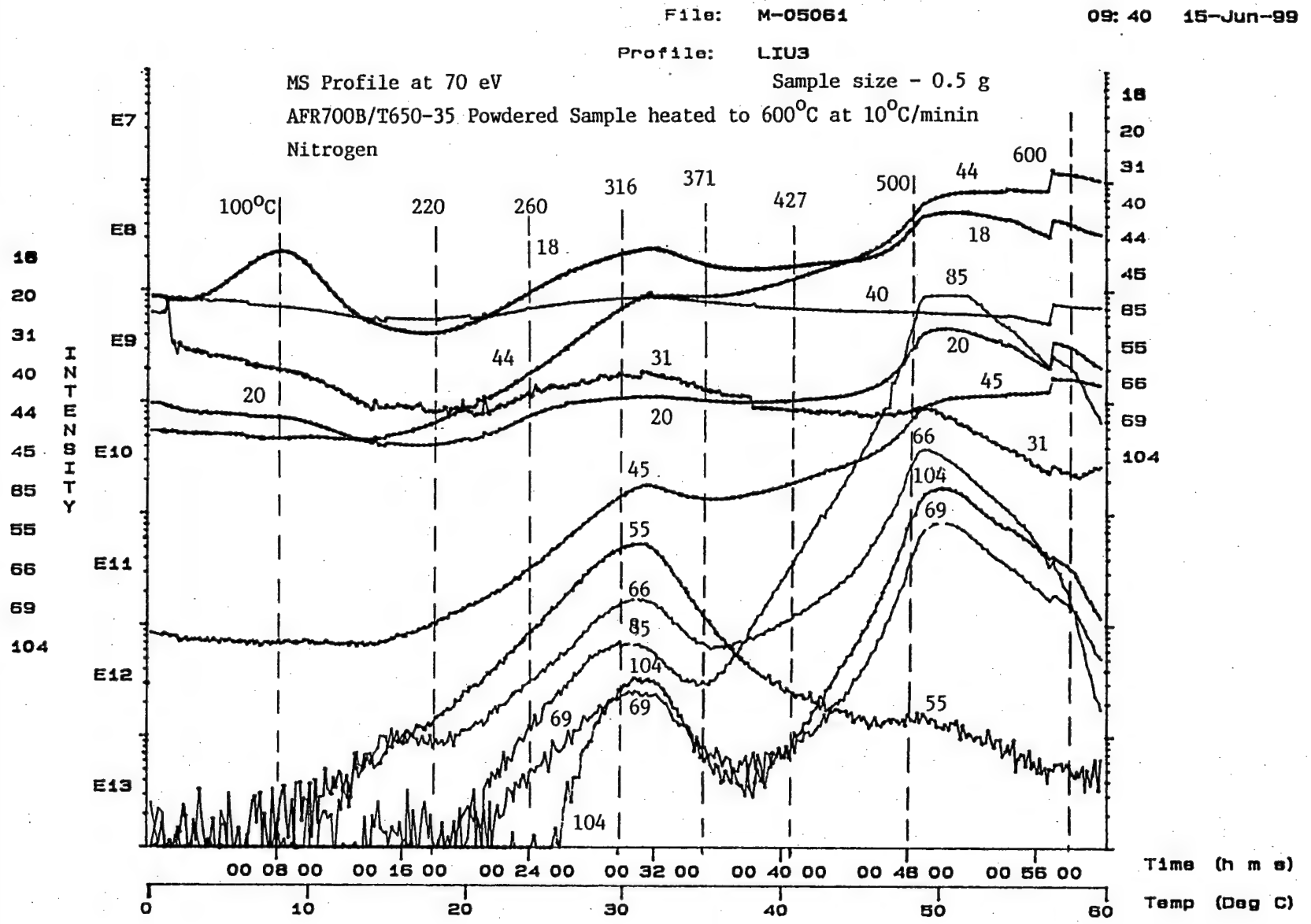

Figure 38 MS Profile for AFR700B/T650-35 Composite, Heated to 600°C in N_2 at 10°C/min

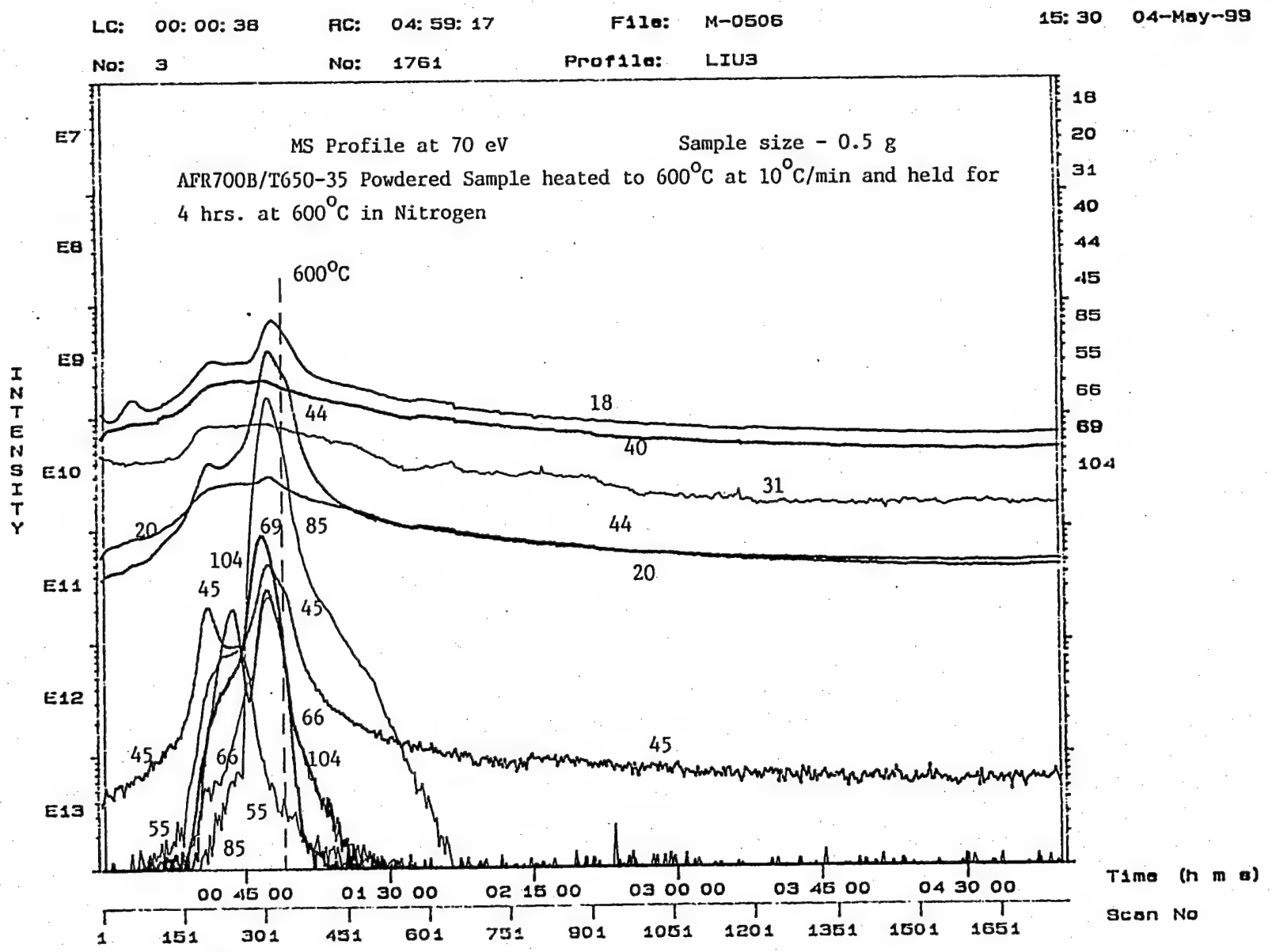

Figure 39 MS Profile for AFR700B/T650-35 Composite, Heated to 600°C in N_2 at 10°C/min and held for 4 hrs at 600°C

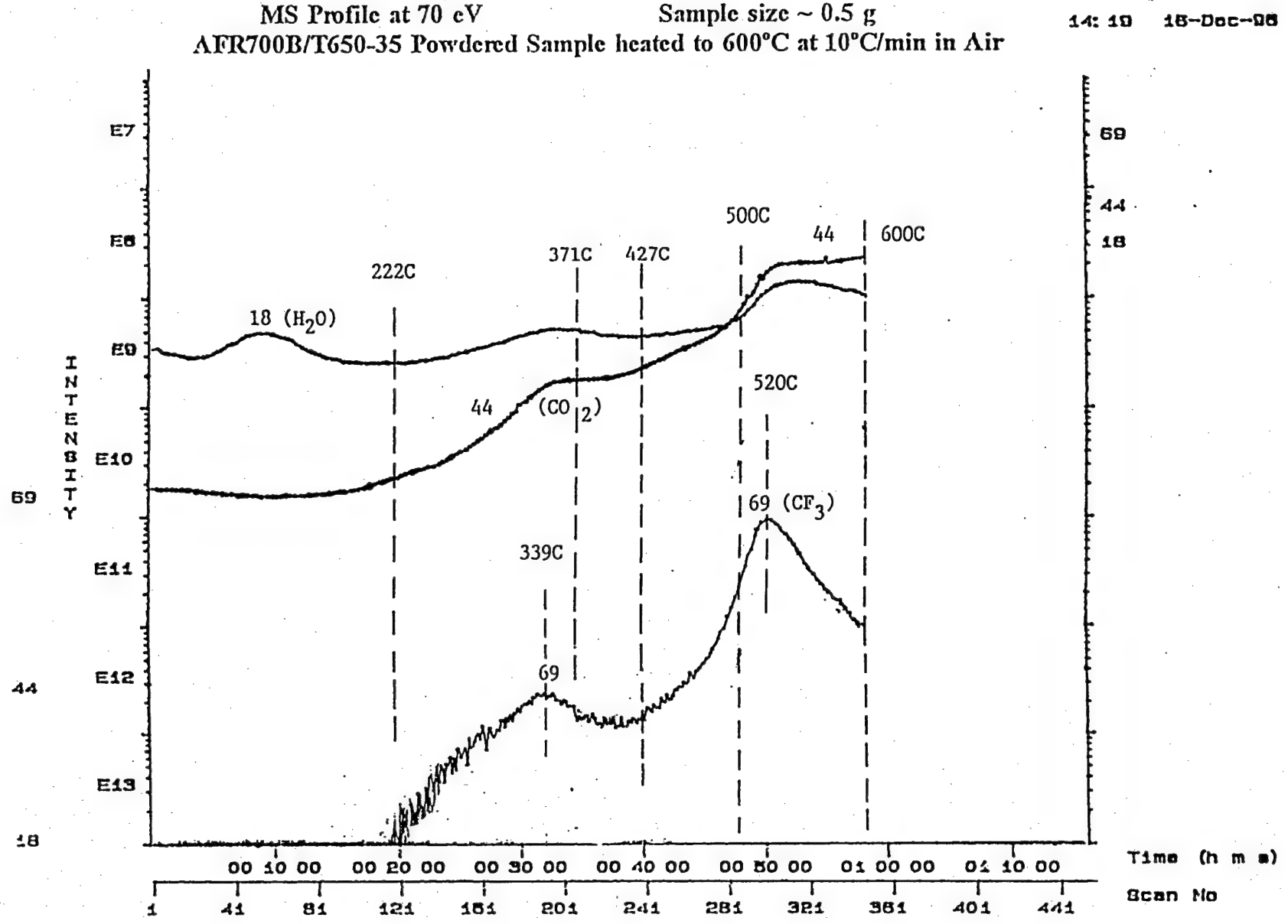

Figure 40 MS Profile for AFR700B/T650-35 Composite, Heated to 600°C in Air at 10°C/min

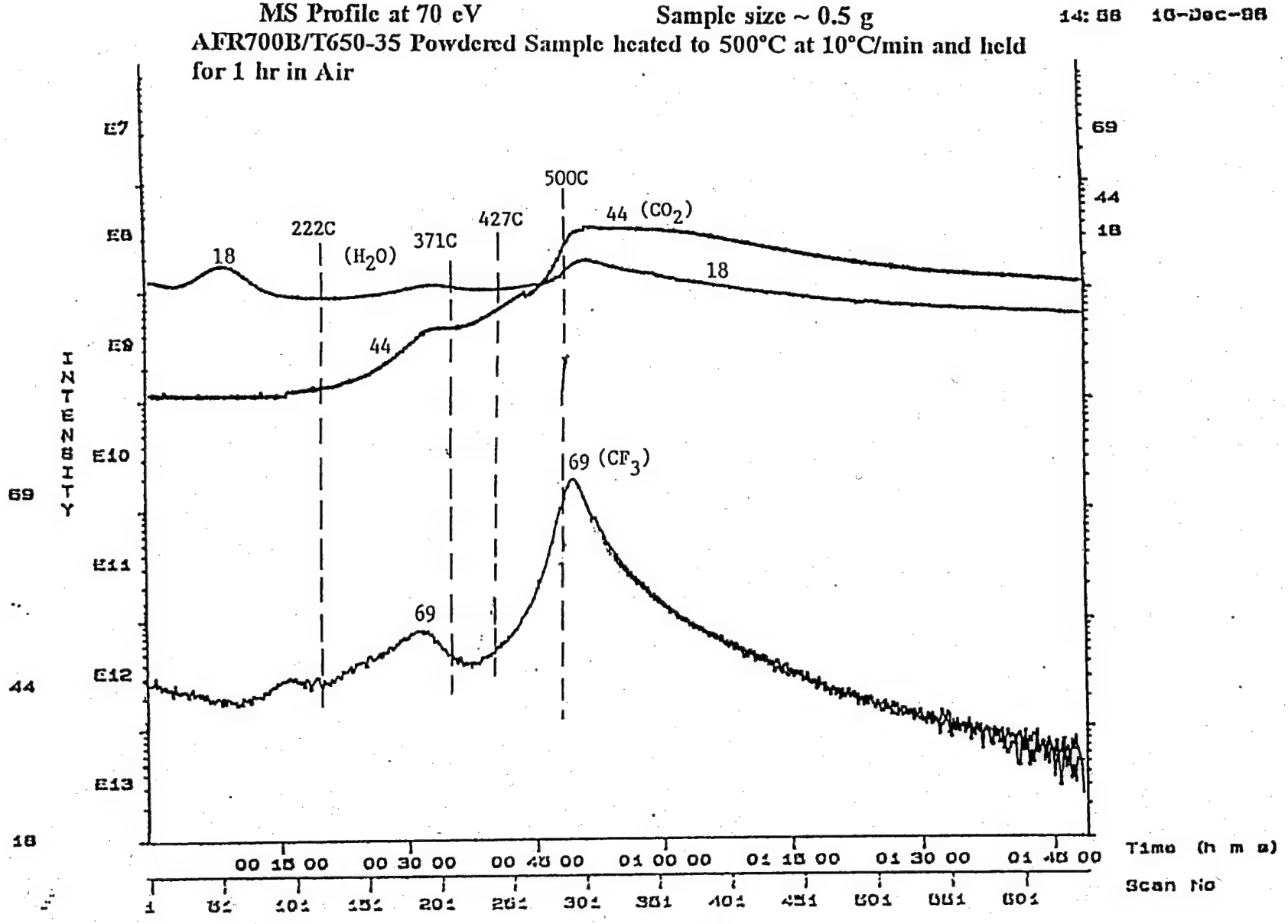

Figure 41 MS Profile for AFR700B/T650-35 Composite, Heated to 500°C in Air at 10°C/min and held for 1 hr at 500°C

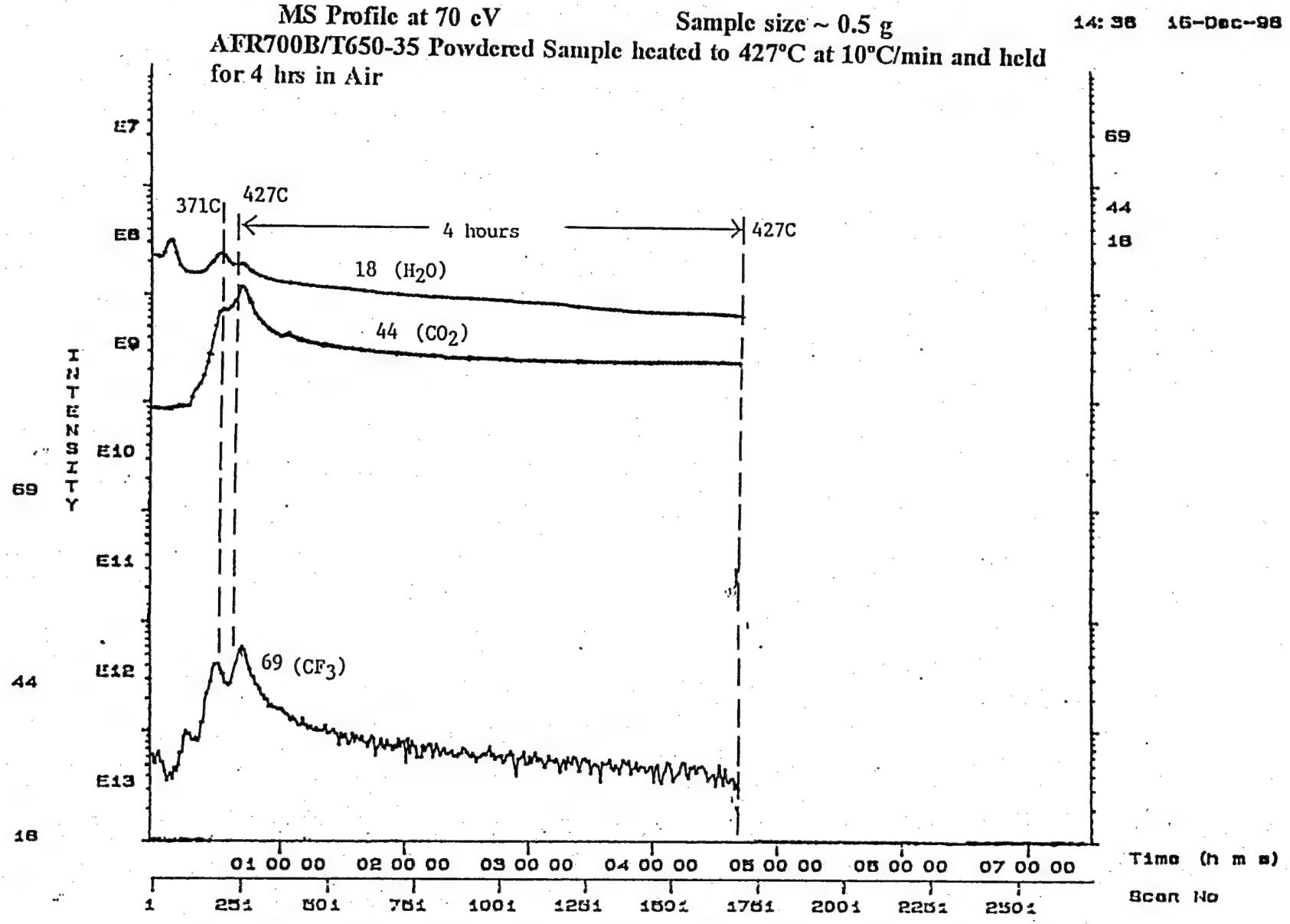

Figure 42 MS Profile for AFR700B/T650-35 Composite, Heated to 427°C in Air at 10°C/min and held for 4 hrs at 427°C

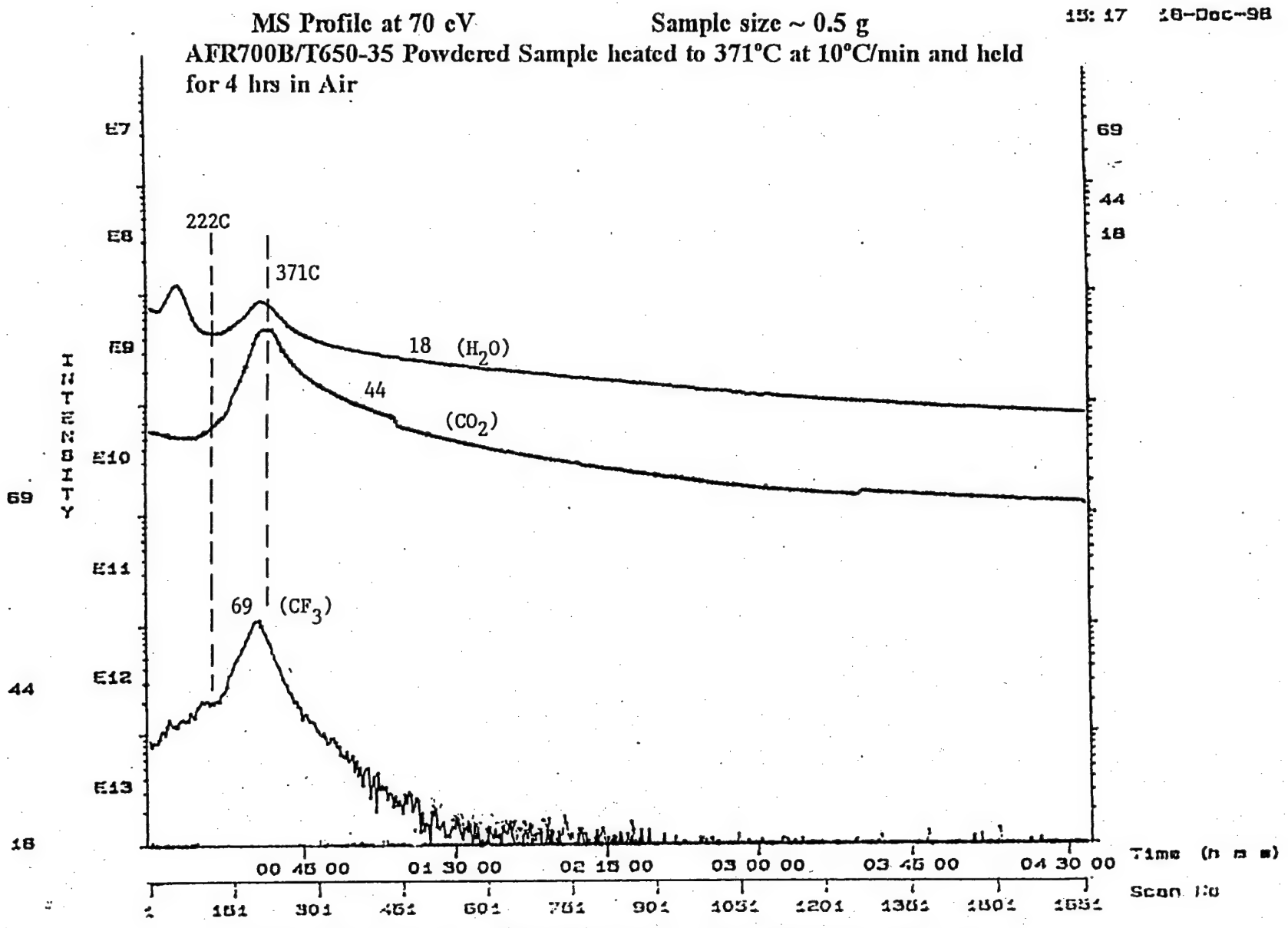

Figure 43 MS Profile for AFR700B/T650-35 Composite, Heated to 371°C in Air at 10°C/min and held for 4 hrs at 371°C

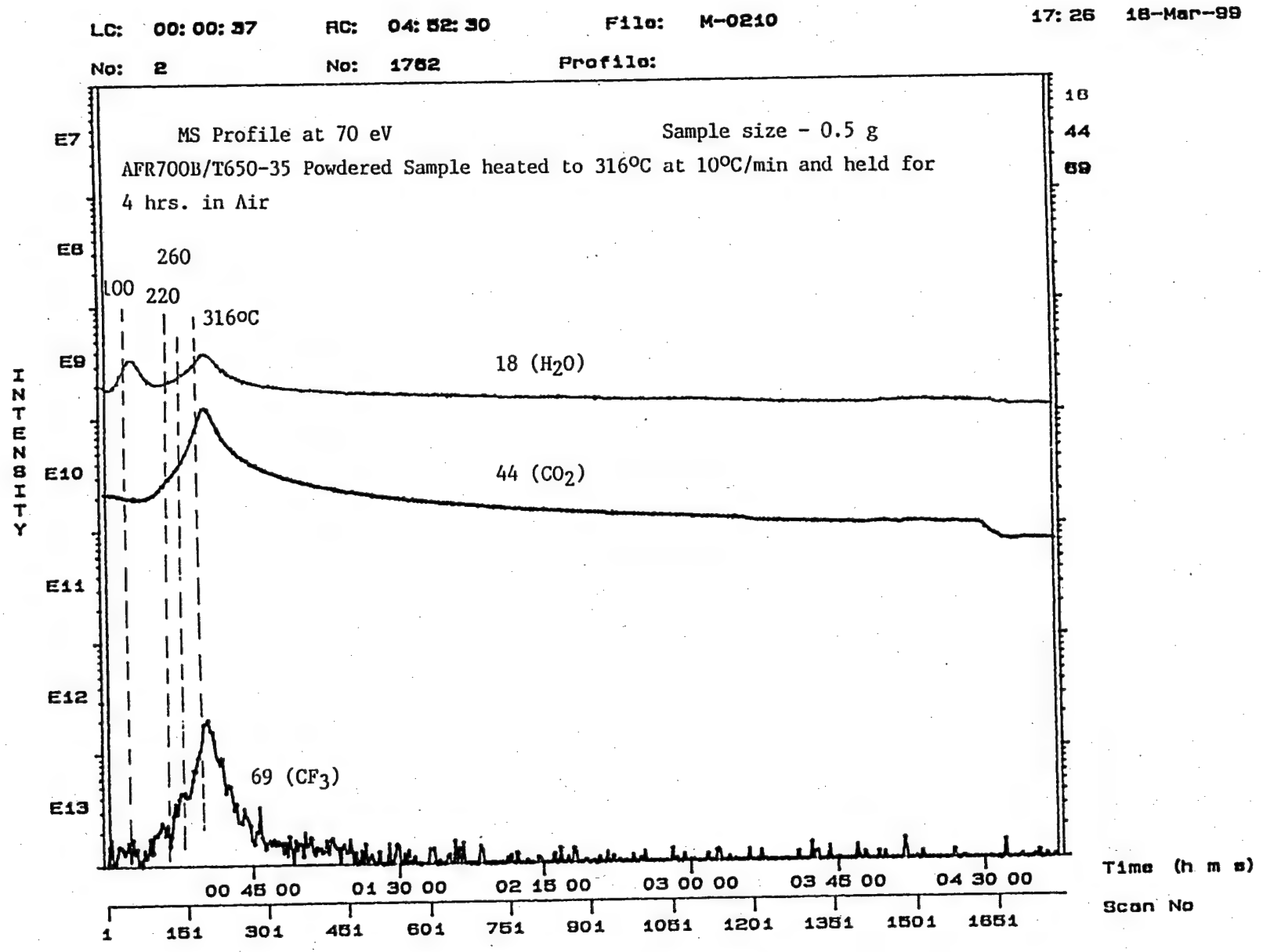

Figure 44 MS Profile for AFR700B/T650-35 Composite, Heated to 316°C in Air at 10°C/min and held for 4 hrs at 316°C

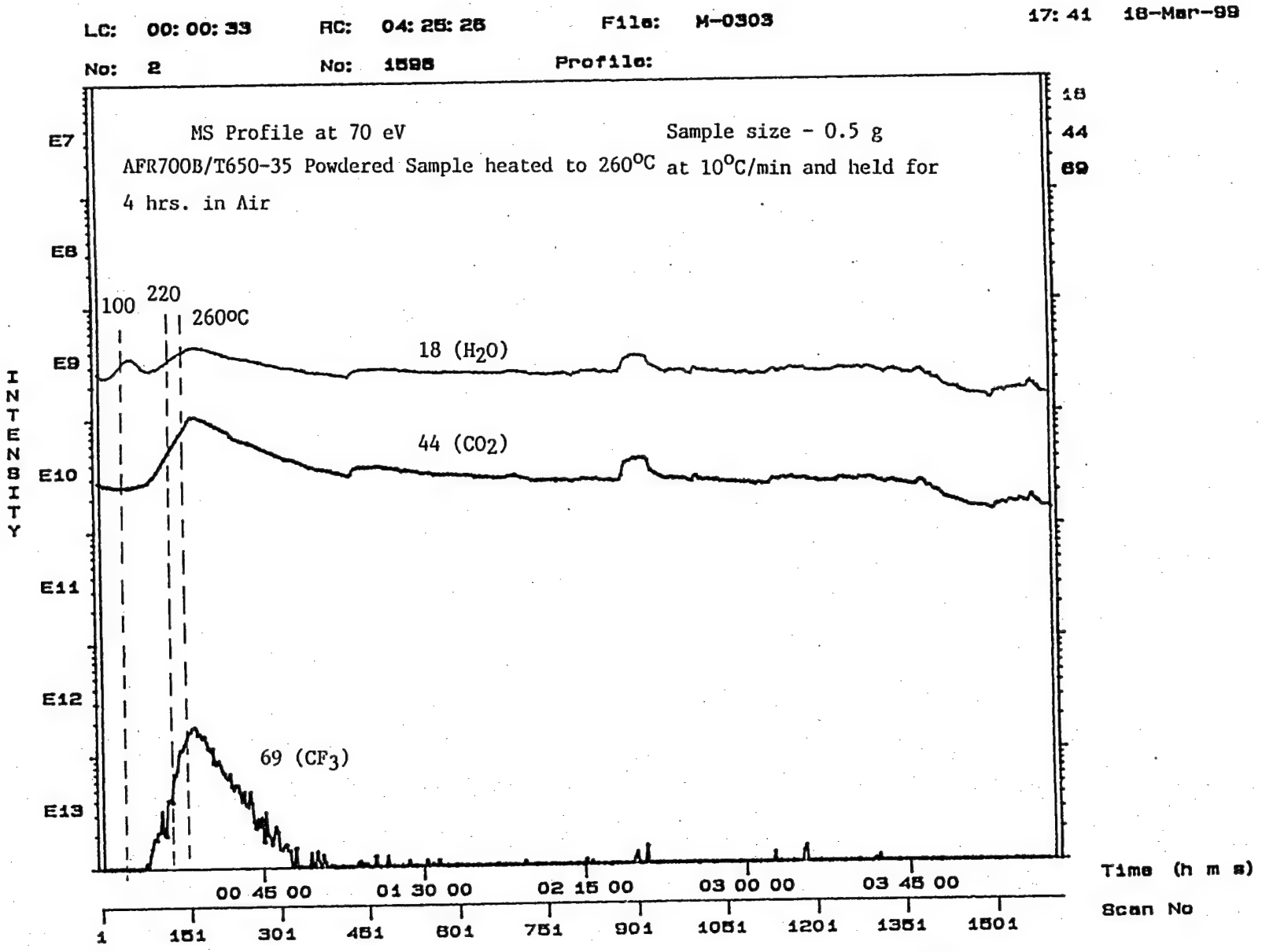

Figure 45 MS Profile for AFR700B/T650-35 Composite, Heated to 260°C in Air at 10°C/min and held for 4 hrs at 260°C

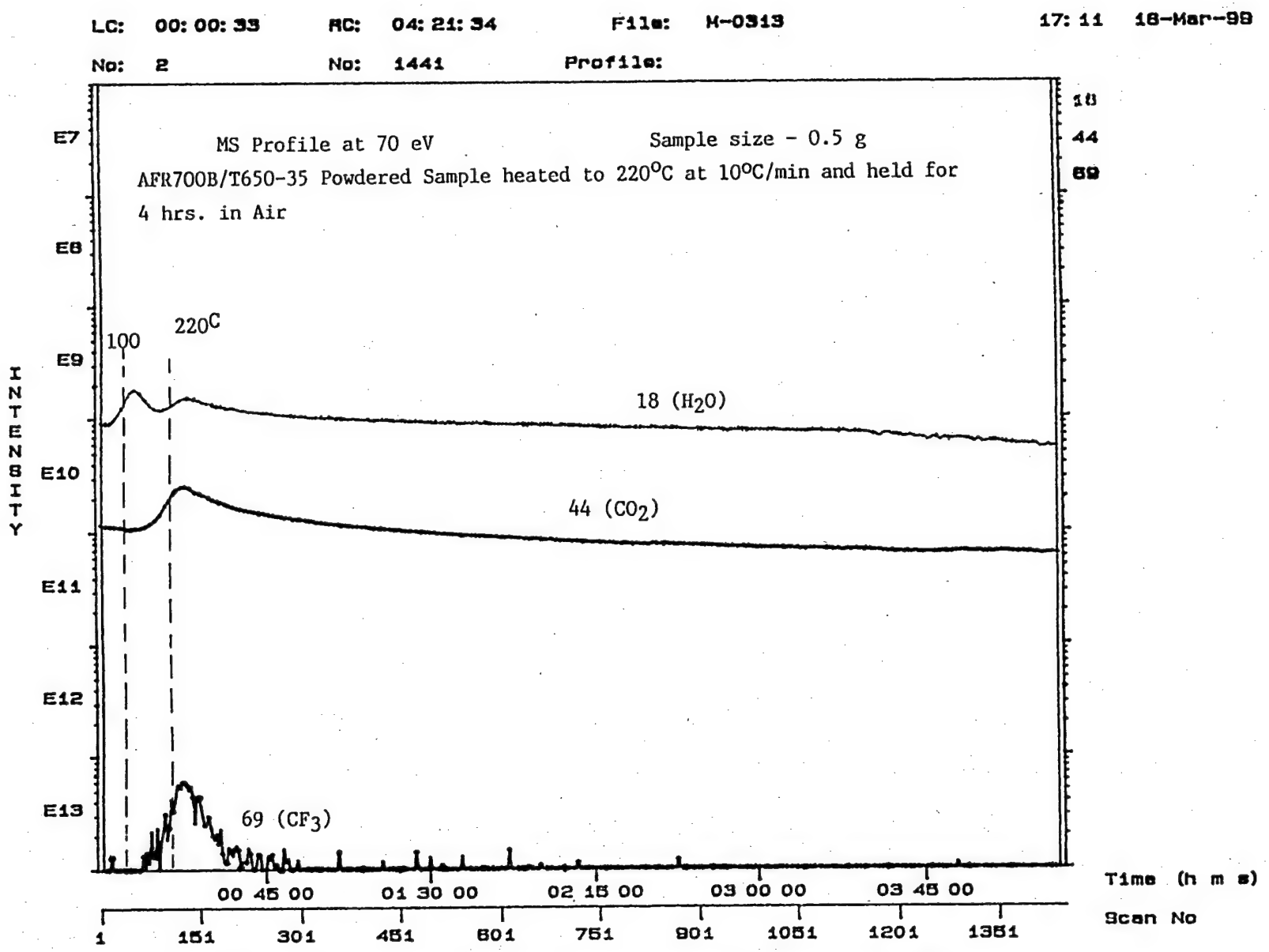

Figure 46 MS Profile for AFR700B/T650-35 Composite, Heated to 220°C in Air at 10°C/min and held for 4 hrs at 220°C

the intensity of the second peak for water, the first peak for carbon dioxide, and the first peak for $-CF_3$ was all small. Extrapolating further downward to a lower aging temperature like 190°C (374°F), one could potentially eliminate the second water peak. Thus, for the production and release of water between 190 and 371°C the decomposition pathways involved were probably similar. Therefore, the limit of its accelerated aging temperature would be 371°C. Beyond 371°C, a different set of water degradation mechanisms would have been started. So, to keep the water degradation mechanism similar for long-term lifetime prediction its accelerated aging temperature should be smaller than 371°C. The accelerated aging temperature limit for carbon dioxide and $-CF_3$ was only slightly different from that for water. For simplicity, 371°C could be applied to all these three degradation off-gases. Hence, any accelerated aging temperatures between 190 and 371°C could be used for AFR700B/T650-35 composite.

Water, carbon dioxide, and tri-fluoro carbon functional group ($-CF_3$) were analyzed for the determination of accelerated aging temperature limit in this study. The primary reasons were two-fold: (1) water and carbon dioxide were the major off-gases from oxidative and thermal degradations; and (2) the tri-fluoro carbon fragment arose from breakage of the weakest bond, $F_3C - C - CF_3$, in AFR700B. Even though only present at a very small intensity, the presence of $-CF_3$ would signal the onset of continuing degradations, and thus, an important event. The other mass fragments such as m/e = 20, 31, 40, 45, 55, 66, 85, and 104 behaved in a similar fashion. Figure 47 exhibited the more complete MS profile for m/e = 18, 20, 31, 40, 44, 45, 55, 66, 69, 85, and 104 for the aging of AFR700B/T650-35 composite in air at 427°C, held at 427°C for four hours, and then, cooled down to 127°C (260°F) at 1.8°C/min. During cooling, the mass fragments continued to decrease in intensity, some more drastically than others. Thus, the inclusion of a cooling period after its isothermal aging at 427°C brought about little unexpected mass intensity changes. Figures 48 – 50 displayed the more complete MS profile for isothermal aging at 371, 316, and 220°C, respectively. Overall, they provided no new information.

Based on the aging of AFR700B/T650-35 composite at 600, 500, 427, 371, 316, 260, and 220°C, the above analysis of the off-gas products seemed to indicate that its accelerated aging temperature should be limited to 371°C or 800°F. Beyond 371°C, its degradation mechanism would have changed. It was the first time that an in-situ chemical analysis made such a limit temperature determination possible.

3.2.5 Summary on AFR700B/T650-35 Composite Stability Study

The use of TGA/FTIR and TGA/MS evolved gas analysis techniques to study the thermal and oxidative stability of AFR700B/T650-35 composite successfully identified, in real time, some of the important off-gas products during aging, such as H_2O, CO, CO_2, HCF_3, HF, CH_3OH, $C_6H_5NH_2$, phenyl isocyanate, cyclopentadiene, etc. In general, they were given off in two separate temperature ranges having the first peak temperature between 300 – 330°C and the second peak temperature at about 500 – 520°C. The higher

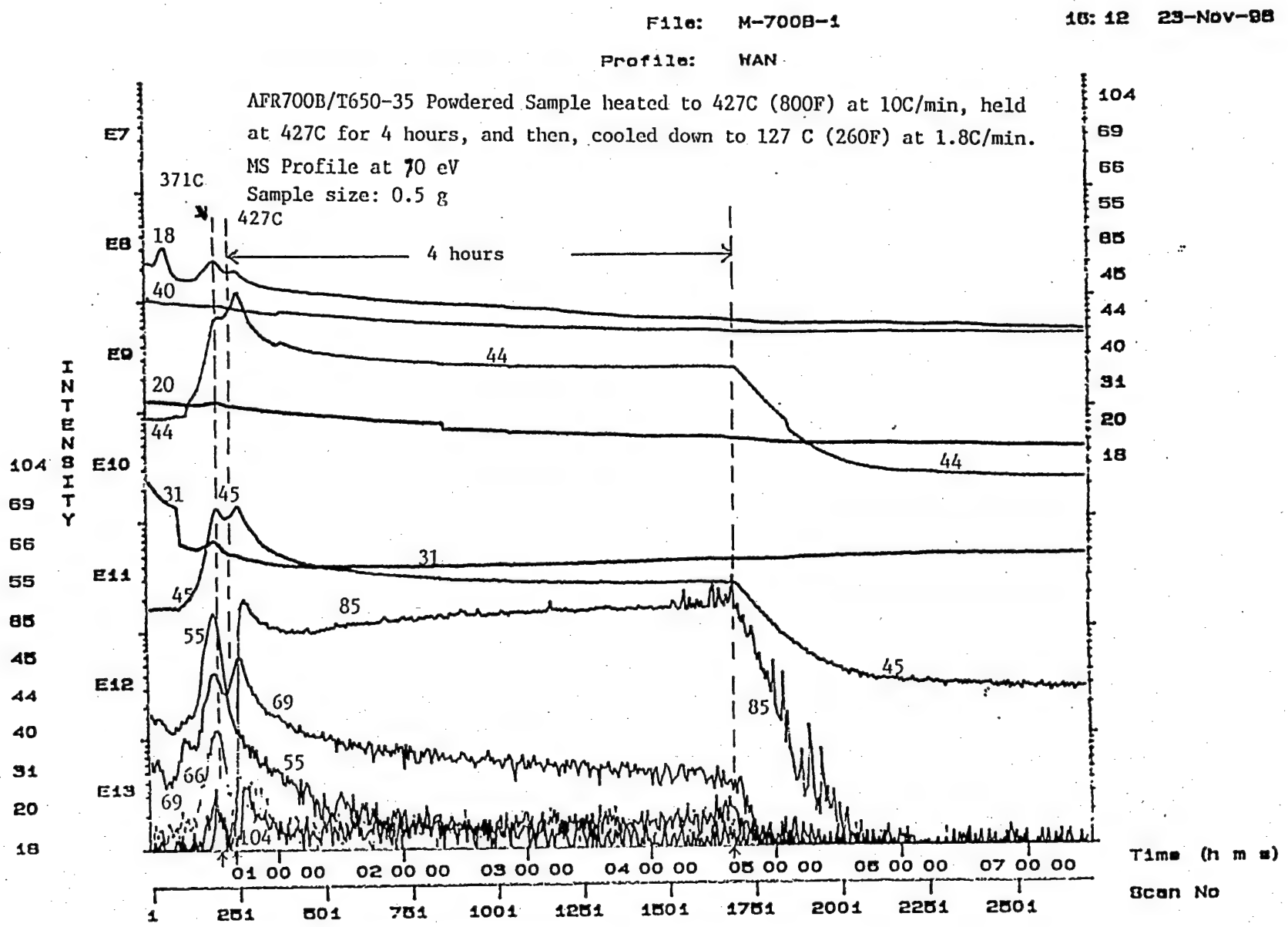

Figure 47 MS Profile for AFR700B/T650-35 Composite, Heated to 427°C in Air at 10°C/min and held for 4 hrs at 427°C with Cooling afterwards

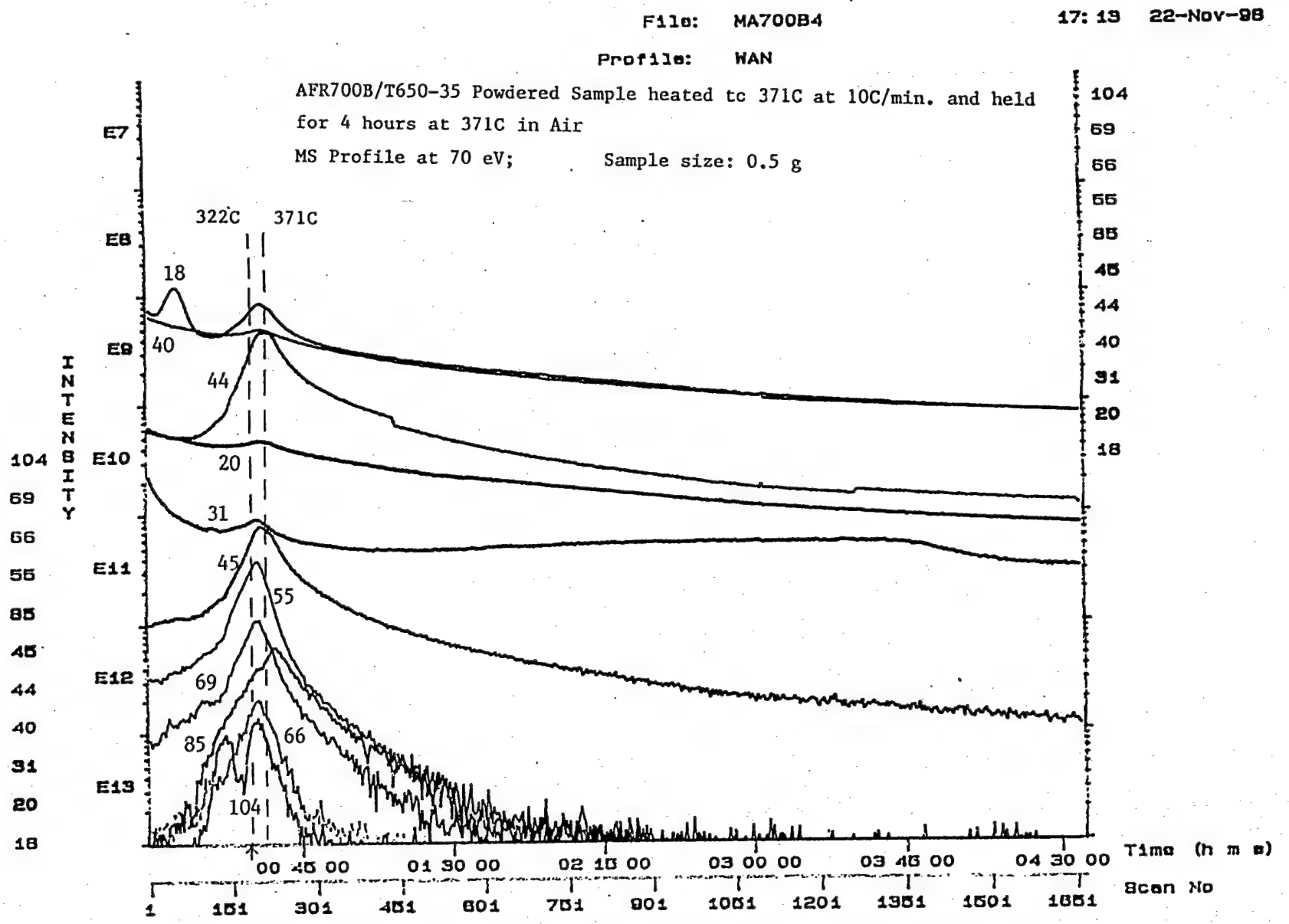

Figure 48 MS Profile (m/e=18-104) for AFR700B/T650-35 Composite, Heated to 371°C in Air at 10°C/min and held for 4 hrs at 371°C

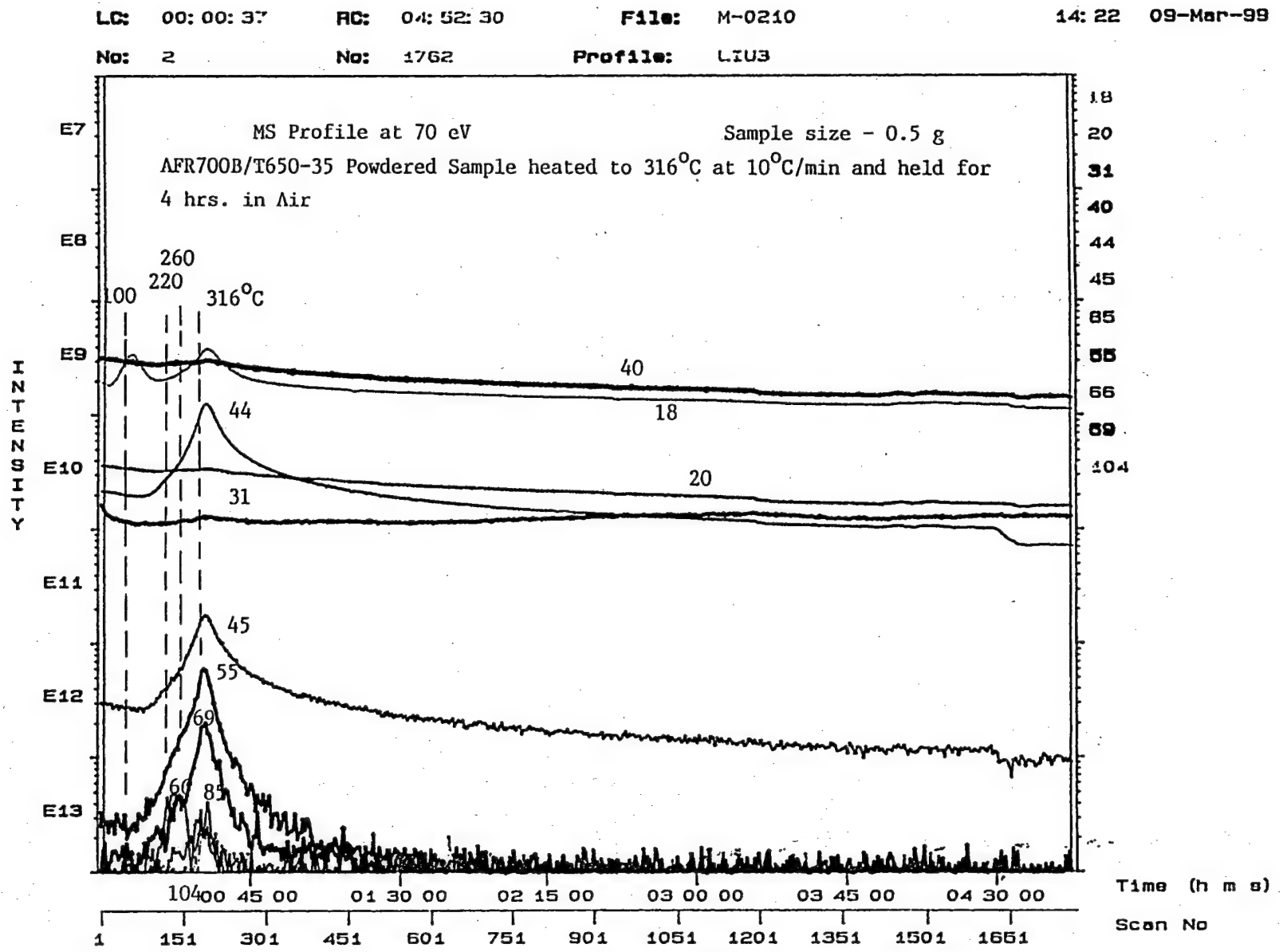

Figure 49 MS Profile (m/e=18-104) for AFR700B/T650-35 Composite, Heated to 316°C in Air at 10°C/min and held for 4 hrs at 316°C

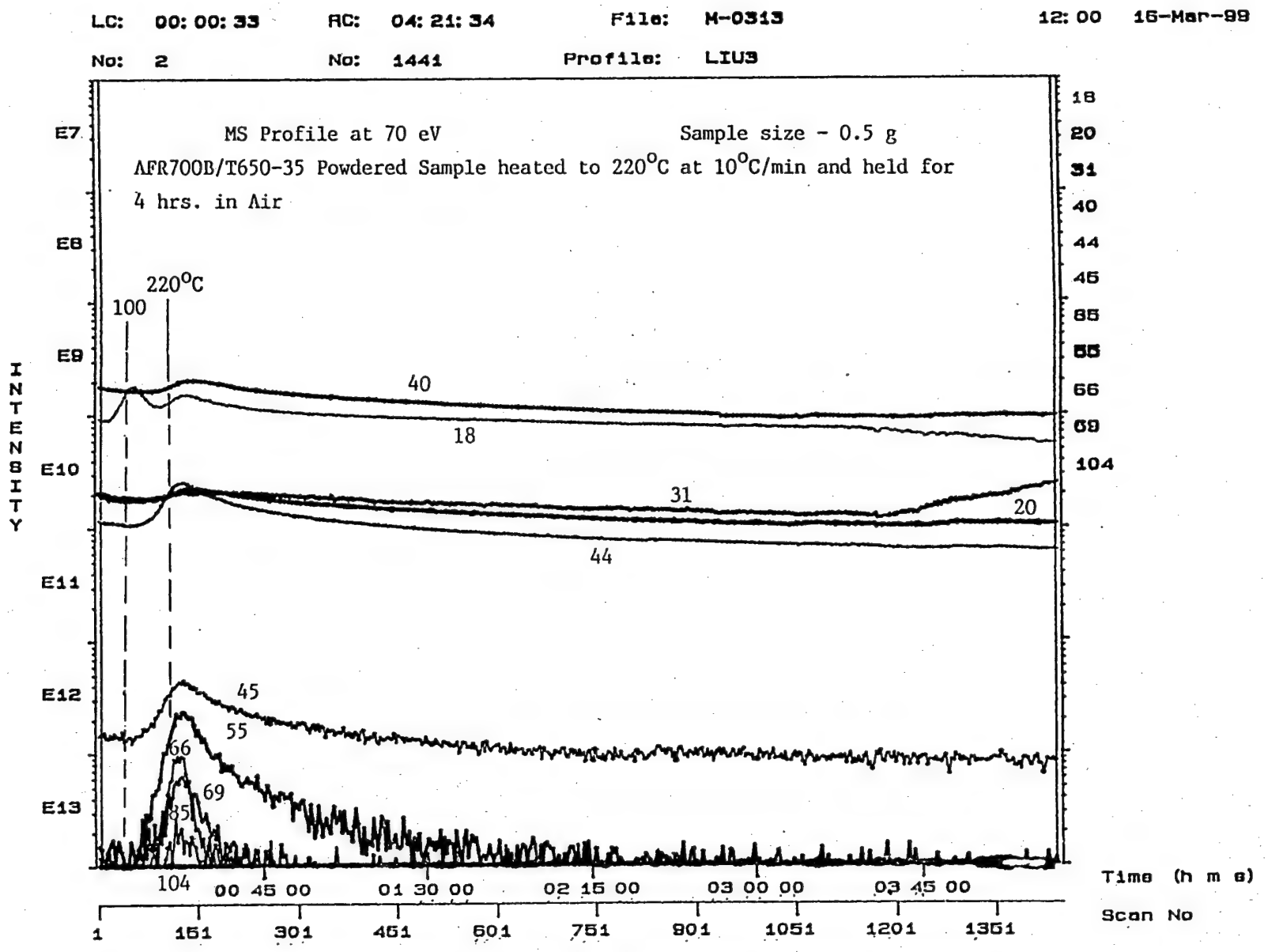

Figure 50 MS Profile (m/e=18-104) for AFR700B/T650-35 Composite, Heated to 220°C in Air at 10°C/min and held for 4 hrs at 220°C

temperature peak was much greater than the first one, suggesting the participation of carbon fiber in the composite.

The onset temperature for the release of these degradation products from chain scissions was surprisingly small at about 190 - 220°C. Furthermore, up to this point the composite degradations proceeded in a similar fashion, regardless of the aging environment used. Beyond 220°C, oxidative degradations gaining in speed started to deviate from thermal degradations, resulting in a larger weight loss and hence, a less stable composite.

The TGA/FTIR and TG/MS evolved gas analysis also provided a convenient means of probing if the thermal oxidative degradations under accelerated aging conditions proceeded according to a similar degradation mechanism by examining the degradation off-gases and their kinetics. When the release of these off-gas products from varying aging temperatures followed the same trend, their degradation mechanisms were deemed to be the same. For the AFR700B/T650-35 composite, its degradation mechanism between 190 and 371°C was found to be similar. Thus, the highest accelerated aging temperature for its long-term lifetime prediction would be 371°C. This marked the first time that an accelerated aging temperature limit was determined according to real-time degradation products.

The use of these evolved gas analysis techniques for studying degradation mechanism detail and hence, composite stability has some limitations. Due to the large number of IR bands and mass fragments present in MS, it was difficult to assign chemical structure to some. Moreover, they appeared simultaneously making detailed degradation pathway determination a challenging task. Lastly, some non-volatile chemical intermediates produced from thermal oxidative degradations would escape detection by evolved gas analysis. Thus, complimentary techniques such as temperature programmable FTIR and NMR may prove useful in monitoring those chemical structures.

In this composite stability study, the emphasis had been placed on its chemical origin instead of mechanical performance. It would be most useful to relate any major chemical changes including chain scissions to composite mechanical property changes. To do so requires the knowledge of oxygen diffusion and heat transfer into a large mechanical property composite specimen. In the ideal case, one would wish to establish an interrelationship among aging environment/temperature/time, the state of chemical degradations, and mechanical property change. Since mechanical property measurement usually involves large composite specimens, it is of paramount importance to be able to determine its corresponding chemical changes during aging and its effects on property to gain a basic understanding of the composite stability.

4. Acknowledgement

The authors of this report wish to express their sincere gratitude to:

1. the Department of Defense's Kentucky Experimental Program to Stimulate Competitive Research (DoD Kentucky EPSCoR) for their financial support of this research,

2. Dr. Charles Y-C Lee of the Air Force Office of Scientific Research for taking the time to be the monitor of this research project,

3. the Sponsored Programs Office at Western Kentucky University for the administration of this external research grant,

4. Dr. William McCormack of General Electric Aircraft Engines for providing the AFR700B/T650-35 prepreg and post-cured composite samples,

5. Dr. Ruth Pater of NASA Langley Research Center for supplying the Larc RP-46/IM7 prepreg, and

6. Dr. James Sutter of NASA Lewis Research Center for providing the VCAP-75/Glass fiber prepreg.

5. References

5.1 Brian Price, "An Evaluation of Two 700° Polyimides," HIGH TEMPLE Workshop XIII, Santa Fe, NM, Jan. 18-21, 1993.

5.2 Tito Serafini, "Ultra-High Temperature Polyimides," HIGH TEMPLE Workshop XIII, Santa Fe, NM, Jan. 18-21, 1993.

5.3 Dan Scola, "Comparative Properties of Polyimides for 370°C Applications," HIGH TEMPLE Workshop XIII, Santa Fe, NM, Jan. 18-21, 1993.

5.4 Richard Cornelia, "The Hot-Wet Stability of Polyimides," HIGH TEMPLE Workshop XIV, Cocoa Beach, FL, Jan. 31 – Feb. 3, 1994.

5.5 T. T. Vuong, "Effect of –18°C Storage on PMR-15 Polyimide Resin," SAMPE Proceeding, 34 (1989) 98.

K. L. Mittal, "Polyimide Synthesis, Characterization and Applications," Vol. 1, Plenum Press, New York, 1984, pp. 311-326 on "The Cure Rheology of PMR Polyimide Resins," by P. J. Dynes et al.

Ibid., pp. 957-975 on "PMR Polyimide Composites for Aerospace Applications, " by T. T. Serafini.

5.6 T. T. Vuong, "Effect of –18°C Storage on PMR-15 Polyimide Resin," SAMPE Proceeding, 34 (1989) 98.

5.7 D. B. Curliss, "^{15}NMR Spectroscopic Investigation of BMI Polymers," HIGH TEMPLE Workshop XIV, Cocoa Beach, FL, Jan. 31 – Feb. 3, 1994.

5.8 Unpublished data at Western Kentucky University, Bowling Green, KY, 1995.

5.9 N. Johnston, "Polyimide Research at NASA-Langley: An Update," HIGH TEMPLE Workshop XIII, Santa Fe, NM, Jan. 18-21, 1993.

5.10 W. M. Lee et al., "Thermal Oxidative Stability of Diketone-Bis-Benzocyclobutene/Graphite Fabric Composites," SAMPE Proceeding, 37 (1992) 679.

5.11 T. Roth, M. Zhang, J. T. Riley, and Wei-Ping Pan, "Thermogravimetric/ Fourier Transformation Infrared Analysis Studies of Combination Fuels," Proceedings, 9th International Coal Testing Conference, Lexington, KY, 1992, 46-49.

5.12 Q. Zhang, Wei-Ping Pan, and W. M. Lee, "Thermal Analysis of Composites by TG/FTIR," Thermochemica Acta, 226 (1993) 115-122.

5.13 W. Zhong, "Degradation Product Analysis of Bismaleimide Composite," M.S. thesis at Western Kentucky University, Bowling Green, KY 42101, 1996.

5.14 William Alston, et al, "TGA Techniques for The Evaluation of The Thermal Oxidative Stability of Polyimides," HIGH TEMPLE Workshop XVII, Monterey, CA, Feb. 10-13, 1997.

5.15 W. M. Lee et al, "Quantum Chemistry Computations of Thermal Oxidative Stability for High Temperature Polyimides," HIGH TEMPLE Workshop XVIII, Hilton Head Island, SC, Jan. 20-22, 1998.

5.16 Both AFR700B/T650-35 prepreg and post-cured AFR700B/T650-35 laminate were provided by William E. McCormack at GE Aircraft Engines, General Electric Company, Cincinnati, OH, 1996.

5.17 James Sutter of NASA Lewis supplied the VCAP-75/Glass fiber prepreg.

5.18 Ruth Pater of NASA Langley provided the RP-46/IM7 prepreg.

5.19 D. A. Scola, Polyimide Resins in Properties of Constituent Materials, "Engineered Materials Handbook – Composites," Vol. 1, p. 83, ASM International, Metals Park, Ohio, 1987.

5.20 T. H. Hu, S. P. Wilkinson, N. J. Johnston, R. H. Pater and T. L. Schneider, "Processing and Properties of IM7/Larc – RP46 Polyimide Composites," High Perform. Polym., 8 (1996) 491-505.

5.21 P. L. Hanst and S. T. Hanst, "Infrared Spectra for Quantitative Analysis of Gases," Gas Analysis Manual for Analytical Chemists, Vol. II.

5.22 M. I. Bessonov, M. M. Koton, V. V. Kudryavtsev and L. A. Laius, "Polyimides – Thermally Stable Polymers," p. 128, Consultants Bureau, New York and London, 1987.